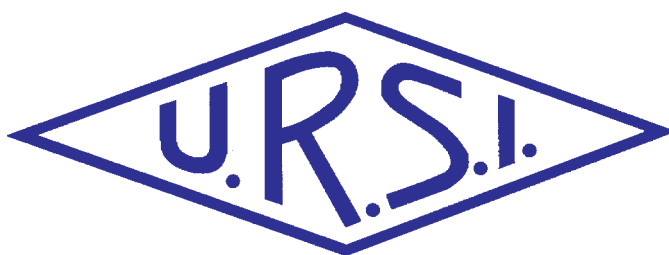


Radio Science Bulletin

ISSN 1024-4530

INTERNATIONAL
UNION OF
RADIO SCIENCE

UNION
RADIO-SCIENTIFIQUE
INTERNATIONALE



No 340
March 2012

URSI, c/o Ghent University (INTEC)
St.-Pietersnieuwstraat 41, B-9000 Gent (Belgium)

Contents

Editorial	3
Electromagnetic Metrology Symposium	5
URSI Commission B 2013 International Symposium on Electromagnetic Theory	6
URSI Accounts 2011.....	7
IUCAF Annual Report for 2011.....	11
Energy Patterns of Pulsed Antennas Illustrated with a Reflector Type of an Impulse-Radiating Antenna (IRA).....	14
Spectrum Management Overview	25
Opportunistic Secondary Spectrum Access : Opportunities and Limitations	29
Recent Advances in Integrated Circuit Immunity to Radio-Frequency Interference.....	34
Radio-Frequency Radiation Safety and Health	53
<i>Are Radio-Frequency or Mobile-Phone Electromagnetic Fields Possibly Carcinogenic to Humans</i>	
Book Reviews for Radioscientists	55
Letter to the Editor	58
Conferences	60
Information for authors	65

Front cover: A photograph of an impulse-radiating antenna (IRA). See the paper by D. V. Giri and F. M. Tesche on pp. 14-24.

EDITOR-IN-CHIEF

URSI Secretary General
Paul Lagasse
Dept. of Information Technology
Ghent University
St. Pietersnieuwstraat 41
B-9000 Gent
Belgium
Tel.: (32) 9-264 33 20
Fax : (32) 9-264 42 88
E-mail: ursi@intec.ugent.be

EDITORIAL ADVISORY BOARD

François Lefeuvre
(URSI President)
W. Ross Stone

PRODUCTION EDITORS

Inge Heleu
Inge Lievens

SENIOR ASSOCIATE EDITOR

J. Volakis
P. Wilkinson (RRS)

ASSOCIATE EDITOR FOR ABSTRACTS

P. Watson

ASSOCIATE EDITOR FOR BOOK REVIEWS

K. Schlegel

EDITOR

W. Ross Stone
840 Armada Terrace
San Diego, CA92106
USA
Tel: +1 (619) 222-1915
Fax: +1 (619) 222-1606
E-mail: r.stone@ieee.org

ASSOCIATE EDITORS

W.A. Davis (Com. A)	R. Lang (Com. F)
G. Manara (Com. B)	J.D. Mathews (Com. G)
M. Luise (Com. C)	O. Santolik (Com. H)
P-N Favennec (Com. D)	R. Strom (Com. J)
A. van Deursen (Com. E)	J. Wiart (Com. K)

For information, please contact :

The URSI Secretariat
c/o Ghent University (INTEC)
Sint-Pietersnieuwstraat 41, B-9000 Gent, Belgium
Tel.: (32) 9-264 33 20, Fax: (32) 9-264 42 88
E-mail: info@ursi.org
<http://www.ursi.org>

The International Union of Radio Science (URSI) is a foundation Union (1919) of the International Council of Scientific Unions as direct and immediate successor of the Commission Internationale de Télégraphie Sans Fil which dates from 1913.

Unless marked otherwise, all material in this issue is under copyright © 2012 by Radio Science Press, Belgium, acting as agent and trustee for the International Union of Radio Science (URSI). All rights reserved. Radio science researchers and instructors are permitted to copy, for non-commercial use without fee and with credit to the source, material covered by such (URSI) copyright. Permission to use author-copyrighted material must be obtained from the authors concerned.

The articles published in the Radio Science Bulletin reflect the authors' opinions and are published as presented. Their inclusion in this publication does not necessarily constitute endorsement by the publisher.

Neither URSI, nor Radio Science Press, nor its contributors accept liability for errors or consequential damages.

This issue of the *Radio Science Bulletin* is an all-Commission E issue. Dr. D. V. Giri has acted as the Guest Editor for this issue, and his efforts and those of the authors of our papers are greatly appreciated.



Our Papers

An impulse radiating antenna (IRA) is designed specifically to maintain the time-domain pulse characteristics of the waveform with which it is excited. It is therefore what is known as a hyperband antenna: it has a very wide bandwidth in the frequency domain. Most of the parameters used to characterize an antenna's performance were chosen with the antenna's frequency-domain performance in mind. However, new parameters may be more appropriate for an IRA. The paper by D. V. Giri and F. M. Tesche looks at the *energy pattern* of an IRA (as contrasted with the power or amplitude pattern of a more-conventional antenna) to characterize how the energy input to the IRA is radiated into space. The authors introduce the energy pattern: the far-field energy density as a function of the spherical angles of a coordinate system centered on the antenna. They then show how the far fields of the IRA can be computed using an aperture-integration method. They apply these results to a prototype IRA, excited by different waveforms. They show that the results of their aperture-integration method agree well with other estimates of the radiation of the IRA. These results and the energy patterns for the IRA serve to provide interesting insights into the performance of this antenna.

Terje Tjelta and Ryszard Struzak have provided us with a very interesting overview of the topic of spectrum management. The paper begins with a review of the demand for spectrum, how this demand has grown, and what the trends in growth foretell. The methods of managing spectrum are then reviewed, noting that spectrum is currently managed at the global, regional, and national levels. The several models in use for managing spectrum are explained. Future trends in spectrum management are explored. Part of this exploration includes a discussion of the tradeoffs among several spectrum-management models, and how these are likely to influence the future of spectrum management. Some interesting arguments are presented for why certain models are more likely to be used than others in the future.

In their paper, Jens Zander and Ki Won Sung report on some results to date from the European Union QUASAR project. The purpose of this project was to assess the amount of spectrum available for secondary users. Secondary users are users that make use of spectrum that is available in either the time and/or spatial domains because primary users are

not making full use of the spectrum. This is the concept behind cognitive radio. The paper begins with a thorough discussion of the major issues associated with opportunistic secondary-spectrum access, and a review of the work that has been done in this area. Secondary-access scenarios are then introduced and reviewed. In common cognitive-radio modes of operation, it is assumed that secondary users can find spectrum to use by sensing the signals from the primary users. The authors point out three major reasons why this approach is likely to result in poor spectrum-utilization performance.

The paper then makes the point that secondary access by a single secondary device is unlikely to be attractive from a business perspective, and that secondary access must therefore scale to support a sufficient amount of traffic. This leads to a quantitative analysis of the interference impact of multiple secondary users. Some results related to the business aspects of the commercial use of secondary access follow. The authors close by drawing some interesting and important conclusions regarding where the use of secondary access to spectrum may be quite viable, and where it may be much less viable.

Etienne Sicard, Mohamed Ramdani, and Samuel Akue Boulingui have provided us with a comprehensive review of the literature and recent results on the effects of RF interference on integrated circuits (ICs), and the developments that have made ICs more immune to such interference. A discussion of the basic concepts of the electromagnetic compatibility of an IC, and possible sources of interference for ICs, is given. The technologies of ICs that are both affected by interference and that provide protection against interference are reviewed, along with the recent advances in this area. The International Electrotechnical Commission's (IEC's) standards for characterizing both emissions from ICs and the susceptibility of ICs are explained in some detail. Several measurement methods for characterizing IC immunity are described. These include the resistive RF injection probe, bulk-current-injection modeling, aging, and on-chip immunity sampling. The methods of modeling IC immunity are described. A number of design guidelines for improving the immunity of ICs are given. This paper provides a comprehensive overview of the topics of IC immunity and interference in a particularly easy-to-read manner.

Our Other Contributions

Kristian Schlegel has brought us reviews of two interesting books. One of these reviews is written by an URSI Young Scientist. Such contributions from our Young

Scientists are particularly welcome. In his Radio Frequency Radiation Safety and Health column, Jim Lin looks at the current status of the question of whether or not radio-frequency electromagnetic fields in general, and/or those associated specifically with mobile phones, are possibly carcinogenic to humans. There are calls for papers for two URSI conferences. Finally, there is also a call for papers for a special issue of the *Radio Science Bulletin* on "The Role of Radio Science in Disaster Management." I urge you to consider contributing to this special issue.

The *Radio Science Bulletin* has a rather short queue of papers at the moment. If you have a paper for which the appropriate audience is radio scientists, please send it to me. The *Bulletin* is an excellent way to reach our community!



URSI GASS Proceedings Available

The *Proceedings of the URSI General Assembly and Scientific Symposium (URSI GASS)* for the past four triennia (2002, 2005, 2008, and 2011) are available from the URSI Web site at

http://www.ursi.org/en/general_assemblies_proceedings.asp



Electromagnetic Metrology Symposium

Organized by Commission A of the International Union of Radio Science

In coordination with the International Conference on Electromagnetics in Advanced Applications (ICEAA 2013) and the IEEE Topical Conference on Antennas and Propagation in Wireless Communications (IEEE APWC 2013)

September 9 – 13, 2013

Torino, Italy

The first Electromagnetic Metrology Symposium (EMS 2013) is organized by Commission A of the International Union of Radio Science (URSI) in coordination with the ICEAA and IEEE APWC Conferences. The three conferences will be held concurrently at the Torino Incontra Conference Center in Torino, Italy from Monday, September 9 through Friday, September 13, 2013. The three conferences share a common organization, registration fee, submission site, welcoming reception, coffee and lunch breaks, banquet, and social program. Detailed information is found on the conferences website: www.iceaa.org. EMS 2013 will consist of invited and contributed papers, workshops and short courses, and business sessions.

Suggested Topics for EMS

Metrology, measurements and standards in all areas of radio science, including:

Microwave to submillimeter measurements/standards

Quantum metrology and fundamental concepts

Time and frequency

EMC and EM pollution

Noise

Materials

Bioeffects and medical applications

Antennas

EM field metrology

Impulse radar

Planar structures and microstrip circuits

Interconnects and packaging

Information for Authors

Authors must submit a full-page abstract electronically by March 1, 2013. Authors of accepted contributions must register electronically by June 7, 2013. Instructions are found on the website. Each registered author may present no more than two papers. All papers must be presented by one of the authors. Authors who want their paper to be published on IEEE Xplore should follow the instructions on the website. Selected authors of EMS will be invited to submit a full-length paper for possible publication in the URSI Radio Science Bulletin.

Deadlines	Abstract submission	March 1, 2013
	Notification of acceptance	April 12, 2013
	Presenter registration	June 7, 2013

EMS Contacts Prof. William A. Davis, EMS Chair wadavis@vt.edu
Prof. Yasuhiro Koyama, EMS Vice-Chair koyama@nict.go.jp

Inquiries Prof. Roberto D. Graglia, Chair of Organizing Committee roberto.graglia@polito.it
Prof. Piergiorgio L. E. Uslenghi, Chair of Scientific Committee uslenghi@uic.edu

URSI Commission B 2013 International Symposium on Electromagnetic Theory

Hiroshima, Japan May 20-24, 2013

www.ursi-emts2013.org

General Information

The "2013 International Symposium on Electromagnetic Theory" (EMTS 2013) is organized by Commission B (Fields and Waves) of the International Union of Radio Science (URSI) and the Electronics Society of The Institute of Electronics, Information and Communication Engineers (IEICE). It will be held on May 20-24, 2013 in Hiroshima, Japan. Its scope covers all areas of electromagnetic theory and its applications.

Important Dates

Nov. 1, 2012	Deadline for receipt of YSA papers
Nov. 15, 2012	Deadline for receipt of papers
Jan. 15, 2013	Notification of authors regarding acceptance of papers, notification of YSA applicants
Mar. 15, 2013	Deadline for pre-registration of authors (All presenting authors must pre-register)
April 30, 2013	Deadline for pre-registration of participants
May 20, 2013	URSI Commission B School for Young Scientists
May 20-24, 2013	Symposium

Young Scientist Awards

Young Scientist Awards (YSA) have been planned for young scientists. For details, visit the website.

Suggested Topics

Contributions concerning all aspects of electromagnetic theory and its applications are welcome. Novel and innovative contributions are particularly appreciated. Special topics will also be announced in the Final Call for Papers in addition to the following list.

- New basic theoretical developments
- Scattering and diffraction
- Inverse scattering and imaging
- Time domain methods
- High-frequency methods
- Guided waves
- Solutions to canonical problems
- Propagation and scattering in layered structures
- Random media and rough surfaces
- Metamaterials and complex media
- Beam and pulse propagation and scattering in lossy and/or dispersive media
- Non-linear phenomena
- Antennas: general aspects
- Antenna arrays, planar and conformal
- Numerical methods: general aspects
- Numerical methods for integral and differential

equations

- Hybrid methods
- Interaction of EM waves with biological tissues
- EM theory and applications for radio systems
- Antennas and propagation for communication systems:
- Smart antennas, UWB systems, etc.
- Mathematical modeling of EM problems

Submission and Further Information

The instructions for the submission of papers and the updated information on the Symposium will be available in the Final Call for Papers and on the conference Web site. Copyrights of all accepted papers are to be transferred to the IEICE.

All accepted and presented papers will be available through IEEE Xplore.

URSI Commission B School for Young Scientists

The "URSI Commission B School for Young Scientists" will be organized for the first time at EMTS 2013 in Hiroshima. In this one-day school, a series of lectures will be delivered by leading scientists in the Commission B community and young scientists are encouraged to learn the fundamentals and future directions in the area of electromagnetic theory. Details will be announced later.

Conference Contacts

General questions and technical program:

Chair, Conference and Commission B of URSI
Prof. Giuliano Manara
Department of Information Engineering,
University of Pisa, Italy
E-mail: g.manara@iet.unipi.it

Questions regarding local arrangements:

Co-Chairs, Local Organizing Committee

Prof. Makoto Ando

Dept. of Electrical and Electronics Engineering
Tokyo Institute of Technology, Japan
E-mail: mando@antenna.ee.titech.ac.jp

Prof. Tsuneki Yamasaki

College of Science and Technology
Dept. of Electrical Engineering
Nihon University, Japan
E-mail: yamasaki@ele.cst.nihon-u.ac.jp

EMTS 2013 Japan Secretariat:

c/o DUPLER CORP.
3F Sun-Arch Bldg., 3-1 Nemoto, Matsudo,
Chiba 271-0077, Japan
Tel: +81-47-361-6030, Fax: +81-47-308-5272
E-mail: secretariat@ursi-emts2013.org

URSI Accounts 2011



URSI held its XXXth General Assembly and Scientific Symposium in Istanbul from 13 till 20 August 2011. Such a General Assembly and Scientific Symposium is both from a scientific point of view, as well as from an organizational point of view a major corner stone in the operation of URSI as a worldwide scientific organization. The impact also extends to the budget of URSI as major expenses normally occur in preparation of and during the General Assembly itself. This impact normally leads to a loss in the year a General Assembly is organized, as is the case for 2011. However for 2011, this loss is limited thanks to the efforts of our hosts within the Turkish National Committee and in particular the

General Chair, Prof. Hamit Serbest, who have put a lot of effort in making the event a success.

Thanks to this success and the careful control on administrative expenses, URSI can, despite the economic crisis, continue its initiatives taken over the past few years targeting Young Scientists and young researchers. These initiatives should stimulate them to participate at URSI events through Student Paper Competitions and Young Scientists awards and consequently link them to URSI for their future career.

Prof. Paul Lagasse
Secretary General of URSI

BALANCE SHEET: 31 DECEMBER 2011

	EURO	EURO
ASSETS		
Dollars		
Merrill Lynch WCMA	0.00	
Fortis	6.64	
Smith Barney Shearson	4,783.19	
		4,789.83
Euros		
Banque Degroof	25.38	
Fortis zichtrekening	128,664.53	
Fortis spaarrekening	382,216.38	
		510,906.29
Investments		
Demeter Sicav Shares	22,681.79	
Rorento Units	111,414.88	
Aqua Sicav	63,785.56	
Merrill-Lynch Low Duration (304 units)	0.00	
Massachusetts Investor Fund	252,722.23	
Provision for (not realised) less value	(7,314.98)	
Provision for (not realised) currency differences	(59,747.62)	
	383,541.86	
684 Rorento units on behalf of van der Pol Fund	12,414.34	
		395,956.20
Petty Cash		1.93
Total Assets		911,654.25
Less Creditors		
IUCAF	14,378.84	
ISES	4,454.13	
		(18,832.97)
Balthasar van der Pol Medal Fund		(11,863.96)
NET TOTAL OF URSI ASSETS		<u>880,957.32</u>

The net URSI Assets are represented by:	EURO	EURO
Closure of Secretariat		
Provision for Closure of Secretariat		100,000.00
Scientific Activities Fund		
Scientific Activities in 2012	45,000.00	
Publications/website in 2012	20,000.00	
Young Scientists in 2012	0.00	
Administration Fund in 2012	105,000.00	
I.C.S.U. Dues in 2012	10,000.00	
		180,000.00
XXX General Assembly 2012/2014 Fund:		
During 2009-2010-2011 (GA 2011)		0.00
During 2012-2013-2014 (GA 2014)		0.00
Total allocated URSI Assets		280,000.00
Unallocated Reserve Fund		600,957.32
		<u>880,957.32</u>

Statement of Income and expenditure for the year ended 31 December 2011

I. INCOME

Grant from ICSU Fund and US National Academy of Sciences	0.00	
Allocation from UNESCO to ISCU Grants Programme	0.00	
UNESCO Contracts	0.00	
Contributions from National Members (year -1)	10,149.00	
Contributions from National Members (year)	162,385.00	
Contributions from National Members (year +1)	38,567.00	
Contributions from Other Members	0.00	
Special Contributions	0.00	
Contracts	0.00	
Sales of Publications, Royalties	680.00	
Sales of scientific materials	0.00	
Bank Interest	4,912.33	
Other Income	88,979.47	
Total Income		<u>305,673.07</u>

II. EXPENDITURE

A1) Scientific Activities		197,329.07
General Assembly 2005/2008/2011	188,168.24	
Scientific meetings: symposia/colloquia	9,160.83	
Working groups/Training courses	0.00	
Representation at scientific meetings	0.00	
Data Gather/Processing	0.00	
Research Projects	0.00	
Grants to Individuals/Organisations	0.00	
Other	0.00	
Loss covered by UNESCO Contracts	0.00	
A2) Routine Meetings		13,303.47
Bureau/Executive committee	13,303.47	
Other	0.00	

A3) Publications		13,227.69
B) Other Activities		2,000.00
Contribution to ICSU	0.00	
Contribution to other ICSU bodies	2,000.00	
Activities covered by UNESCO Contracts	0.00	
C) Administrative Expenses		110,668.29
Salaries, Related Charges	83,169.19	
General Office Expenses	3,774.86	
Travel and representation	13,488.40	
Office Equipment	2,742.47	
Accountancy/Audit Fees	5,747.50	
Bank Charges/Taxes	3,062.50	
Loss on Investments (realised/unrealised)	(1,316.63)	
Total Expenditure:		<u>336,528.52</u>

Excess of Expenditure over Income		30,855.45
Currency translation diff. (USD => EURO) - Bank Accounts		12.55
Currency translation diff. (USD => EURO) - Investments		505.83
Currency translation diff. (USD => EURO) - Others		134.92
Accumulated Balance at 1 January 2011		911,159.47
		<u>880,957.32</u>

Rates of exchange		
January 1, 2011	1 \$ = 0.7610 EUR	
December 31, 2011	1 \$ = 0.7630 EUR	

Balthasar van der Pol Fund		
684 Rorento Shares : market value on December 31 (Aquisition Value: USD 12.476,17/EUR 12.414,34)		33,789.60
Book Value on December 31, 2011/2010/2009/2008		12,414.34
Market Value of investments on December 31, 2011-2008		
Demeter Sicav		70,679.40
Rorento Units (1)		642,200.00
Aqua-Sicav		89,696.64
M-L Low Duration		0.00
Massachusetts Investor Fund		185,659.63
		988,235.67
Book Value on December 31, 2011/2010/2009/2008		395,956.20

(1) Including the 684 Rorento Shares of v d Pol Fund

APPENDIX : Detail of Income and Expenditure

I. INCOME

Other Income		
Income General Assembly 2008	0.00	
Income General Assembly 2011	88,234.00	
Young scientist support (Japan)	0.00	
Support Kogamidal	0.00	
Closure Radio Science Press	0.00	
Commission B+C	0.00	
Mass investors growth stock Fund	0.00	
Other	745.74	
		88,979.74

II . EXPENDITURE

General Assembly 2008		
Organisation	0.00	
Vanderpol Medal	0.00	
Young scientists	0.00	
Expenses officials	0.00	
Support Commissions	0.00	
General Assembly 2011		
Organisation	38,181.05	
Vanderpol Medal	0.00	
Young scientists	28,535.00	
Expenses officials	73,681.44	
Support Commissions	47,770.75	
		188,168.24
Symposia/Colloquia/Working Groups		
Commission A	0.00	
Commission B	0.00	
Commission C	0.00	
Commission D	0.00	
Commission E	1,000.00	
Commission F	0.00	
Commission G	2,500.00	
Commission H	1,000.00	
Commission J	981.38	
Commission K	0.00	
Central Fund	2,796.75	
Central Fund (Student Award MC)	882.70	
		9,160.83
Contribution to other ICSU bodies		
FAGS	0.00	
IUCAF	2,000.00	
		2,000.00
Publications		
Printing 'The Radio Science Bulletin'	5,671.46	
Mailing 'The Radio Science Bulletin'	7,556.23	
		13,227.69



1. Introduction

The Scientific Committee on Frequency Allocations for Radio Astronomy and Space Science, IUCAF, was formed in 1960 by its sponsoring Scientific Unions, URSI, the IAU, and COSPAR. Its brief is to study and coordinate the requirements of radio frequency allocations for passive (i.e., non-emitting or receive-only) radio sciences, such as radio astronomy, space research and remote sensing, in order to make these requirements known to the national administrations and international bodies that allocate frequencies. IUCAF operates as a standing inter-disciplinary committee under the auspices of ICSU, the International Council for Science. IUCAF is a Sector Member of the International Telecommunication Union (ITU).

2. Membership

At the end of 2011 the membership for IUCAF was:

URSI	S. Ananthkrishnan (Com J)	India
	S. Reising (Com F)	USA
	I. Häggström (Com G)	Sweden
	A. Tzioumis (Com J)	Australia
	W. van Driel (Com J)	France
IAU	H. Chung	rep. of Korea
	H.S. Liszt (Vice Chair)	USA
	M. Ohishi (Chair)	Japan
	K.F. Tapping	Canada
	A. Tiplady	South Africa
COSPAR	Y. Murata	Japan
		the
at large:	W.A. Baan	Netherlands
	D.T. Emerson	USA

IUCAF also has a group of correspondents, in order to improve its global geographic representation and for issues on spectrum regulation concerning astronomical observations in the optical and infrared domains. It is noted that K.F. Tapping (Canada) has already retired, and his successor needs to be appointed.

3. International Meetings

During the period of January to December 2011, its members and correspondents represented IUCAF in the following international meetings:

February	Conference Preparatory Meeting towards the WRC2012	Geneva, Switzerland
May-June	ITU-R Working Party 1A (Spectrum Engineering Techniques)	Geneva, Switzerland

June	Space Frequency Coordination Group meeting (SFCG-31)	San Francisco, USA
August	URSI General Assembly and Scientific Symposium	Istanbul, Turkey
September	ITU-R Study Group 7 (Science services) and Working Party 7D (Radio Astronomy)	Geneva, Switzerland

Additionally, IUCAF members and correspondents participated in numerous national or regional meetings (including CORF, CRAF, RAFCAP, the FCC etc.), dealing with spectrum management issues, such as the preparation of input documents to various ITU meetings.

IUCAF member A. Tzioumis, is the chairman of ITU-R Working Party 7D (radio astronomy) and IUCAF member H. Chung, is the vice-chairman of ITU-R Study Group 7 (Science Services). IUCAF member, S. Ananthkrishnan, is president of URSI Commission J (radio astronomy).

4. IUCAF Business Meetings

During 2011 IUCAF had face-to-face committee meetings. Before and during the WP7D meeting IUCAF ad-hoc meetings were held to discuss further its meeting strategy. In the business meeting during the URSI GASS, financial issues, recruitment of new members, initiatives and future contributions to international spectrum management meetings and so on were discussed.

Although such face-to-face meetings have been convenient and effective, throughout the year much IUCAF business is undertaken via e-mail communications between the members and correspondents.

5. Protecting The Passive Radio Science Services

At the ITU, the work in the various Working Parties of interest to IUCAF was focused on the relevant agenda items that were adopted in 2007 for WRC-12 of ITU, the World Radiocommunication Conference in 2012, as well as on creation and maintenance of various ITU-R Recommendations and ITU-R Reports. Although the WRC2012 was held between January and February, 2012, it is worthy to mention in this activity report results of this important meeting for the passive radio services.

The frequency range between 275 and 3000 GHz is used by the radio astronomy observations of important spectral lines and continuum bands which assist in the study and understanding of the Universe. This frequency range is

also of interest by the Earth science community by means of passive satellite observations.

New receiver technology and new instruments (both ground-based and space-based) being used in the 275-1000 GHz region are helping to refine the results of radio astronomy observations in this spectrum range, while similar developments in the 1 000-3 000 GHz range are leading to a better understanding of specific spectral lines and specific atmospheric windows that are of interest to radio astronomers. Significant infrastructure investments are being made under international collaboration for the use of these bands between 275 and 3 000 GHz. The Atacama Large Millimeter/submillimeter Array (ALMA), an international facility located in northern Chile, started its first operation period in 2011, which is expected to provide new insights on the structure of the Universe through observations in the 30-1000 GHz range. Space-based highly sensitive telescopes observe spectral lines from a variety of molecules and atoms and continuum thermal radiation from very small particles (cosmic dust).

Although no frequency allocations have been made above 275 GHz, the radio astronomy community and the Earth science community have identified a list of specific bands of interest which need to be protected by each government. Thus a WRC-12 agenda item to review the use of the radio spectrum between 275 and 3000 GHz was most relevant to the passive radio science concerns. Fortunately a preliminary agreement was made towards updating a footnote (5.565) in the Radio Regulations of the ITU during the Conference Preparatory Meeting held in February, 2011. The preliminary agreement was confirmed at the WRC 2012, resulting in better protection of passive radio sciences between 275 and 3000 GHz. The new regulatory measure will be in effect in 2013.

Power Line Communications utilizing the High Frequency range (2-30 MHz) is a technology to send electrical signals through the power lines for communication purposes. This technology aims to enable broadband Internet access and the home LAN by means of the “existing” power lines. Since the power lines are designed and installed to carry current at 50/60Hz only, there has been a serious concern that the electromagnetic field radiated from the power lines may cause harmful interferences to the radio communication services such as broadcasting, communication, and radio astronomy observations. In this regard IUCAF members participated in the ITU-R Working Party 1A (Spectrum Engineering Techniques), and submitted several contribution papers regarding radiation mechanisms from power lines. These study results were welcomed by the ITU-R Working Party 1A, and were adopted as a part of ITU-R Report SM.2158-2 (Impact of power line telecommunication systems on radiocommunication systems operating in the LF, MF, HF and VHF bands below 80 MHz) and ITU-R Report SM.2212 (Impact of power line telecommunication systems on radiocommunication systems operating in the VHF and UHF bands above 80 MHz).

At the Space Frequency Coordination Group (SFCG) meeting in San Francisco in June 2011, details were finalized to implement a set of web-based resources that will allow better coordination of radio astronomy observations with orbiting high-power earth-sensing and cloud-sensing radars; broadcasts from these radars could have seriously deleterious effects on radio astronomy receivers during main-beam encounters. These new resources are the result of a several year-long cooperative effort between IUCAF and SFCG.

6. Contact with the Sponsoring Unions And ICSU

IUCAF maintains regular contact with its supporting Scientific Unions and with ICSU. The Unions play a strong supporting role for IUCAF and the membership is greatly encouraged by their support.

IUCAF continued its activities towards strengthening its links with other passive radio science communities, in particular in space science, and defining a concerted strategy in common spectrum management issues.

During its GASS 2011 in Istanbul, URSI held a lunch time session, “Special Meeting on URSI-ITU relations”. The session aimed to enhancing the relationship between URSI and the ITU since there are many radio science experts within URSI, whose participation in ITU activities would be beneficial for both organizations. The IUCAF chairman was invited to the special session, and gave a talk titled “IUCAF and its activities within ITU-R”; since IUCAF has long experience in the ITU, the IUCAF chairman summarized the ITU structure, working procedures, how to submit technical information, study results, views from URSI. Since introduction of new radio technologies developed by URSI experts may lead to new RFI problems, it was mentioned that advanced coordination within URSI would be needed before problems really show up and tough coordination takes place in the ITU.

The IUCAF chair, M. Ohishi, is the president of IAU Commission 5 on Documentation and Astronomical Data. IUCAF member, W. van Driel, is the president of IAU Commission 50. Two IUCAF members, A. Tzioumis and M. Ohishi, worked as the Organising Committee members of IAU Commission 50. IUCAF member, W.A. Baan is the chair of the IAU Working Group on RFI mitigation. M. Ohishi chairs the Working Group on Astrophysically Important Spectral Lines of Division X, IAU. He is also appointed as the official liaison between the IAU and the ITU.

The preparation towards the next IAU General Assembly in 2012 is ongoing. IUCAF will hold a business session during the IAU GA. Many IUCAF members have already submitted papers to be presented at this GA.

The 39th scientific assembly of the COSPAR will be held in July, 2012, in Mysore, India. Some IUCAF members plan to attend this COSPAR meeting.

7. Publications and Reports

IUCAF has a permanent web address, <http://www.iucaf.org>, where the latest updates on the organization's activities are made available. All contributions to IUCAF-sponsored meetings are made available on this website.

8. Conclusion

IUCAF interests and activities range from preserving what has been achieved through regulatory measures or mitigation techniques, to looking far into the future of high frequency use, giant radio telescope use and use by large-scale distributed radio telescopes. Current priorities, which will certainly keep us busy through the next years, include study of the effects of automotive collision avoidance radars at around 79 GHz region (a new agenda item for WRC 2015) and study of high-frequency power line communications (HF-PLC). As well IUCAF is contributing to studies off

conditions that will allow the successful operation of future giant radio telescopes.

IUCAF plans to hold the 4th Summer School on Spectrum Management in 2013 or 2014; its possible venue is Santiago, Chile. If this summer school is actually held in Chile, it would be a very good opportunity for radio scientists in South America to learn how to protect the radio quiet environment that is needed for passive radio science services.

IUCAF is grateful for the moral and financial support that has been given for these continuing efforts by ICSU, COSPAR, the IAU, and URSI during recent years. IUCAF also recognizes the support given by radio astronomy observatories, universities and national funding agencies to individual members in order to participate in the work of IUCAF.

Masatoshi Ohishi, IUCAF Chair
IUCAF website : <http://www.iucaf.org>
IUCAF contact : iucafchair@iucaf.org

Energy Patterns of Pulsed Antennas Illustrated with a Reflector Type of an Impulse-Radiating Antenna (IRA)



D.V. Giri
F.M. Tesche

Abstract

A question that often comes up in the context of an IRA is, “How is the transient energy from the pulser radiated in space”? Of course, the electromagnetic fields (both E and H), the power density, and the energy density have their maxima on the boresight. The power pattern is a well-defined frequency-domain concept, but it is a cumbersome descriptor for hyperband antennas such as an IRA because of the multitude of frequencies involved. In this note, we explore the concept of an energy pattern that holds good both in the time and frequency domains. An energy pattern is useful in visualizing where the transient energy provided to the IRA is going. It is further noted that the energy and power patterns are identical for a CW antenna, while they can be vastly different for pulsed antennas.

1. Introduction

An easy way to remember the performance parameters of an antenna is through an acronym, “BRIDGE.” The individual letters denote:

- Beamwidth
- Radiation pattern
- Input impedance
- Directivity
- Gain
- Effective area

All of these parameters are well defined in the frequency domain, and are functions of frequency. In the context of pulsed antennas, where many frequencies are

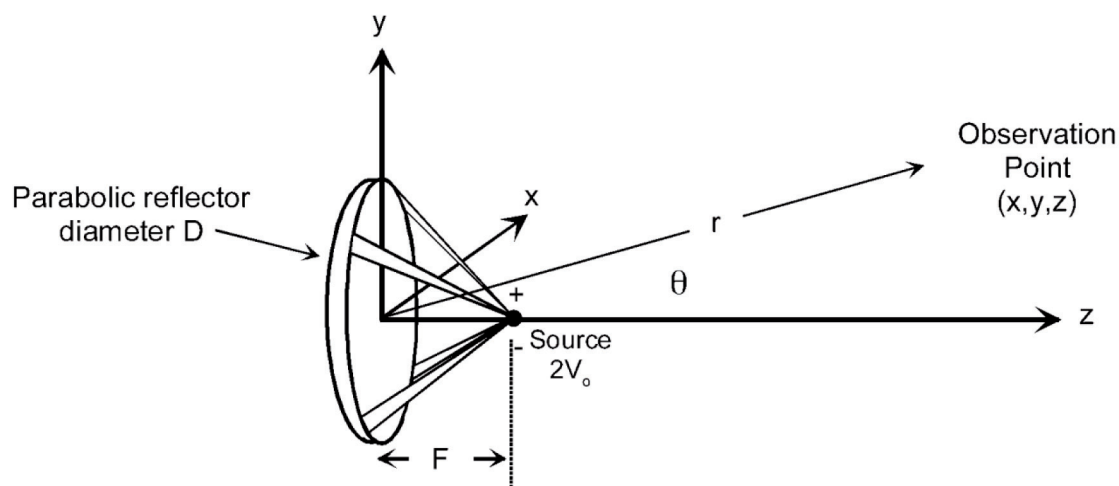


Figure 1. The IRA geometry and coordinate system.

D. V. Giri is with Pro-Tech, 11-C Orchard Court, Alamo, CA 94507-1541; and the Department of Electrical & Computer Engineering, University of New Mexico, Albuquerque, NM 87131, USA; e-mail: Giri@DVGiri.com. F. M. Tesche is with EMConsultant, 1519 Miller Mountain Road, Saluda, NC 28773; and the Holcombe Department of Electrical and Computer Engineering, College of Engineering & Science, 337 Fluor Daniel Building, Box 340915, Clemson, SC 29634-0915, USA; e-mail: Fred@Tesche.com.

simultaneously fed into the antenna, the use of frequency-dependent parameters is useful, but cumbersome.

Let us consider a reflector type of an IRA as an example of a hyperband [1] antenna [2-4]. The radiation pattern of an IRA is a strong function of frequency, as was reported in [5]. The lower frequencies of the input pulse have lower gain and large beamwidths, while the higher frequencies have a higher gain and smaller beamwidths. In the next section, we consider an *energy pattern* of the IRA, which is a simple and unique descriptor. It is indicative of how the input energy is radiated into all of space.

2. Energy Pattern

Let us denote the energy pattern of the IRA by $U(\theta, \phi)$ in the far field or Fraunhofer zone. This quantity is measured in Joules/steradians. Figure 1 shows the geometry, and the Cartesian and spherical sets of coordinates with the origin at the center of the radiating aperture. The diameter and the focal length of the reflector are denoted by D and F . The Fraunhofer zone is known to begin at an axial distance given by [6]

$$r_{far} = \frac{D^2}{2c\tau_{mr}}, \quad (1)$$

where c is the speed of light and τ_{mr} is the maximum rate of rise of the voltage wave launched onto the reflector, which is not necessarily the rate of rise of the transient source's waveform.

Let $\bar{E}_f(R, \theta, \phi, t)$ and $\bar{E}(R, \theta, \phi, \omega)$ denote the far electric field at an arbitrary location in the time and frequency domains, respectively. The energy pattern can be defined as

$$U(\theta, \phi) = \frac{1}{Z_0} \int |\bar{E}_f(r, \theta, \phi, t)|^2 r^2 dt \quad (2)$$

$$= \frac{1}{2\pi Z_0} \int |\bar{E}(r, \theta, \phi)|^2 r^2 d\omega$$

[Joules/steradian].

Note that Equation (2) represents an energy density, and not the total radiated energy. In Equation (2), Z_0 is the characteristic impedance of free space, and the value of r needs to be in the far field, satisfying Equation (1). It is noted that energy content of a signal is the same whether one computes it in the time domain or the frequency domain, as per Parseval's Theorem [7]. It is also observed while the

electromagnetic fields depend on the radial distance, r , the energy pattern in the far field is independent of r , simply because the electric field falls off like r . We can rewrite Equation (2) in shorthand notation as

$$U = \int_0^\infty r^2 \frac{[\bar{E}(t)]^2}{Z_0} dt \quad \text{[Joules/steradian]}. \quad (3)$$

In Equation (3), $\bar{E}(t)$ denotes the total electric field or the vector sum of all nonzero components. At an arbitrary point (r, θ, ϕ) in the far field, the electric field has a vanishing radial field, and there are only θ and ϕ components. The usual relationships between the rectangular and spherical components are applicable here, if one chooses to compute the Cartesian components of the electric field:

$$E_r = 0,$$

$$E_\theta = E_x \cos(\theta) \cos(\phi) + E_y \cos(\theta) \sin(\phi) - E_z \sin(\theta),$$

$$E_\phi = -E_x \sin(\phi) + E_y \cos(\phi), \quad (4)$$

$$E_x = E_\theta \cos(\theta) \cos(\phi) - E_\phi \sin(\phi),$$

$$E_y = E_\theta \cos(\theta) \sin(\phi) + E_\phi \cos(\phi),$$

$$E_z = -E_\theta \sin(\theta).$$

The square of the magnitude of the total electric field in the time domain is given by

$$|\bar{E}(r, \theta, \phi, t)|^2 = [E_\theta^2 + E_\phi^2] \quad (5)$$

$$= [E_x^2 + E_y^2 + E_z^2].$$

Of course, in practice, the integration in Equation (3) is carried out over time-limited or band-limited ranges.

3. Estimation of Far Fields by Aperture-Integration Method

The electric field at any arbitrary observation point in the far field can be estimated by the method of aperture

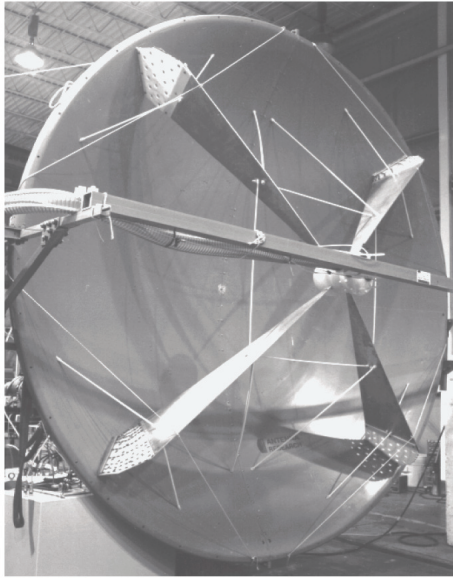


Figure 2. A photograph of the prototype IRA.

integration, which takes into account the presence of the feed arms. Initially, the field on the aperture plane is computed. The radiated field can then be computed by an integration of the magnetic current (tangential electric field) on the aperture. The relevant equations are given below [8], with reference to Figure 1.

The magnetic current on the aperture is given by

$$\vec{M} = -2\vec{I}_z \times \vec{E}_{aperture}, \quad (6)$$

and the electric-field components in terms of the magnetic current on the aperture are given by

$$E_x = \frac{1}{4\pi} \iint (z-z') M_y \frac{1+jkr}{r^3} e^{-jkr} dx' dy',$$

$$E_y = \frac{1}{4\pi} \iint (z-z') M_x \frac{1+jkr}{r^3} e^{-jkr} dx' dy', \quad (7)$$

$$E_z =$$

$$\frac{1}{4\pi} \iint [(y-y') M_x - (x-x') M_y] \frac{1+jkr}{r^3} e^{-jkr} dx' dy'.$$

From the estimation of all components of the electric field in frequency domain, the total transient electric field is found by Fourier inversion, and then used in Equation (3) to get the energy pattern.

Some comments about the aperture-integration method outlined above are in order.

The aperture-integration method for a hole in an

Parameter	Value
Reflector diameter, D	3.66 m
Focal length, F	1.22 m
F/D	0.33
Number of arms	4
Arm configuration	90°
Impedance, Z_{in}	200 ohms
Geometrical factor $f_g = Z_{in}/Z_0$	0.53
Polarization	Linear/Vertical

Table 1a. The details of the antenna parameters of the prototype IRA

Parameter	Value
Peak voltage, V_p	$\sim \pm 60 \text{ kV} \sim 120 \text{ kV}$
Peak rate of rise, $\left(\frac{dV}{dt}\right)_p$	$\sim 1.2 \times 10^{15} \text{ V/s}$
Maximum rate of rise, $t_{mr} = \frac{V_p}{\left(\frac{dV}{dt}\right)_p}$	$\sim 100 \text{ ps}$
Pulse repetition frequency (PRF)	$\sim 200 \text{ Hz}$
Pulse decay time, t_d	$\sim 20 \text{ ns}$
Duty cycle, $\tau = t_d \text{ PRF}$	$\sim 4 \times 10^{-6}$
Peak power, $P_{in} = \frac{V_p^2}{Z_{in}}$	$\sim 72 \text{ MW}$
Average power	$\sim 72 \times 4 \times 10^{-6} \sim 288 \text{ W}$

Table 1b. The details of the pulser parameters of the prototype IRA.

infinite screen is quite accurate in the direction of the main beam, but the accuracy deteriorates as the angle θ increases. This is due to the various approximations used to obtain an analytical solution to this problem. In the EM model used here for the dish, the tangential E and H fields are normally needed over the aperture, and are assumed to be zero elsewhere on the aperture plane away from the dish. However, we use only the tangential E-field distribution, and assume the corresponding TEM value for the tangential H field (and this results in an equivalent magnetic current of $M = 2E_a$ over the aperture).

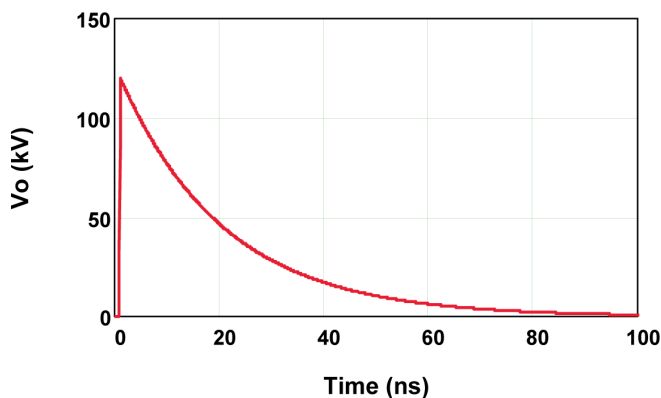


Figure 3. A plot of the excitation waveform $V_0(t)$.

For this idealized aperture source, the radiated field in the E plane when $\theta = \pm 90^\circ$ is zero, due to geometrical projection reasons. In the H plane, the radiated field does not vanish for $\theta = \pm 90^\circ$, because the equivalent source is radiating in free space, and this observation point is broadside to the magnetic-current source. If there were an infinite, perfectly conducting plate in the plane of the aperture, there the field in the H plane would go to zero at $\pm 90^\circ$ due to the boundary condition of $E_{tan} = 0$ on the screen. We also observe that the aperture-integration model will not give good results on the back side of the aperture plane. In fact, the radiation pattern from the equivalent sources is the same in the back as in the front.

In summary, the aperture-integration model gives good responses in the forward direction, but not in the backward direction. The numerical errors also increase as the observation point approaches the plane of the aperture.

4. Energy Pattern of the Prototype IRA

In this section, we consider the prototype IRA and evaluate its energy pattern. A photograph of this prototype IRA is shown in Figure 2.

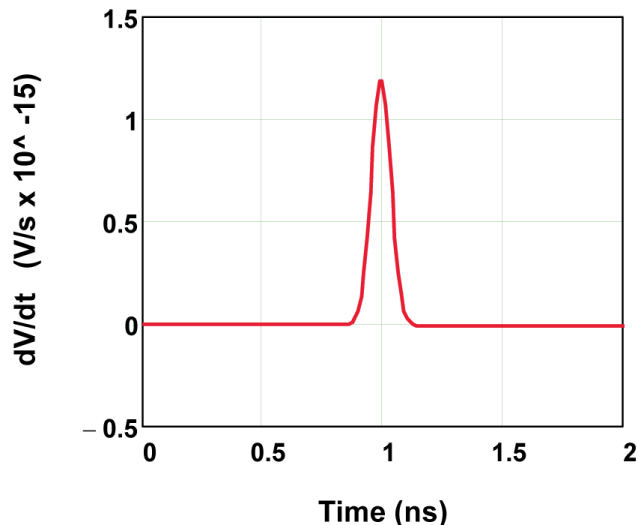


Figure 4. A plot of the time rate of change of the excitation waveform $dV_0(t)/dt$.

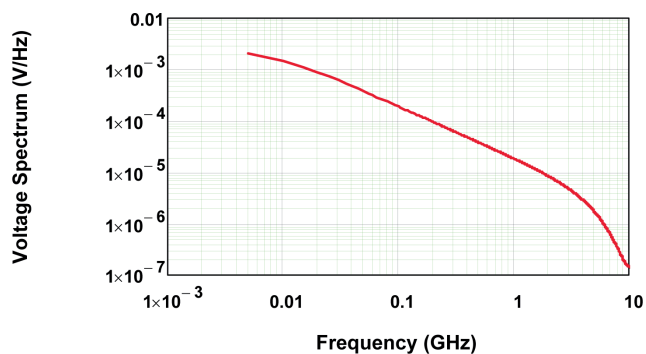


Figure 5. A plot of the spectral magnitude of the excitation waveform.

The parameters of the prototype IRA are summarized in Table 1, where we have separately listed the geometry of the reflector and the pulser parameters. Having outlined the salient features of the prototype IRA, we now proceed to compute the radiated fields and the energy patterns.

The excitation voltage of the IRA is the total plate voltage situated at the focal point of the dish, and is denoted as $V_0(t)$. As outlined in [6], one possible representation of a fast pulse is given by the expression

$$V_0(t) = V_{peak} (1 + \Gamma) e^{-\beta \left(\frac{t-t_s}{t_r} \right)} \left\{ 0.5 \operatorname{erfc} \left(-\sqrt{\pi} \frac{t-t_s}{t_r} \right) u[-(t-t_s)] + \left[1 - 0.5 \operatorname{erfc} \left(\sqrt{\pi} \frac{t-t_s}{t_r} \right) \right] u(t-t_s) \right\}. \quad (8)$$

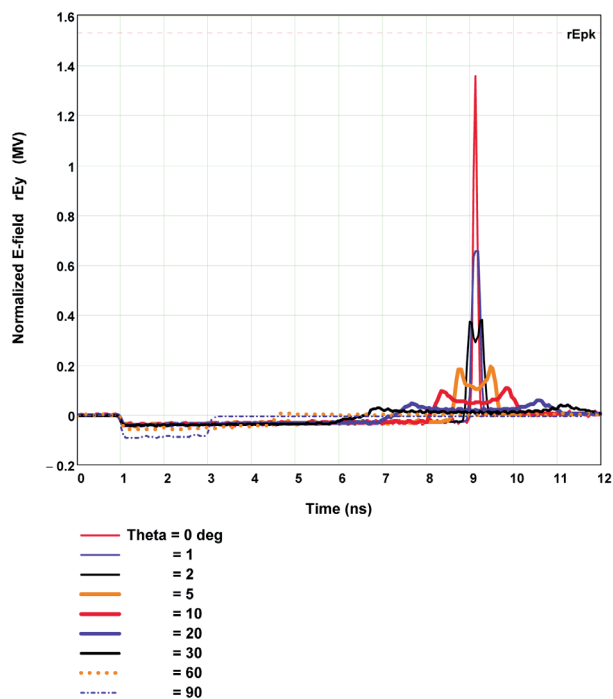


Figure 6. An overlay of the principal (E_y) field components for various values of the angle θ , computed in the horizontal plane (the H plane) in the far zone of the IRA (for a 120 kV/100 ps/20 ns pulse excitation).

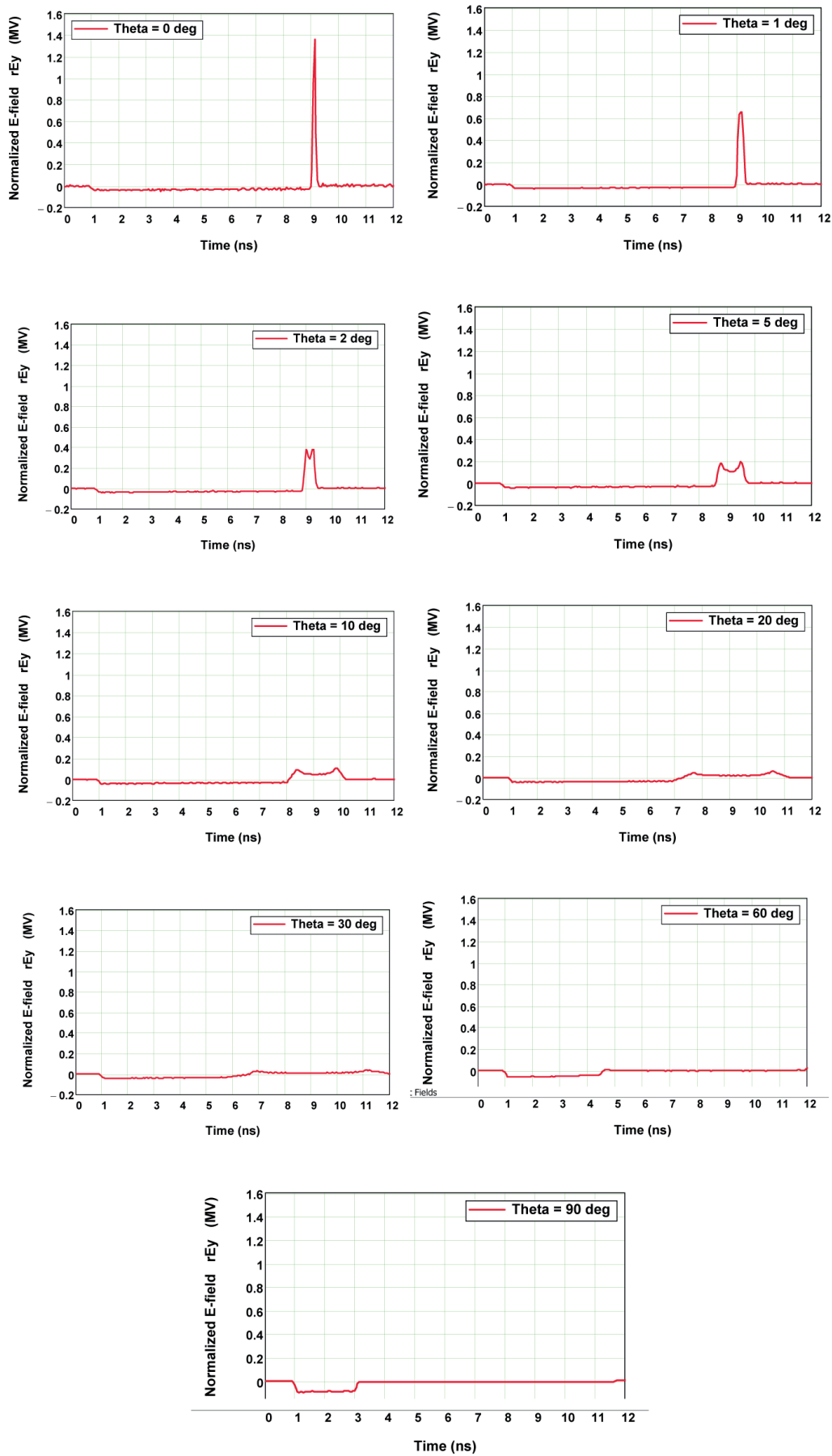


Figure 7. An illustration of the individual principal (E_y) field components in the horizontal plane (the H plane) in the far zone of the IRA (for 120 kV/100 ps/ 20 ns pulse excitation).

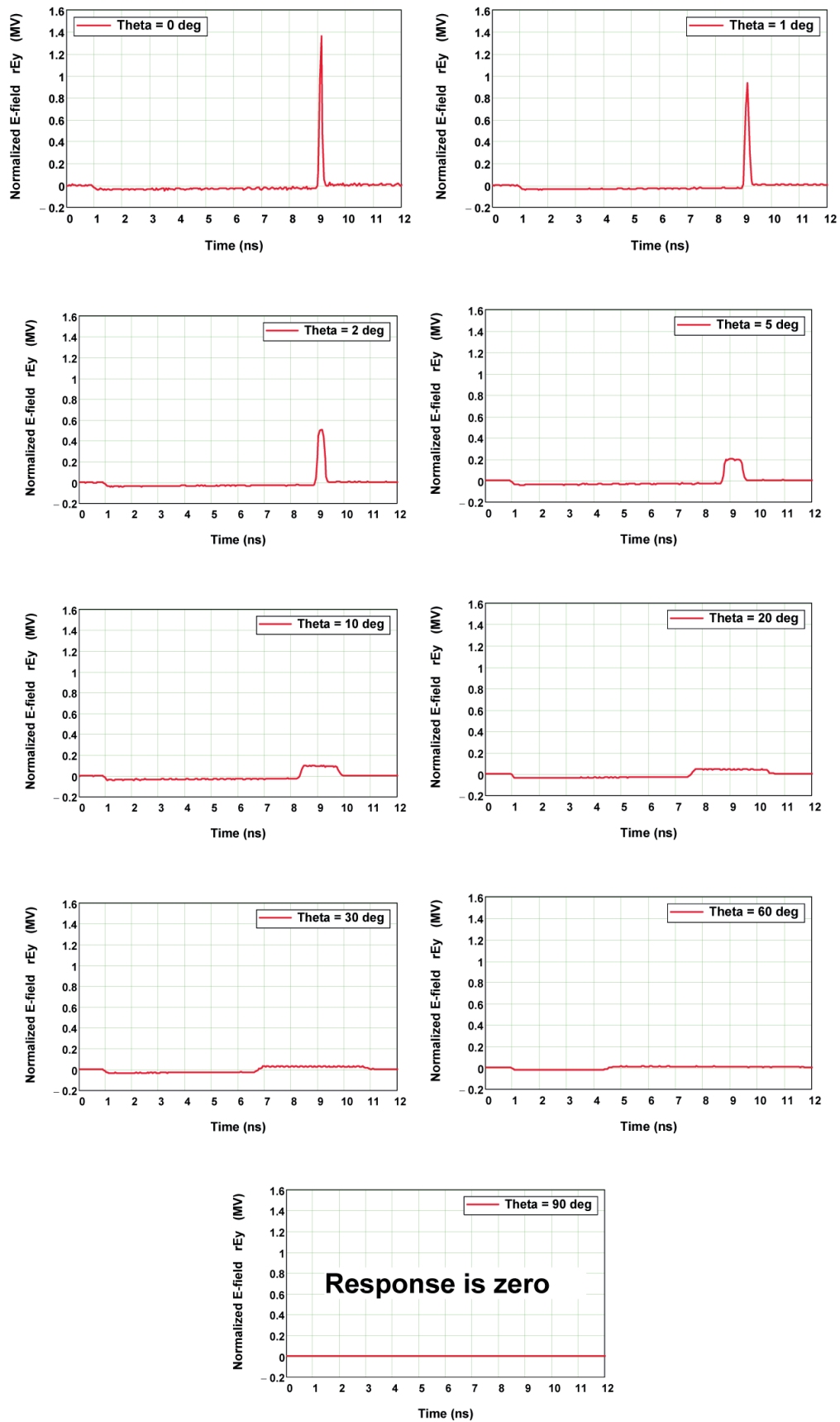


Figure 9. An illustration of the individual principal (E_y) field components in the vertical plane (the E plane) in the far zone of the IRA (for 120 kV/100 ps/ 20 ns pulse excitation).

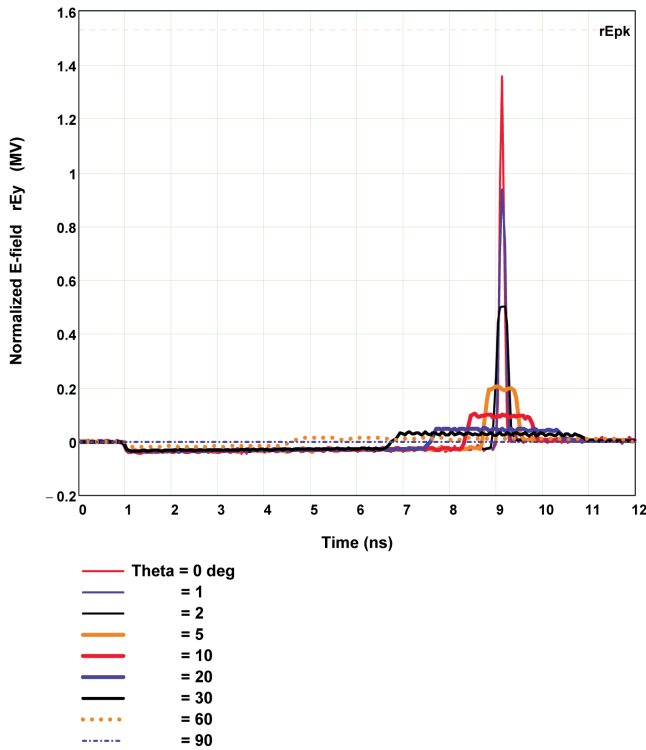


Figure 8. An overlay of the principal (E_y) field components for various values of the angle θ , computed in the vertical plane (the E plane) in the far zone of the IRA (for 120 kV/100 ps/20 ns pulse excitation).

In Equation (8), the term $\text{erfc}(\cdot)$ denotes the complementary error function, and $u(\cdot)$ is the unit step (Heaviside) function. For the calculations here, the following parameters were used:

- $V_{peak} = 120$ kV (peak value of the transient waveform)
- $\Gamma = 0.006$ (amplitude adjustment factor)
- $\beta = 0.005$ (fall-time coefficient)
= risetime/fall time = 100 ps/20 ns
- $\tau_r = 100$ ps (waveform risetime)
- $\tau_s = 1.0$ ns (time shift)

Figure 3 presents the waveform $V_0(t)$ for late and early times, respectively, and Figure 4 illustrates the time derivative $dV_0(t)/dt$ of the waveform. The spectral magnitude of the waveform is provided in Figure 5.

The calculation of the radiated far-field response of this antenna was done using an aperture-integration method, which was described in [9]. The TEM field illuminating the dish was approximated, and this formed the aperture field over the dish that was integrated to yield the impulse portion of the response. In addition, the radiation from the feed-line currents and the source itself was determined, and this provided the pre-pulse contribution to the field.

Overlay plots of the principal components of the transient E fields for this antenna are presented in Figure 6 for the H plane and in Figure 8 for the E plane. Individual plots

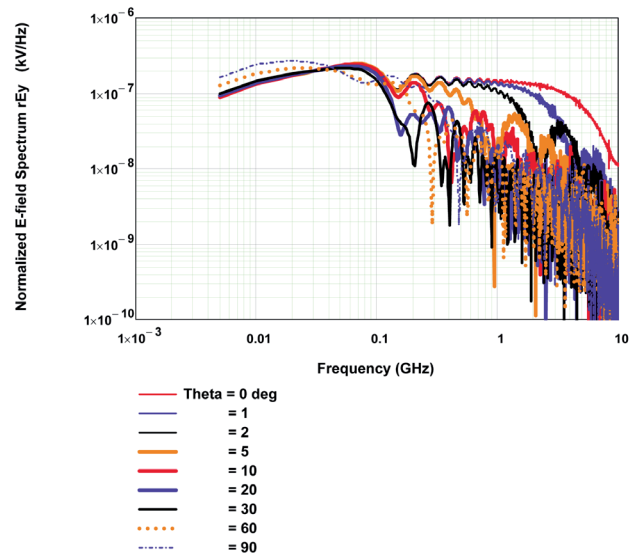


Figure 10. A plot of the spectral magnitudes of the principal (E_y) field components computed in the horizontal plane (the H plane) in the far zone of the IRA (for 120 kV/100 ps/20 ns pulse excitation).

of these transient waveforms for each angle of observation are plotted on the same scale in Figure 7 and Figure 9 for the H and E planes, respectively.

As a check of these results, Giri [6] provided the following estimation of the peak value of the impulse portion of the normalized radiated E field on-axis ($\theta, \phi = (0^\circ, 0^\circ)$)

$$rE_{peak} \approx \frac{D}{4\pi c f_g} \left. \frac{\partial V_0}{\partial t} \right|_{peak} \sqrt{2} \text{ [V]}. \quad (9)$$

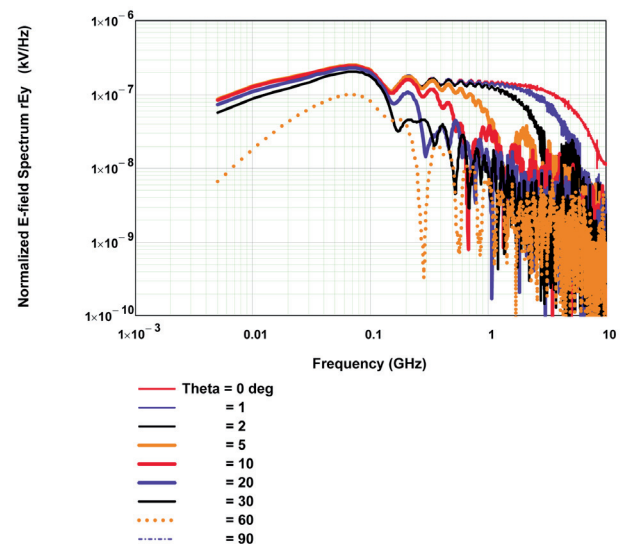


Figure 11. A plot of the spectral magnitudes of the principal (E_y) field components computed in the vertical plane (the E plane) in the far zone of the IRA (for 120 kV/100 ps/20 ns pulse excitation).

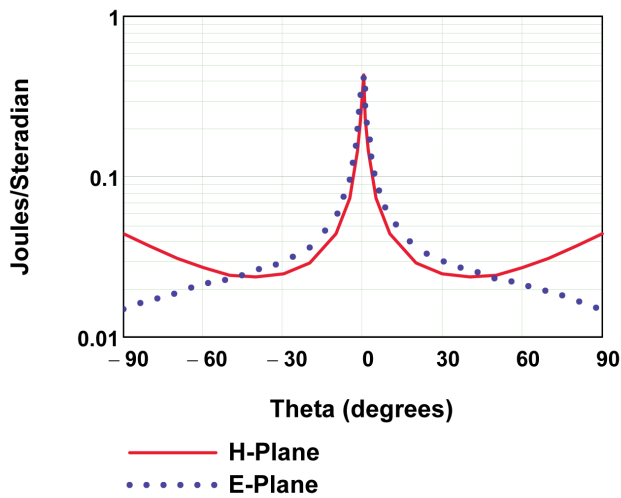


Figure 12. A plot of the radiated-energy pattern in the horizontal (H) and vertical (E) planes for the IRA with the voltage excitation of Figure 3 (the ordinate is a logarithmic scale).

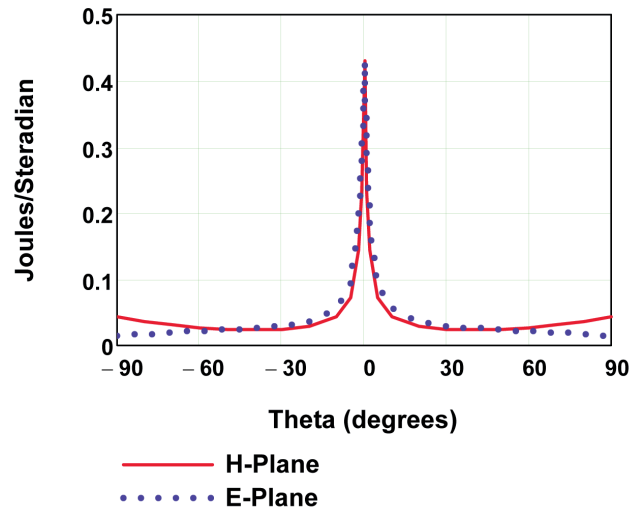


Figure 13. A plot of the radiated-energy pattern in the horizontal (H) and vertical (E) planes for the IRA with the voltage excitation of Figure 3 (the ordinate is a linear scale).

In this expression, $\partial V_0 / \partial t|_{peak} \approx 1.184 \times 10^{15}$ V/sec from Figure 4, and $f_g = 1.06$. This provided an estimate of $rE_{peak} \approx 1.534$ MV, which is shown in the figures and agreed well with the present aperture-integration calculations.

In these responses, it should be noted that the large impulse-like response occurred only in the boresight direction. It occurred in a very narrow beam around $(\theta, \phi) = (0^\circ, 0^\circ)$, and even at a value of $\theta = 1^\circ$ there was a substantial reduction of the peak. Moreover, the waveforms became more dispersed in time as the angle θ increased. It was also noted that the waveforms in the H plane and in the E plane were different.

Although the E_x and E_z field components are not plotted here, it suffices to note that they were both either zero or negligible compared with the principal E_y component.

The spectral responses of the E_y field components in the H plane and the E plane were also of interest. These are plotted as overlay plots for different values of the observation angle θ in Figures 10 and 11, respectively.

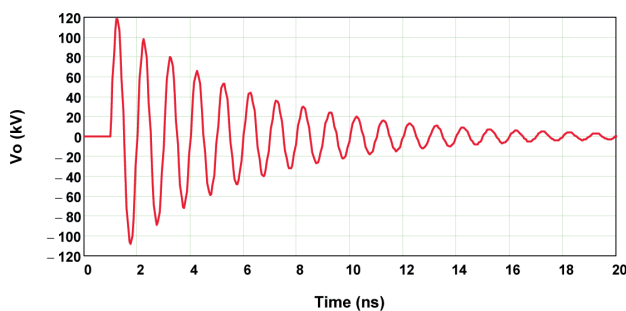


Figure 14. A plot of the excitation waveform $V_0(t)$.

For the driving waveform of Figure 3 into an impedance of 200 ohms (the net IRA impedance), the total energy delivered to the antenna could be estimated to be

$$U_{in} = \frac{1}{200} \int_0^{\infty} V_0^2(t) dt \quad (10)$$

$$\approx \frac{\Delta t}{200} \sum_{k=0}^{N-1} (V_{0k}^2) = 0.727 \text{ Joules}$$

Of interest is the spatial distribution density (in Joules/steradian) of the radiated energy from the IRA. Equation (3) was evaluated in both of the observation planes, and the results are presented in Figures 12 and 13 for different scales for the y axis. In this calculation, all vector components of the calculated E field were used, even though the x and y components were very small.

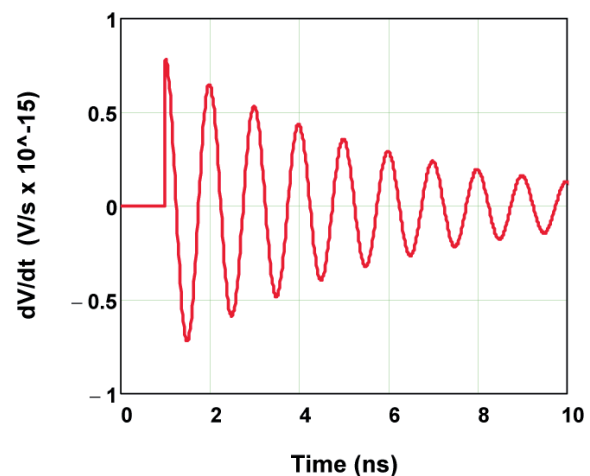


Figure 15. A plot of the time rate of change of the excitation waveform $dV_0(t)/dt$.

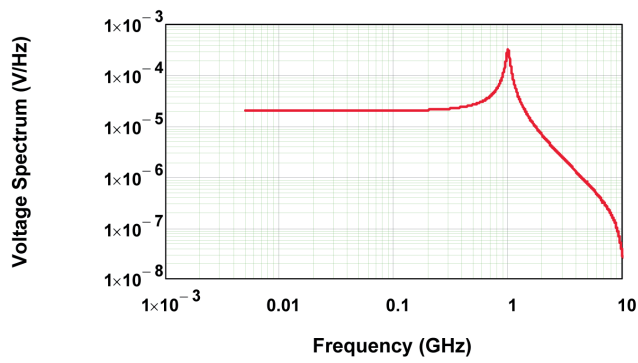


Figure 16. A plot of the spectral magnitude of the excitation waveform.

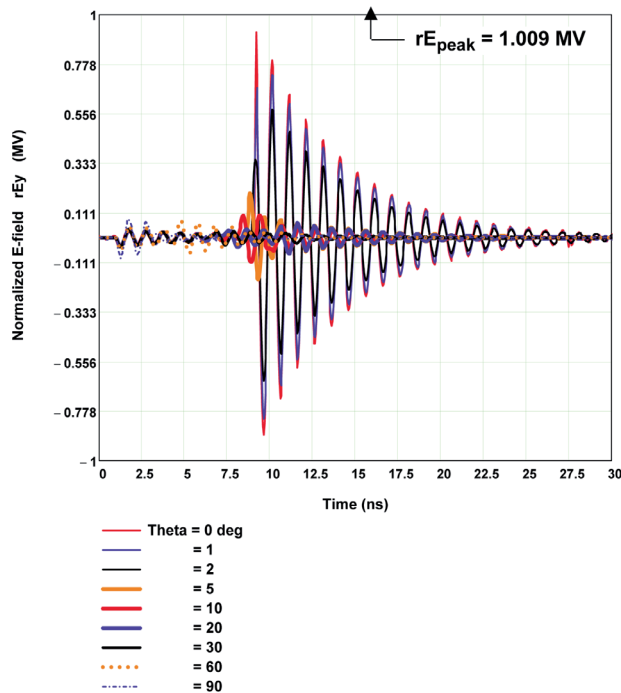


Figure 17. An illustration of the principal (E_y) field component computed in the horizontal plane (the H plane) in the far zone of the IRA (for 120 kV/1 GHz damped-sinusoidal-pulse excitation).

It was clear that the IRA sends more energy in the boresight direction. It is important to note that this radiated energy pattern will be different for other excitation sources, because it depends on the frequency content of the excitation voltage.

5. Calculations for the Prototype IRA with a Damped Sine Wave Excitation

Because the radiated energy pattern depends on the waveform exciting the IRA, it is interesting to consider an alternate excitation function. In this section, we examine a damped sine waveform with a center frequency of $f_0 = 1$

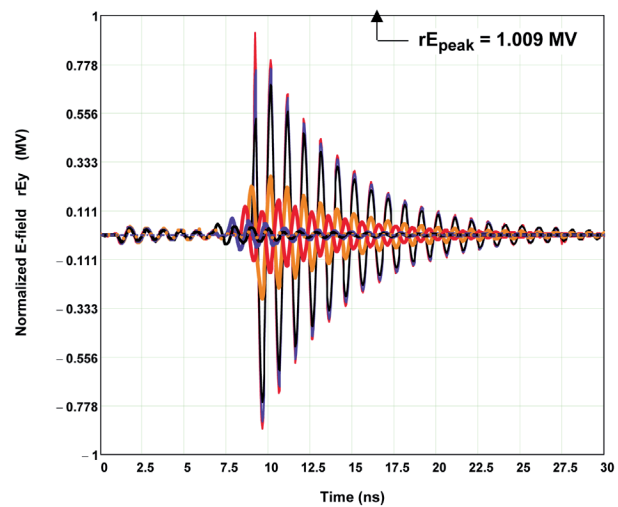


Figure 18. An illustration of the principal (E_y) field component computed in the vertical plane (the E plane) in the far zone of the IRA (for 120 kV/1 GHz damped-sinusoidal-pulse excitation)

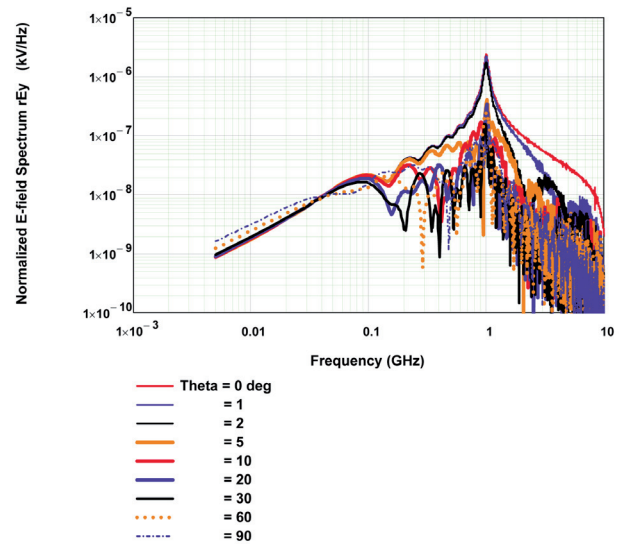


Figure 19. A plot of the spectral magnitudes of the principal (E_y) field component computed in the horizontal plane (the H plane) in the far zone of the IRA (for 120 kV/1 GHz damped-sinusoidal-pulse excitation).

GHz, and an exponential damping constant of $\alpha = 2 \times 10^8 \text{ sec}^{-1}$. The peak amplitude of this waveform was adjusted to provide the same value as the previous pulse waveform, namely $V_{max} = 120 \text{ kV}$. Figure 14 illustrates this waveform, and its derivative is shown in Figure 15. The spectral magnitude is provided in Figure 16. For this waveform, the resulting transient responses in the H and E planes are shown in Figures 17 and 18, and the spectral

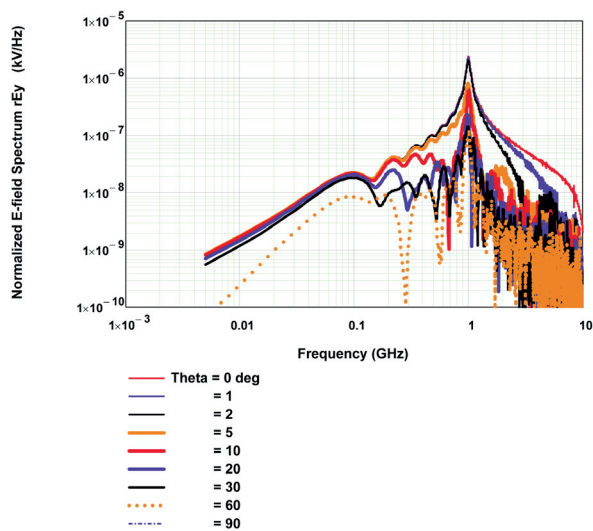


Figure 20. A plot of the spectral magnitudes of the principal (E_y) field component computed in the vertical plane (the E plane) in the far zone of the IRA (for 120 kV/1 GHz damped-sinusoidal-pulse excitation).

responses are in Figures 19 and 20. It was clear that the responses for this excitation were considerably different from those of the fast pulse.

Note that the estimated peak value of $rE_{peak} = 1.009$ MV from Equation (9) agreed well with the computed results. It was also worth noting that the low-amplitude early-time ringing in the waveforms of Figures 17 and 18 was not an FFT problem, but rather this was the pre-pulse response from the IRA.

Figures 21 and 22 present the radiated energy pattern for this damped-sine excitation. It was noted that there was more energy radiated in the main beam for this excitation than for the fast pulse. In addition, there were significant sidelobe variations in the pattern for off-axis directions. This was not the case for the fast-pulse excitation, because this former excitation contained many frequencies with similar amplitudes, and the sidelobes tend to wash out in the transient response. This was not the case for the damped sine wave, which had a rather narrow range of significant frequencies in the spectrum.

6. Summary

We have explored the concept of energy patterns (measured in Joules/steradian) for a pulsed antenna such as the IRA. In the case of CW antennas, the radiated power and energy patterns are the same. This is not the case for pulsed antennas. The radiated power pattern for a pulsed antenna is a strong function of frequency, and can be computed for various frequencies.

In this note, we have considered the prototype IRA and estimated its energy pattern for two different inputs with the same peak-voltage amplitude of 120 kV. One input was

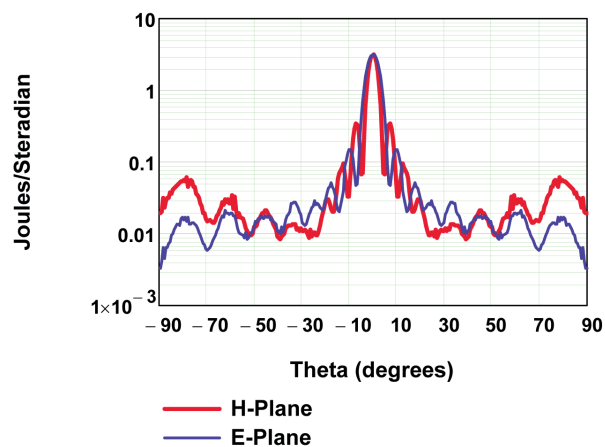


Figure 21. A plot of the radiated energy pattern in the horizontal (H) and vertical (E) planes for the IRA with the damped-sinusoidal voltage excitation of Figure 13 (the ordinate is a logarithmic scale).

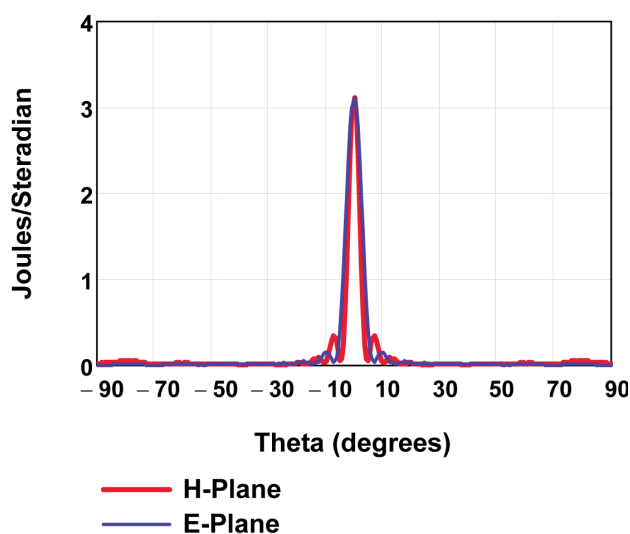


Figure 22. A plot of the radiated energy pattern in the horizontal (H) and vertical (E) planes for the IRA with the voltage excitation of Figure 13 (The ordinate is a linear scale)

a fast-rising (100 ps), slowly decaying (20 ns) monopolar pulse, while the second was a 1 GHz damped sinusoidal voltage, which was bipolar.

The transient energies of the two input voltages had vastly different frequency components. The fast pulse had frequencies extending from dc to a few GHz, while the damped-sinusoidal input was a moderate-band source, centered at 1 GHz. As a consequence of this, the energy patterns of the same prototype IRA were considerably different for the two input voltages.

In summary, the energy patterns are useful in visualizing where the transient energy provided to the IRA is being radiated in front of the antenna.

7. References

1. D. V. Giri and F. M. Tesche, "Classification of Intentional Electromagnetic Environments (IEME)," *IEEE Transactions on Electromagnetic Compatibility*, **46**, 3, August 2004, pp. 322-328.
2. C. E. Baum, "Radiation of Impulse-Like Transient Fields," *Sensor and Simulation Note* 321, November 25, 1989.
3. C. E. Baum and E. G. Farr, "Impulse Radiating Antennas," in H. L. Bertoni et al. (eds.), *Ultra-Wideband Short Pulse Electromagnetics*, New York, Plenum Press, 1993, pp 139-147.
4. D. V. Giri, M. Lehr, W. D. Prather, C. E. Baum, and R. J. Torres, "Intermediate and Far Fields of a Reflector Antenna Energized by a Hydrogen Spark-Gap Switched Pulsar," *IEEE Transactions on Plasma Science*, **28**, 5, October 2000, pp. 1631-1636.
5. K. Sunitha, D. V. Giri, and J. Thomas, "Radiation Patterns of a Reflector Type of Impulse Radiating Antenna (IRA) Relating Time and Frequency Domains," *Sensor and Simulation Note* 545, October 25, 2009.
6. D. V. Giri, *High-Power Electromagnetic Radiators: Nonlethal Weapons and Other Applications*, Cambridge, MA, Harvard University Press, 2004.
7. C. D. McGillem and G. R. Cooper, *Continuous and Discrete Signal and System Analysis, Second Edition*, New York, Holt, Reinhart and Winston, 1984.
8. C. A. Balanis, *Antenna Theory Analysis and Design*, New York, John Wiley & Sons, 2005.
9. F. M. Tesche, "Swiss Impulse Radiating Antenna (SWIRA) Characterization," report for Armasuisse contract 4500314446, August 8, 2005.

Spectrum Management Overview



Terje Tjelta
Ryszard Struzak

Abstract

Radio frequencies are of increasingly high value for wireless telecommunications services, as well as for science services. Spectrum simply must be efficiently utilized, and more so with the very high interest currently seen for radio applications. This involves developing good radio equipment, able to operate under challenging conditions; a high degree of spectrum reutilization of close-by spatial locations or temporal time slots; and, obviously, cost-effective spectrum-management regimes. The pressure to make suitable additional spectrum available is getting high, in particular for mobile data services. The management at all levels must address the new challenges. Some communities trust traditional command and control methods, other communities argue for liberalized market mechanisms. Some want to keep most of the spectrum for specific and well-defined radio services and systems; others want a free utilization in spectrum commons, and technology-neutral allocations. The way forward is preferably an evolutionary path where the laws of physics must be respected, but advanced technology allowed, and more flexible and efficient spectrum-management regulatory regimes put to work.

1. Introduction

The utilization of radio spectrum has been growing dramatically for many years. Broadband mobile data services and other personal wireless communication systems have become particularly heavy spectrum users in recent decades. In fact, fixed-broadband-access radio technology dominates with respect to first-meters technology choices, such as through wireless local-area networks (WLANs).

Along with the incredible growth of personal wireless communication, spectrum management has either changed as well or is in the middle of a process where new efficient regimes are sought. The pressure on management comes from several angles: to serve businesses, to deliver cost-efficient services to users, and to efficiently utilize the

electromagnetic-wave frequencies. The discussion includes to what extent regulatory authorities shall control the spectrum and its use, or whether other mechanisms – such as commercial spectrum trading – are more appropriate, or should more common spectrum be available with no control other than determination of basic frequency bands and transmitting power limits? At present, there is a mixture of methods depending on the part of the spectrum and country, from almost no control, through regulations with detailed bureaucratic means.

This paper discusses aspects of the management mechanism, and indicates some possible routes for future improved spectrum management. It is a revision of the paper presented at the URSI General Assembly and Scientific Symposium in 2011 [1].

2. Demand for Spectrum

Ever since the radio was invented more than a hundred years ago, there has been an increasing demand for radio frequencies for various purposes. The trend is to both use higher frequencies, and to increase the degree of utilization, such that the total gross capacity can meet the higher and higher demand for radio-based services. The latter point has resulted in radio systems that both make better use of radio waves in terms bit/s/Hz and gross area capacity, and that can tolerate more interference.

One of the most remarkable recent drivers towards improved spectrum utilization and demand for more spectrum is mobile data traffic, i.e., to use the mobile network for the Internet both using handsets (small screens), or laptops and stationary computers (large screens). The predictions from various sources indicate a dramatic growth in total mobile data traffic, as depicted in Figure 1 from the Cisco source [2] shown together with forecasts since 2008. Busy-hour Western European traffic is shown in Figure 2, from Telenor research [3, 4]. The exponential growth indicates total monthly mobile data traffic doubling rates of about a year, and also dramatic busy-hour traffic in Western Europe. Without identifying detailed spectrum

Terje Tjelta is with Telenor, Snarøyveien 30, 1331 Fornebu, Norway; e-mail: terje.tjelta@telenor.com. Ryszard Struzak is with the National Institute of Telecommunications, Wrocław, Poland; e-mail: struzak@gmail.com.

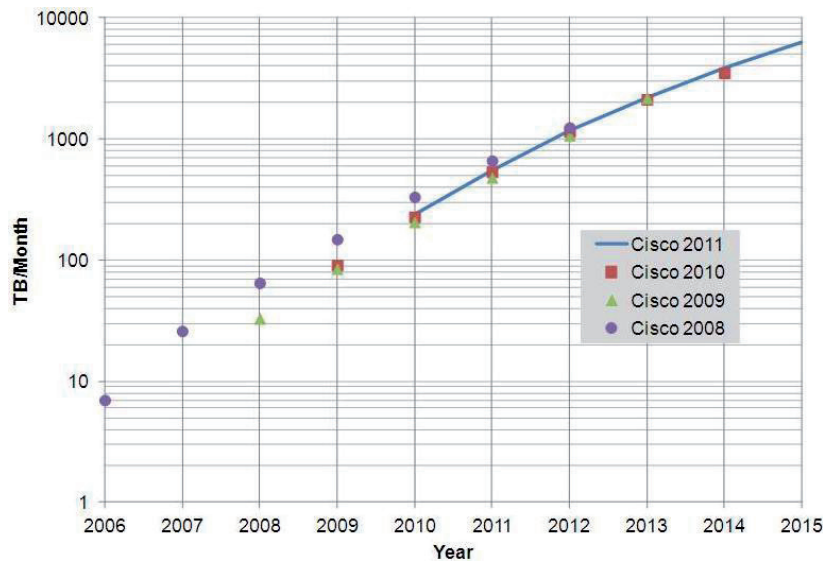


Figure 1. Mobile data growth in terms of total global traffic per month [2].

requirements, it is clear that mobile data traffic will become more and more demanding in its requests for spectrum resources in suitable frequency bands [5].

However, the trend indicates that the growth rate for mobile data [2] is reduced, with a traffic-doubling rate towards longer periods than a year, and that earlier year predictions somewhat overestimated the expected traffic. However, a challenge remains clear to make available, regulate, and manage spectrum for this branch of the radio business.

3. Management Methods for Radio Frequencies

In the first years of utilization of radio frequencies for communication or broadcasting, there was no harmonization or management. However, it did not take long before it was necessary to manage the spectral resources, and to reach agreements, in 1903, to regulate the utilization of the

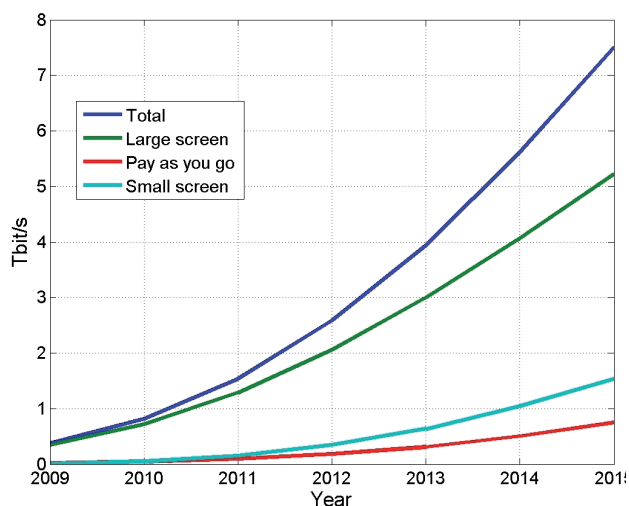


Figure 2. Busy-hour traffic for Western Europe [3].

spectrum [6, 7]. The main driver was probably avoiding destructive interference.

Today, there are three spectrum-management levels: the global, the regional, and the national levels. The Radiocommunication Sector of the International Telecommunication Union (ITU-R) issues Radio Regulations (RR) [8] every three or four years. The Radio Regulations give the basic set of rules for the utilization of the radio spectrum, for radio-based services such as mobile or fixed, and for international-coordination procedures. The main spectrum-allocation table just split the world into three regions, but numerous footnotes make many of the allocations valid or invalid at national levels, irrespective of the table's allocations.

The Radio Regulations have a major impact on global business, in the sense that radio systems and services are developed according to their allocations. For global systems such as satellite and mobile services, it is desirable to achieve common frequency bands for the whole world, or for areas as large as possible. The more fragmented the allocations are – for example, set by countries in footnotes to the Radio Regulations allocation table – the more complicated the radio system becomes. The Radio Regulations were created in a highly democratic process, taking into account the interests of all interested parties, treating the radio spectrum as a common heritage of all of humanity. At the national level, the practical management is done to provide a right to use part of the spectrum for a specified service. The regional level is used for harmonization within a geographical area, and sometimes to align policies.

National regulatory authorities manage spectrum following an “administrative model,” a “trading model,” or a “free model.” The administrative model, which some call “command and control,” allows the authority to decide in much detail to whom to give rights to use the spectrum, for how long, and for what purpose. The authority will normally follow the ITU-R Radio Regulations with respect

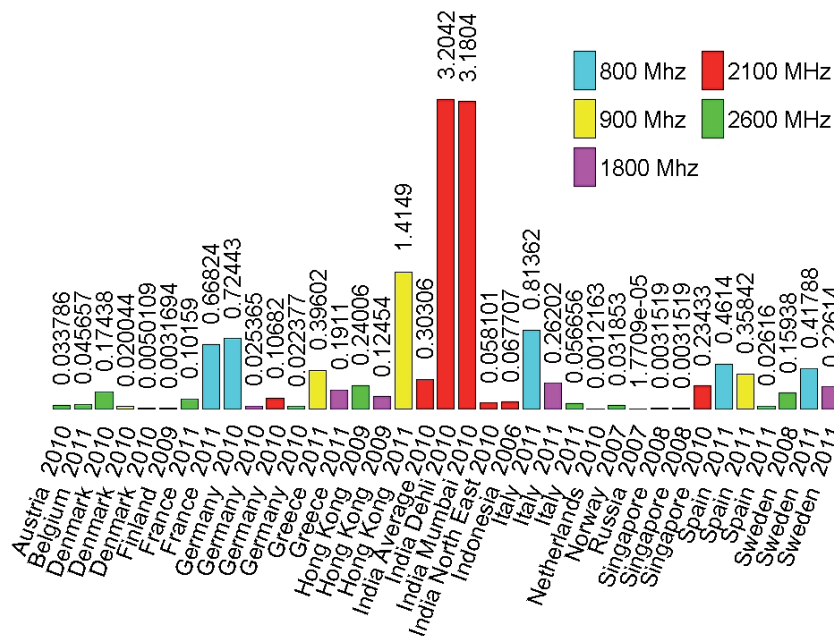


Figure 3. Auction prices given in EUR/MHz/Pop for paired spectrum, using exchange rates at the time the auctions were held. (Note: This is for paired spectrum. EUR/MHz/Pop was based on historical exchange rates when the different auctions were worked out. When calculating EUR/MHz/Pop, the sum of uplink and downlink bandwidth was taken into account. In auctions where paired/unpaired spectrum was sold in bundles, the amount of paired spectrum was used.)

to frequencies for type of service, but may deviate. Operators may apply for use of the spectrum with a certain proposal, and if there are more applicants than can be offered rights, it is sometimes called a “beauty contest” to obtain rights. This is not easy to judge, and not easy to apply, either. The trading approach replaces the beauty contest by a market mechanism, and is commonplace today in most developed countries and in some developing countries. Operators are willing to pay a lot of money for spectrum, although this varies from country to country. Figure 3 shows example auction prices in Euros (EUR) per MHz and population (Pop) for paired spectrum for mobile operations over a five-year period. However, there have been cases where in spite of paying a large amount in an auction, the operators did not deploy the service as promised, for one reason or another.

The trading model can be taken further in dealing with spectrum rights (to use as any other good model [9]) and in allowing these to be sold to others. That is to say, the market mechanisms are not limited to the primary access to spectrum, but spectrum can be treated also as a good that can be traded on a secondary basis. The regulator may again try to ensure that spectrum is used for its original purpose, but it is the market that is in control and not the authority, unless explicit in national regulations. Some see this as necessary for the future, not only to efficiently handle the spectrum, but to also get new technology into use. New technology is apparently assumed to make better use of the spectrum [10].

4. Future Development Trends

Global radio regulations remain very important for the vendor industry and operators for developing new radio systems, in particular to lower the cost of services. Obviously, no one will develop a system that cannot be

widely used. For example, mobile-communication vendors and operators will hesitate to develop unique products for small national markets. Depending on circumstances, the services offered may become expensive. Expensive services lead to less spectrum utilization. In such cases, a spectrum-management problem is solved, but society is not served as well as it should be.

Market mechanisms have increasingly been recently deployed, although this is not a new concept [9]. Several argue for more spectrum to become available under a liberalized market-mechanism regime, to both promote development of new radio systems and to lower the cost. Some indicate that more frequencies should become spectrum commons, using the same type of arguments.

One success story is WLAN, beyond no doubt used by very many for first-meter broadband access. However, note that there are also examples of WLANs where no service is possible, simply because of spectrum pollution due to interference.

Market laws are not good enough on their own: the laws of physics must be respected. Radio waves propagate according to physical laws under particular technical designs such as spectrum occupied, transmitted power, and the antenna radiation pattern. Regulatory or economic principles have no influence once the radio transmitter is turned on, i.e., the radio system is put into operation. The radio transmitter can cause destructive interference to others using the same portion of the spectrum, and it can be affected itself.

Market institutions are geared toward economic growth, and provide only private goods at the expense of public goods. In the 1950s, John Kenneth Galbraith argued that society was too focused on the market provision of private goods and neglected public goods such as education,

infrastructure, public health, and so on, which would better improve quality of life. Today, not only is the importance of public goods provided by nature recognized, but it is known that the production of market goods inevitably degrades them.

Technology is evolving quickly, such that radio systems will increasingly be able to adapt to the environment, making it possible to increase spectrum utilization. A modern radio system can handle more interference – up to some limits. If pushed beyond inherent limits, gross throughput will be reduced and, even ultimately, no service can be provided in that part of the spectrum in that geographic area.

Radio-communication services can very much look the same, whether they are provided by a fixed, mobile, or even broadcast technology. The traditional allocation to such services is becoming obsolete as convergence takes place such that it is not really possible to distinguish among them. At local levels, spectrum rights should be provided while not specifying technology: they should be technology neutral.

Trends like these put spectrum management under pressure to change. From a regulatory authority point-of-view, it might look easier to let the actors make decisions based on their views of market development, while not regulating at a too-detailed level. Developments clearly point toward higher pressure on the most suitable parts of the electromagnetic spectrum, such as for mobile data services. How should spectrum management deal with the future: use command and control, trading, or free commons? Considering mobile data, the context is global business for convergent services.

Clearly, an administrative approach at national levels has severe drawbacks when focusing only on a small geographical area. A market-oriented approach can quickly lead to fragmentation of the spectrum for various services, and, if there is a motivation for alternative air interfaces, a large number of complex radio systems will have to deal with broadband traffic as well as difficult interference scenarios. With fragmented spectrum spread over several frequency bands, the equipment has to deal with very variable radio channels, as well as with the complexity created within the radio circuits themselves, to communicate using an aggregated number of narrower bands taken from a much wider total bandwidth. The commons approach is obviously attractive as long as the radio system works; the opposite is equally obvious, since many users can simply result in congestion and blocking.

Growing total gross traffic leads to careful consideration of how much spectrum a certain system needs in a geographical area. There is a limit, hard or soft, where the load is too high, and throughput will be reduced and even blocked. Technical and operational characteristics of

various services need to be precisely coordinated – more and more, in an automated way – to cope with that challenge.

5. Conclusion

The pressure on suitable radio frequencies is increasing in several radio-based business areas. Spectrum management is challenged to become more efficient, to adapt to a technology world with convergent services and fast-developing technology. It is possible to become more efficient and still respect physical and technical constraints. Spectrum trading, along with administrative command and control, may well be the road to continue to follow. More spectrum commons are also possible, but concomitant destructive interference will increase the more services in such bands are used, and, in such cases, it is difficult to guarantee satisfactory quality of experience.

6. Acknowledgments

Many thanks to Kjell Stordahl, Nils Kristian Elnegaard, and Terje Ambjørnsen, who provided busy-hour traffic and auction-price data.

7. References

1. T. Tjelta and R. Struzak, "Physical, Technical, Practical, Economical, and Regulatory Aspects of Spectrum Management," Proceedings of 2011 XXXth URSI General Assembly and Scientific Symposium, Istanbul, Turkey, August 13-20, 2011.
2. Cisco, "Cisco Visual Networking Index: Forecast and Methodology, 2010-2015," Cisco White Paper, June 1, 2011.
3. K. Stordahl, "Long-Term Mobile Broadband Traffic and Subscription Forecasts," Proceedings of the 31th Annual International Symposium on Forecasting, Prague, Czech Republic, June 26-29, 2011.
4. K. Stordahl, "Market Development up to 2015," Celtic project MARCH Deliverable D3.4, December 2, 2010; available at http://projects.celtic-initiative.org/march/march/UserFiles/file/CP5-013-MARCH-D3_4-final.pdf.
5. M. Lazarus, "The Great Spectrum Famine," *IEEE Spectrum*, 47, 10, October 2010, pp. 26-31.
6. E. Lie, "Radio Spectrum Management for a Converging World," ITU Workshop, February 16-18, 2004.
7. R. Struzak, "Trends in Use of RF Spectrum," *Journal of Telecommunications and Information Technology*, 4, 2009, pp. 95-100.
8. ITU-R, "Radio Regulations," Geneva, ITU, 2012.
9. R. Struzak, "Spectrum Market or Spectrum Commons," Proceedings of EMC Europe 2010, September 13-17, 2010, Wroclaw, Poland.
10. I. Chochliouros, A. Spiliopoulou, S. Chochliouros, and T. Doukoglou, "European Challenges Towards Forming and Promoting an Innovative Radio-Spectrum Policy in a Fully Converged Communications Market," *Journal of the Communications Network*, 6, Part 2, April-June 2007, pp. 60-67.

Opportunistic Secondary Spectrum Access : Opportunities and Limitations



Jens Zander
Ki Won Sung

Abstract

The dynamic spectrum-sharing technique (“cognitive radio”), where secondary users opportunistically utilize temporarily or locally unused spectrum, has emerged as a prime candidate technology for relieving the perceived spectrum shortage in the lower frequency bands. Making a realistic assessment of the amount of spectrum available for secondary services was the objective of the EU FP7 QUASAR project. In the project, it was found to be fundamentally difficult to reliably determine which part of the spectrum is available. This leads to large safety margins and to poor spectrum utilization, in general. Furthermore, the business success of future systems depends on the scalability of the secondary-access techniques. Results from the project indicate that in large-scale deployment, the aggregate interference from the secondary devices is the key bottleneck. This aggregate interference is difficult for the individual secondary-spectrum user to assess. In addition, the vast majority of spectrum opportunities are strongly dependent on the intended use. They are highly localized in time and space, and not obviously suitable for reliable service provisioning. The exception has been shown to be short-range, indoor communications, where the low transmitter power, walls, and other obstructions successfully provide these margins.

1. Introduction

The need for more radio-spectrum resources to fulfill the demands of the rapidly growing mobile and converged broadband-access services is evident. Abundant and fast access to spectrum has three main advantages: it fosters rapid innovation in wireless systems and services, lowering entry barriers to the market; it enables affordable broadband access to all; and it potentially improves services and business models of established mobile operators.

Among the candidate “expansion” frequency bands, secondary use of already licensed but underutilized

spectrum allotments in “low-frequency bands” (below 6 GHz) has been proposed as an interesting alternative to previously promoted millimeter-wave bands (10 GHz and above). In addition to lower equipment cost, the attractive propagation conditions in the lower-frequency bands allow for much-simpler and thus lower-cost deployment. Low spectrum occupancy in a number of measurement campaigns worldwide has been the basis for claims of large gains in spectrum efficiency by cognitive radio and opportunistic spectrum access (see, e.g., [1, 2]). However, little research has been done to substantiate these claims with technological, regulatory, or economic feasibility studies. For discussions on issues and a feasibility analysis of the generic problems related to secondary-spectrum access, see [3,4]. Except for secondary use of TV white space, which has been extensively studied (e.g., [5] and references therein), there are few concrete studies of other sharing scenarios. The EU FP7 QUASAR [6] project aimed at bridging this gap between the claims made in conventional cognitive-radio research and practical implementation. This was done by assessing and quantifying the “real-world” benefits of secondary (opportunistic) access to primary (licensed) spectrum. In this paper, we will report some of the initial findings of the project, and their (high-level) consequences. We will primarily discuss four areas of concern.

It is important to set the scene for secondary-spectrum access in the quantitative assessment of the availability. This can be done by defining the models and parameters of the secondary access in a comprehensive manner, which we term a “scenario.” A complete scenario consists of the following three elements: a primary system and spectrum, a secondary system and usage, and methods and context of spectrum sharing.

Spectrum-detection schemes and technical parameters of the secondary system make a huge impact on the amount of practically available spectrum. In many popular scenarios, the fundamental reliability of the techniques for determining which part of the spectrum is available is usually not sufficient to protect the primary users. This leads to large safety margins for secondary-spectrum use

Jens Zander and Ki Won Sung are with the KTH Royal Institute of Technology, Electrum 229, 164 40, Stockholm, Sweden; e-mail: jenz.@kth.se; sungkw@kth.se.

and, consequently, to poor spectrum utilization (more-limited availability of secondary spectrum). Limited knowledge/flexibility regarding the system parameters (a.k.a. technology neutrality) has a similar effect.

Further, scalability is essential for business success. Most previous work has provided more “anecdotal evidence” of successful use, and has been focused on the availability of spectrum for a single user. The business success of future systems depends on widespread and reliable use of secondary-access techniques. This means that the effect of aggregate interference on primary users in large-scale usage is of significant importance.

Conventional economic models for spectrum trading fail, since spectrum opportunities largely depend on the technical parameters of the intended user and the potential interference victim. Creating exclusive and technology-neutral spectrum is therefore often associated with massive losses in efficiency.

In the remainder of this paper, we will exemplify these findings with preliminary results/studies from the QUASAR project.

2. Secondary-Access Scenarios

A *secondary-access scenario* is composed of a primary system and spectrum, a secondary system and usage, and the methods and the context of spectrum sharing. First of all, we should exactly know the characteristics of the target primary system and spectrum to protect the legacy system already in use. It is important that the protection of the primary system and the exploitation of the spectrum should be done without excessive cost. Ideally, the secondary systems should have accurate information about the technical features and usage pattern of the primary system. Large chunks of spectrum allocated to the primary system is preferred for the secondary users to achieve economy of scale. Attractive propagation characteristics (e.g., 300 MHz to 3 GHz: UHF band) can also be an advantage to the secondary users. Primary systems investigated in the QUASAR project included the TV broadcasting system, radars, and navigation systems.

The technical feasibility of a given scenario depends not only on the primary system and spectrum, but also on the characteristics of secondary systems. For a scenario to be promising – i.e., in order to allow for successful spectrum sharing – the secondary system should have usage requirements that are different from the usage pattern of the primary system. Examples of secondary-use cases include short-range and low-power wireless, indoor and hotspot broadband, wide-area wireless, backhaul and relay, and machine-type communications.

The way in which the spectrum is shared between primary and secondary systems is specified by sharing techniques and opportunity-discovery schemes that have

to meet regulatory requirements mainly designed to protect the primary users. Licensing and medium-access control schemes then describe the sharing among the secondary devices and/or systems. The above constraints determine the behavior of the secondary system, which determines its interference footprint, and this in turn determines the performance of both primary and secondary systems.

A scenario is completely described when all of the elements described above are combined with the primary and secondary user locations and the propagation characteristics of the geographical area under investigation. The radio propagation is determined by the terrain and buildings in the area. The demographics are good indicators of the secondary user’s locations and demand, which can be a further input to the analysis of business viability.

Interesting secondary-access scenarios defined in the QUASAR project can be found in [7, 8]. These scenarios enabled us to assess the availability and scalability of secondary access. The results of both technical and economic analysis were then fed back into the scenario-making process. Through this iterative refinement of the scenarios, the benefit of secondary access was better quantified, and, finally, decisions for regulation and business investment could be made.

3. Reliability of Finding Opportunities by Signal Detection

In the traditional and widely published “cognitive radio” concept, it is usually assumed that by sensing the primary signals, secondary transmitters will be able detect which frequency to use for their transmissions. These vacant frequencies are usually referred to as “spectrum holes” or “spectrum opportunities.” However, previous work and several publications of the QUASAR project have shown that spectrum sensing based access leads to quite poor performance in terms of spectrum utilization in realistic scenarios [9]. There are mainly three reasons for this:

1. The detection of the primary-system transmitter’s (T_P in Figure 1) signal over the path (G_{PS}) does not provide very reliable information regarding the properties of the critical path, the path between the secondary transmitter (T_S) and the primary receiver (R_P), nor of the primary user’s desired path gain (G_{PP});
2. The required protection of legacy primary systems is usually very high: less than a few percent of the primary receiver can be allowed not to reach their signal-to-interference ratio (SIR) targets; and
3. When large numbers of secondary users access the spectrum, their aggregate interference cannot be reliably assessed by the individual secondary transmitters.

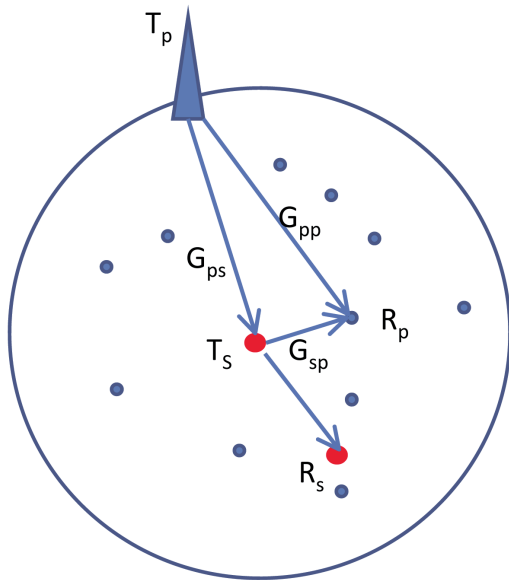


Figure 1. The secondary-use and interference scenario.

Let us use a simple TV white-space scenario in Figure 1 to provide examples of the first two difficulties. The aggregate interference problem will be addressed in the next session. Assume that the secondary transmitter (T_S) knows the primary user's transmitted power, and thus can perfectly estimate the path gain, G_{PS} . The SIR in the primary receiver is then (in dB)

$$\Gamma = P_P - P_S + G_{PP} - G_{SP} \quad (1)$$

$$= P_P - P_S + G_{PP} + 10\alpha \log_{10}(r_{SP}) - X_{SP},$$

where we have used a simple propagation model with an inverse α power-law distance dependence and a log-normal shadow-fading component, X . The distance between T_S

and R_P is denoted by r_{SP} . Now, assume that we can express the wanted path gain, G_{PP} , by using the estimated gain, G_{PS} :

$$G_{PP} = G_{PS} + (1 - \beta) X_{PP}, \quad (2)$$

where the constant $\beta \in [0, 1]$ is a measure of the correlation between the observed path gain, G_{PS} , and the primary path gain, G_{PP} . The SIR is then given by

$$\Gamma =$$

$$P_P - P_S + G_{PS} + 10\alpha \log_{10}(r_{SP}) + [(1 - \beta) X_{PP} - X_{SP}]. \quad (3)$$

In Equation (3), the last two terms represent the uncertainty related to the unknown distance to the primary receiver and the uncertainty due to shadow fading, respectively. Table 1 illustrates the required interference margin in some practically interesting cases where the victim receiver can be nearby. The table suggests that the key problem is not knowing the location of the primary receiver. The interference margin in this case is excessively high, and secondary reuse becomes impractical in the whole area – unless the secondary user's transmitted power (and the data rate) are extremely low. Even “perfect” sensing of the primary transmitter does not make any sense (!): a database indicating that the channel is used (somewhere) in the same geographical area provides this information in a more-reliable way. Using the database may lead us to knowing that the primary receiver is relatively far away, which lowers the variance of X_{SP} . However, in this case the correlation, β , tends to zero, which again means that sensing is meaningless.

Sensing becomes more interesting when the path loss to the primary receiver becomes known: e.g., in those cases where the primary system is a two-way communication system, where the primary system has very short range

Scenario	Standard Deviation	IM (95%)	IM (99%)	Rate (IM = 95%)	Rate (IM = 99%)
Low detection correlation ($\beta = 0$)	23.0	37.8	53.5	1.66E-04	4.51E-06
High detection correlation ($\beta = 1$)	21.5	35.4	50.1	2.86E-04	9.75E-06
Known primary receiver position	11.3	18.6	26.3	1.38E-02	2.33E-03
Known path gain G_{SP}	8.0	13.2	18.6	4.83E-02	1.38E-02
Genie aided access (full knowledge)	0	0	0	1	1

Table 1. The required interference margins, IM , and achievable relative secondary transmission rates for 95% and 99% availability for nearby primary receivers and various detection scenarios. The shadow-fading standard deviation was 8 dB, and the primary receivers were assumed to be uniformly distributed over the area. As a consequence, the distance to the nearest primary receiver was exponentially distributed. The standard deviation of the distance term for $\alpha = 4$ was roughly 20 dB.

(T_p is very close to R_p), or where the primary transmitter and receiver are collocated (e.g., radio-navigation and radar systems). In other cases, sensing adds very little to the information about primary systems that cannot be provided by geo-location-based access schemes, where secondary access is allowed when the area around the secondary systems is known to be free from primary receivers. Such access schemes, based on centralized databases with primary user information, are also the preferred access method in the TV bands, as discussed below.

4. Scalability of Secondary Access

Availability of secondary access in a particular location by a single secondary device will not be attractive enough from a business perspective. Secondary access is commercially interesting only when it is scalable, i.e., when it can support sufficient secondary traffic in a large area. This means that the primary spectrum should be “reused” by multiple secondary users. However, the impact of multiple secondary users has not been properly addressed in the existing regulatory approaches.

In TV white spaces, the recent ECC report 159 proposed a method to regulate transmission powers of secondary users and to assess the value of the spectrum [10]. In a nutshell, the method can be described as follows: a large geographical area is divided into pixels. The maximum allowed transmission power for a secondary user, $P_{S,max}$, is then calculated in each pixel with the constraint of the TV coverage probability, as follows:

$$\Pr[RX_P \geq RX_{P,min} + I_{TV} + I(P_{S,max}) + IM] \geq q, (4)$$

where q is the required TV-coverage probability, RX_P is the received signal power at a TV receiver, $RX_{P,min}$ is the minimum TV-receiver sensitivity, I_{TV} is the interference from other TV transmitters, and $I(P_{S,max})$ is the interference from the secondary user as a function of $P_{S,max}$. The safety margin and multi-user margin are accounted for by the term IM . It should be noted that the methodology in [10] took only a single secondary transmitter into account. Although the effect of multiple secondary users can be considered by IM , a method for obtaining the proper IM value has not yet been established yet. A conservative value of IM will result in the loss of spectrum opportunity, while insufficient multi-user margin has a risk of failing to protect TV receivers.

Another example of secondary access is the use of radar spectrum at 5 GHz by low-power devices such as WLANs. ETSI standard EN 301 893 specifies the thresholds and requirements for the secondary devices [11]. The transmission decision of each secondary user is regulated

by an individual-detection result: a secondary device with a power density of 10 dBm/MHz can use the primary spectrum if a detected radar signal power is less than -62 dBm. Notably, the detection threshold of -62 dBm remains constant, regardless of the number of secondary devices.

The impact of aggregate interference generated by multiple secondary users should be studied in order to overcome the drawback of existing regulatory approaches. In [12], a mathematical framework to describe the aggregate interference in the radar spectrum was proposed under the assumption of uniformly distributed secondary users. Key findings of the study were as follows. First, aggregate interference hugely depends on the propagation environment. Accurate description of propagation loss is thus a prerequisite for reliable interference modeling. Second, the impact of multiple secondary users should not be ignored, particularly when path loss does not quickly attenuate, e.g., for rural or line-of-sight propagation environments. A similar result was reported when pieces of airborne equipment were considered to be the potential primary users [13]. Recent advances in the aggregate interference models and their applications to the practical secondary-access scenarios in TV white space and radar spectrum can be found in [14].

5. Business Considerations for Commercial Operation in Secondary Spectrum

Traditional economic models for trading tell us that an efficient market requires assets that are general enough to attract the interests of many potential players [15]. The more constraints that are put on the use of the asset, the lower is the expected value. In opportunistic spectrum access, the vast majority of spectrum opportunities are not “spectrum holes” that anyone can use anywhere and for any purpose, but instead they are highly localized in time and space. Furthermore, if there are opportunities to be found, these strongly depend on the technical parameters of the intended user. QUASAR results showed that in many cases there is plenty of such “specific availability” of spectrum for a specific transmission at a given place and time, but this is not very useful to others—not even in the local surroundings. Making the spectrum asset more general, in the sense that it should be available over large geographical areas and for a wide range of applications (a.k.a. “technology neutrality”), requires significant interference margins, as demonstrated in Section 2. This lowers the spectrum availability by many orders of magnitude. Examples of how difficult it is to come by exclusive and technology-neutral spectrum are the recent spectrum reallocations in the 800 and 900 MHz bands, due to conflicts with legacy systems (e.g., GSM-R and TV-broadcasting).

Secondary spectrum, with its erratic availability, is therefore not very well suited for applications where wide-area coverage and guaranteed availability are required.

Wide-area broadband mobile access is a good example where long-term exclusive licensing is a much better option, in particular regarding the significant, long-term investments in infrastructure that are needed. An example where secondary spectrum is of significant commercial interest is short-range and/or indoor wireless access in hotspots in the TV or radar bands. Here, systems are deployed to complement wide-area systems, and infrastructure investments are usually very limited (low-cost equipment “piggy-backed” onto existing wired infrastructure). On the average, plenty of spectrum is available for this application. If higher capacity should be locally needed, deploying additional access points is a low-cost alternative. Another example where secondary spectrum is a viable alternative is rural broadband access. In this scenario, most primary systems have a very low geographical utilization, also allowing for wide-area secondary use.

6. Conclusion

One of the key findings demonstrated in the QUASAR project thus far is that there is plenty of availability of spectrum for opportunistic reuse, in particular when it comes to short-range secondary systems. Broadcast spectrum is more difficult to reuse, since spectrum sensing does not provide sufficient information for protecting the broadcast receivers. Scalability, i.e., the effects of massive secondary spectrum usages, is identified as a significant problem for further study. Short-range, indoor systems have been identified as one of the “commercial sweet spots” of secondary-spectrum access.

7. Acknowledgments

The research leading to these results received partial funding from the European Union’s Seventh Framework Programme FP7/2007-2013 under grant agreement No. 248303 (QUASAR).

8. References

1. J. M. Peha, “Sharing Spectrum Through Spectrum Policy Reform and Cognitive Radio,” *Proceedings of the IEEE*, 97, 4, April 2009, pp. 708-719.
2. A. Tonmukayakul and M. B. Weiss, “Secondary Use of Radio Spectrum: A Feasibility Analysis,” *Proceedings of Telecommunications Policy Research Conference*, October 2004.
3. J. M. Peha and S. Panichpapiboon, “Real-time Secondary Markets for Spectrum,” *Telecommunications Policy*, 28, 7, August 2004, pp. 603-618.

4. S. Srinivasa and S. A. Jafar, “The Throughput Potential of Cognitive Radio: A Theoretical Perspective,” *IEEE Communications Magazine*, 45, 5, May 2007, pp. 73-79.
5. M. Nekovee, “Cognitive Radio Access to TV White Spaces: Spectrum Opportunities, Commercial Applications and Remaining Technology Challenges,” *Proceedings of IEEE Symposium on New Frontiers in Dynamic Spectrum (DySPAN)*, Singapore, April 2010.
6. INFSO-ICT-248303 QUASAR Project, <http://www.quasarspectrum.eu/>.
7. J. Kronander, M. Nekovee, K. W. Sung, J. Zander, S.-L. Kim, and A. Achtzehn, “QUASAR Scenarios for White Space Assessments and Exploitation,” *Proceedings of EMC Europe Conference, URSI Special Session*, Wroclaw, Poland, September 2010.
8. QUASAR Deliverable D5.1, “Model Integration and Spectrum Assessment Methodology,” March 2011, available at <http://www.quasarspectrum.eu/>.
9. J. Zander, “Can We Find (and Use) ‘Spectrum Holes’? Spectrum Sensing and Spatial Reuse Opportunities in ‘Cognitive’ Radio Systems,” *Proceedings of IEEE 69th Vehicular Technology Conference (VTC)*, Barcelona, Spain, April 2009.
10. ECC Report 159, “Technical and Operational Requirements for the Possible Operation of Cognitive Radio Systems in the ‘White Spaces’ of the Frequency Band 470-790 MHz,” January 2011, available at <http://www.ero.dk/>.
11. ETSI EN 301 893 V1.5.1, “Broadband Radio Access Networks (BRAN); 5 GHz High Performance RLAN; Harmonized EN Covering the Essential Requirements of Article 3.2 of the R&TTE Directive,” December 2008, available at <http://www.etsi.org/>.
12. M. Tercero, K. W. Sung, and J. Zander, “Impact of Aggregate Interference on Meteorological Radar from Secondary Users,” *Proceedings of IEEE Wireless Communications and Networking Conference (WCNC)*, Cancun, Mexico, March 2011.
13. K. W. Sung, E. Obregon, and J. Zander, “On the Requirements of Secondary Access to 960-1215 MHz Aeronautical Spectrum,” *Proceedings of IEEE Symposium on New Frontiers in Dynamic Spectrum (DySPAN)*, Aachen, Germany, May 2011.
14. QUASAR Deliverable 4.3, “Combined Secondary Interference Models,” March 2012, available at <http://www.quasarspectrum.eu/>.
15. P. Crocioni, “Is Allowing Trading Enough? Making Secondary Markets in Spectrum Work,” *Telecommunications Policy*, 33, 8, September 2009, pp. 451-468.

Recent Advances in Integrated Circuit Immunity to Radio-Frequency Interference



Etienne Sicard
Mohamed Ramdani
Samuel Akue Boulingui

Abstract

In recent years, the electromagnetic compatibility (EMC) of integrated circuits (ICs) has been addressed by the scientific and industrial community to measure and model parasitic emissions, as well as susceptibility to radio-frequency interference, in order to compare, predict, and improve the EMC performance of components. The EMC community has made significant progresses on the emission aspects, with the release of mature standards, models, tools, and guidelines. However, the immunity of ICs is still under extensive research. The goal of this paper is to highlight the most-recent advances in immunity measurement, modeling at the integrated-circuit level, and to highlight research publications giving design guidelines for improved immunity. The visions of the standardization committee on the immunity-measurement methods and modeling approaches are also detailed.

1. Introduction

Electromagnetic compatibility (EMC) research focusing on integrated circuits (ICs) is not just a recent topic. Early electrical simulators, such as *SCEPTRE* – forerunners of the well-known *SPICE* simulation tools – were originally designed for simulating the susceptibility of electronic devices to radio-frequency interference (RFI). This paper aims at reviewing the state-of-the-art of EMC modeling of integrated circuits.

In the past ten years, concerns about EMC have risen in importance as low emissions and high immunity to interference have emerged as key differentiators in overall IC performance [1]. Advances in process integration, higher switching speeds, and more-complex circuits tend to increase the amount of parasitic emissions generated by ICs. Reduced supply voltages and an increased number of interfaces tend to decrease the immunity to radio-frequency

interference. EMC has become one of the major causes of IC redesign, mainly due to inadequate design methods and lack of expertise in parasitic noise reduction and immunity improvement.

The first collaborative book focused on EMC at the IC level was published in 2006 [2]. For the 30th anniversary of the special issue devoted to the effects of radio-frequency interference on ICs in 1979 [3], a review paper was published in 2009 [4] with an emphasis upon early papers in the field, the status of the standard measurement methods, and a discussion of standard modeling approaches. Various approaches for emission reduction, and predictive simulations of conducted and radiated noise interference have been presented. A recent book was published by Redouté [5], wherein the authors described the design of analog integrated circuits that achieved a higher degree of immunity against electromagnetic interference.

In the past five years, a significant effort has been made by expert engineers, scientists, and standardization committees to handle immunity modeling and its predictive simulation. Specific workshops and dedicated sessions in major conferences have enhanced dialogue and exchanges within the EMC community, focusing on integrated-circuit immunity.

The goal of this paper is to highlight the most-recent advances in immunity measurement, modeling at the integrated-circuit level, and to highlight research publications giving design guidelines for improved immunity. Section 2 presents a general introduction to EMC applied at the IC level, including a brief review of immunity-measurement methods. The status of international standardization and a focused look at two novel approaches are included. Section 3 explores recent advances in immunity modeling, covering analog, digital, and mixed-signal IC case studies. In Section 4, publications dealing with design guidelines for improved immunity are presented, followed by a conclusion.

Etienne Sicard is with INSA de Toulouse, 135, avenue de Ranguel, 31077 Toulouse Cedex 4, France. Mohamed Ramdani is with ESEO, 4, rue Merlet-de-la-Boulaye, BP 30926, 49009 Angers Cedex 01, France; e-mail: Mohamed.RAMDANI@eseo.fr. Samuel Akue Boulingui is with ABB France, 10, rue Ampère, 69685, Chassieu, France.

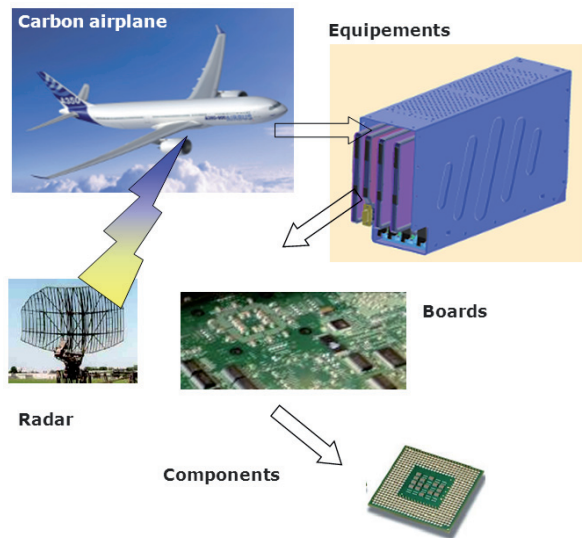


Figure 1. Illustrating the concept of moving from system to component susceptibility.

2. Electromagnetic Compatibility of Integrated Circuits

2.1 Generalities

Electromagnetic compatibility (EMC) is the ability of an electric or electronic device to satisfactorily operate in its electromagnetic environment without itself introducing intolerable electromagnetic disturbances to another device that is in this environment. To reach satisfactory compatibility, the device must:

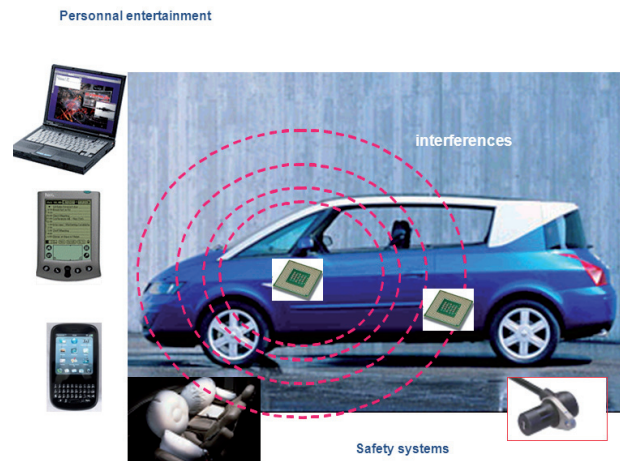


Figure 2. IC emissions and possible electromagnetic interference at the system level.

- Limit the unwanted-emissions levels from each piece of equipment so as not to disturb other equipment;
- Be sufficiently immune to interference from other equipment, or, more generally, from the environment.

This introduces the concepts of an EM victim and source. The IC as a victim is illustrated in Figure 1, in the case of a carbon airplane illuminated by a radar wave. The resulting electrical overstress may jeopardize the electronic equipment by coupling onboard and altering the IC's behavior. Against a radio-frequency disturbance, the IC's behavior may range from no reaction to destruction through malfunctions.

Year of Production	1995	1999	2003	2007	2011	2015
Technology	0.35 μm	0.18 μm	90 nm	45 nm	22 nm	13 nm
Internal supply (V)	3.3	1.8	1.2	1.0	0.9	0.8
Die dimensions (mm)	18 \times 18	20 \times 20	25 \times 25	30 \times 30	30 \times 30	30 \times 30
Million gates/mm ²	0.09	0.15	0.4	1.5	5.0	9.0
Average switching delay/gate, typical load (ps)	50	30	20	15	10	7.0
Average capacitance/gate (fF)	5	3	1	0.4	0.25	0.15
Average current/gate (μA)	1500	1200	800	500	300	200
Max. operating frequency [GHz]	0.3	0.8	2.0	4.0	7.0	10.0
Max I/O count	800	1000	1500	2000	3000	4000
Max peak switching current (A)	5	30	100	500	1000	1500
Interconnects						
Layers	5	6	8–10	8–12	8–12	8–15
Materials	Tu+Alu	Tu/Alu/	Cu+low K	Cu+Low K	Cu+ultra-low K	Cu+ultra-low K
1mm resistance (Ω)	500	2000	2500	5000	10000	15000
Data rate (Mb/s)	100	300	900	1200	2000	4000
Packaging	QFP	BGA, MCM	μBGA , double die	CSP, Multi-die	System-in-package, stacked dies	3D system-in-package, multi-stacking
EMC						
Conducted emission (dB μV)	50	70	80	80	80	80
Max. freq of interest	300 MHz	1 GHz	2 GHz	5 GHz	10 GHz	30 GHz
Noise margin (mV)	300	150	120	100	90	80
IO model	Ibis v2.1	Ibis v3.2	Ibis v4.1	Ibis v4.2	Ibis v5.0 [10a]	Ibis v5.x
EMC model	n.a.	IMIC	ICEM-CE	ICEM-RE	ICIM-CI	ICIM-RI

Table 1. Key parameters for IC technology, interconnects, and EMC as a function of technology nodes over a period of 20 years (1995-2015), based on ITRS technology roadmaps [7] and EMC roadmaps [2].

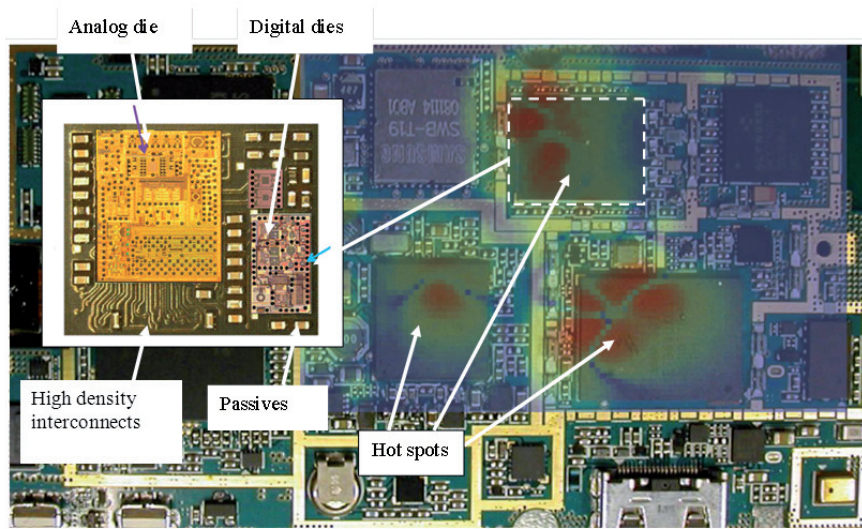


Figure 3. The near-field magnetic scan of a 3G+ mobile platform at 26 MHz revealed several hot spots [6].

In Figure 2, the IC as a disturbance source generates parasitic signals that may couple to victim devices, either by wire coupling (conducted mode), or by radiated coupling. This is illustrated in Figure 2 in the case of a car. Hundreds of embedded microcontrollers generate important levels of switching and communication noise that may interfere with personal devices such as smart phones, and may also erroneously trigger safety devices, such as the anti-lock brake system (ABS) and airbags.

2.2 Application to Integrated Circuits

The EMC of integrated circuits concerns the study of the emission and immunity of one or several components embedded in a package. Components may be active, passive, or a combination of both. The potential noise sources and victims can be within the same die or the same package. EMC at the IC level also addresses “system-on-chip” (SoC) and “system-in-package” (SiP), including three-dimensional integration of multi-dies within the same package. Figure 3 shows a near-field magnetic-field scan of a commercial 3G+ mobile platform at 26 MHz. Several “hot spots” were observed above the surface of some components at that specific frequency. Most of these devices include several dies and passives in the same package, mixing digital, logic, and power devices, using heterogeneous technologies.

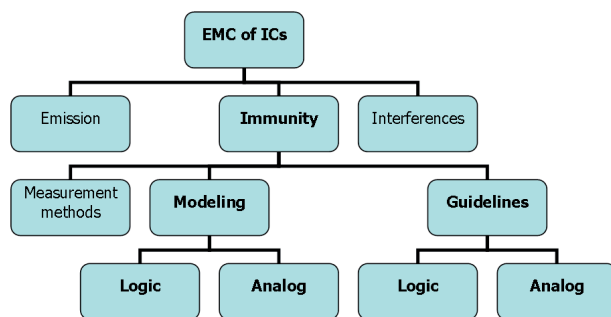


Figure 4. A general classification of research domains in the EMC of ICs, with a closer look at immunity.

Continuous technological advances [7] at the silicon and packaging levels enable increased gate density, and thus more-complex functions within a single package. Interference problems between internal blocks within the same silicon substrate, or between dies within the same high-density package, may jeopardize the benefits of improved integration.

Research in the EMC of integrated circuits may be classified into three general topics, as illustrated in Figure 4. These topics concern parasitic emission, immunity to radio-frequency interference, and interference between blocks. Concerning immunity, which is the main focus of this review paper, we may consider three subcategories: innovative measurement methods, modeling approaches for immunity simulation, and guidelines for improved immunity.

2.3 Integrated-Circuit Technology

As detailed in Table 1, progress in lithography and materials has enabled a tremendous increase in integration capabilities, together with a steady increase in operating frequencies. In 2011, the most-advanced technology node corresponded to an average feature size around 22 nm [8,

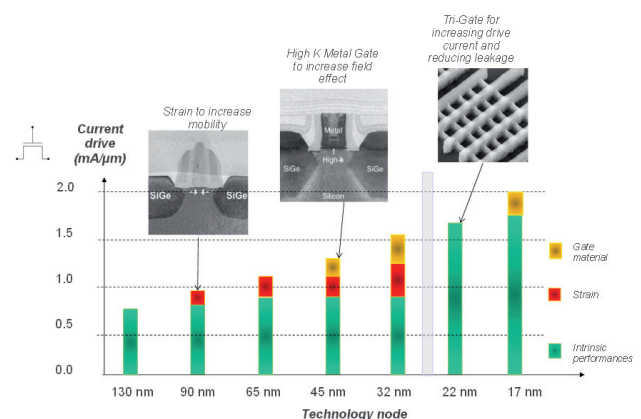


Figure 5. The improvement of switching-device performance due to enhanced gate material and mechanical strain [9, 10].

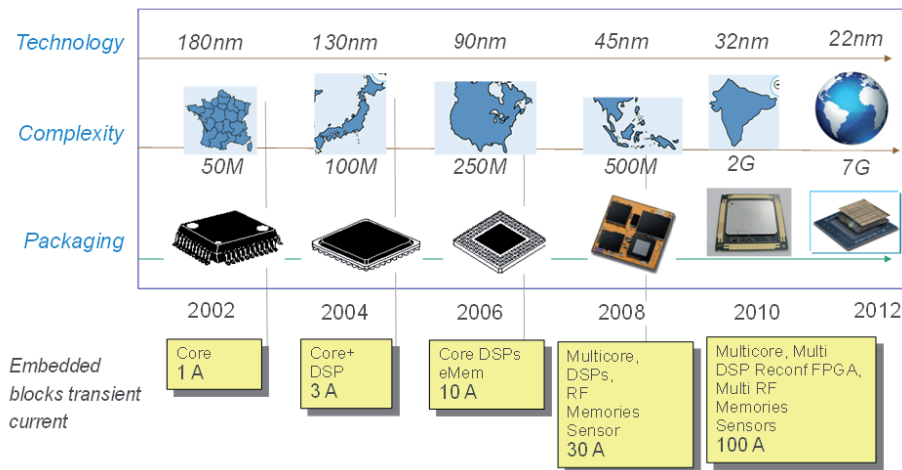


Figure 6. Breaking the records in terms of complexity and package density.

9], with more than one billion transistors on a single die. The interconnect layers have also increased, together with the input/output data rate and package integration. From an EMC viewpoint, the EMC specifications at the IC level were extended to a higher frequency range (1 GHz in 2000, 10 GHz in 2010). Due to the rapid voltage-supply reduction, the static noise margins were also decreased, down to the 100 mV range in 45 nm technology. Models for I/Os are mostly based on the I/O buffer-information specification IBIS [10], while EMC models rely on ICEM approaches [11] for emission and ICIM for immunity [12].

At the MOS-switch level, the decrease of lateral dimensions had a limited impact on the current drive, as may be seen in Figure 5. Strained silicon was introduced starting with the 90-nm technology to boost carrier mobility, which enhances both the n-channel and p-channel transistor performance. Intel introduced a so-called “Replacement Metal Gate” in its 32 nm technology node [9] to further increase the channel strain. The combination of reduced channel length, high-permittivity dielectric, metal gate, and enhanced channel strain achieved a substantial gain in drive current for both nMOS and pMOS devices. Starting with the 22-nm technology node, Tri-Gate technology (also known as 3D-FinFET) was introduced, which provides more than a 30% percent performance increase compared to planar transistors.

As illustrated in Figure 6, the IC complexity has literally exploded within a 10-year period. In 22-nm, a four-die FPGA from XLINX [13] embedded seven billion devices in a single package, which is equal to the worldwide human population. Two important trends may also be noted: more-efficient packages, enabling several thousand interconnecting pins per cm², thanks to micro-ball and high-density interconnect technologies; and more transient current at each clock edge, due to a tremendous complexity increase and therefore many more logic gates switching synchronously.

An important trend in IC technology is the steady reduction in the power supply. In Figure 7, three voltage trends are shown: the I/O voltage, which tends to be reduced step-by-step (5 V, 3.3 V, 2.5 V, 1.2 V); the core supply, which has constantly decreased from 5 V (0.5 μm node) to around 1 V (32 nm node); and the associated dc noise margin, which has been cut by a factor of five. A reduced noise margin means an increased sensitivity to external interference, and consequently an increased immunity. The IC package dimensions correspond approximately (Figure 8) to the quarter-wavelengths of the UHF and SHF bandwidths. Furthermore, the IC die itself, with dimensions close to one cm², may act as a patch antenna for similar bandwidths. This emphasizes the potential risk of IC immunity far above 1 GHz, as recently confirmed by [14] for an ASIC circuit

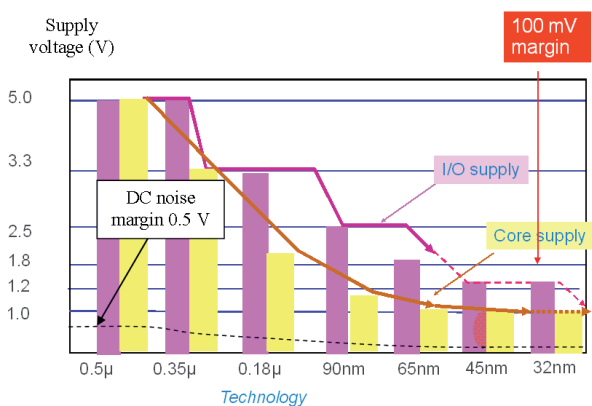


Figure 7. The steady reduction of the IC power-supply voltage has led to decreased noise margins.

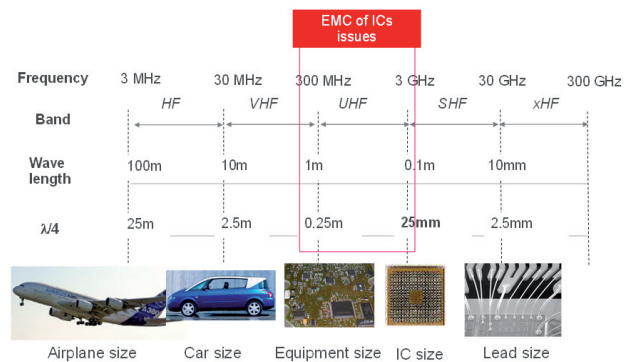


Figure 8. The IC and printed-circuit-board dimensions match a quarter-wavelength in the UHF and SHF bands.

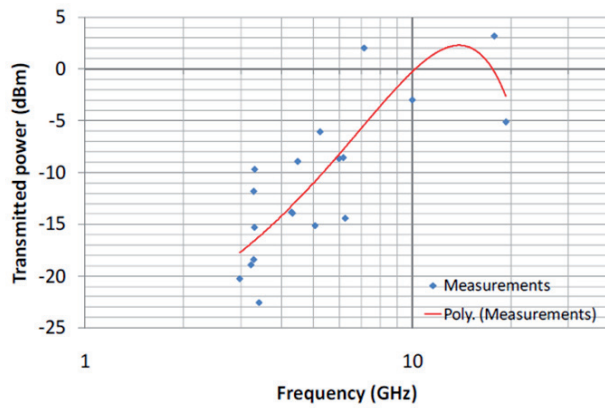


Figure 9. The susceptibility over 1 GHz for low radiated emission level.

in conventional 0.25 μm technology, which proved to be sensitive to radiated interference within the 1 mW range (Figure 9) at 10 GHz.

2.4 IEC standards for Immunity Characterization

Within the International Electrotechnical Commission (IEC), technical committees have released standards applicable to IC emission and IC susceptibility characterization. These standards ease the exchanges of EMC information between ICs suppliers and users. As many

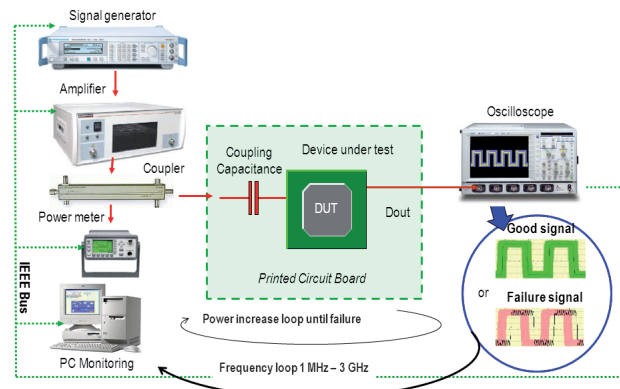


Figure 10. A typical direct power injection (DPI) setup, as part of the IEC 62132 standard measurement methods [15].

as eight measurement methods were proposed by the IEC under project 62132 [15], for characterizing IC immunity, as reported in Table 2.

Probably the most popular immunity method is the direct-power-injection (DPI) method. Its advantages are power efficiency; simple modeling of the injection device (a single capacitance, as illustrated in Figure 10); and its possible extension to the GHz range. Two major drawbacks may be pointed out: the unmatched coupling path, and the single-pin approach. As the coupling path and terminations are not adapted to 50 Ω , the reflected and transmitted powers may vary significantly over the

Standard	Description	Advantages	Drawbacks
IEC 62132-1	General <i>Conditions</i> and Definitions		
IEC 62132-2	<i>Radiated Immunity – TEM Cell and Wideband TEM Cell Method</i>	GTEM cell extended to 18 GHz. 50- Ω adapted method. Global perturbation. May be used for emission.	TEM cell limited to 1 GHz. Canonical field. Poor yield. Specific EMC board required.
IEC 62132-3	Bulk Current Injection (BCI)	Close to equipment BCI. Global injection through cables. No need for a specific EMC board.	Limited to 400 MHz. Difficult to scale. Needs for external buses/wires. Poor yield. Unmatched method. Dangerous: shielded room required.
IEC 62132-4	Direct <i>RF</i> Power Injection (DPI)	Power-efficient. May be extended to 18 GHz with careful injection design.	Unmatched, risk of PA damage. Limited to 1 GHz. Single-pin method. Specific EMC board required.
IEC 62132-5	Work Bench Faraday Cage (WBFC)	Close to equipment immunity. May be used for emission. A specific board can be avoided. Reasonable cost.	Insufficient support and publications on its modeling. Resonances at GHz-range frequencies.
IEC 62132-6	Local Horn Injection Antenna (LIHA)	Local injection up to several GHz. A specific EMC board can be avoided. Low cost.	The grounding has a strong influence on results. Unmatched method.
IEC 62132-7	Mode stirred chamber	Close to equipment measurement. Non-canonical field. Power-efficient method.	Need for specific EMC board and specific setup. Very high hardware cost. Cannot be used below 100 MHz.
IEC 62132-8	Micro strip-line	Up to 5 GHz. 50- Ω adapted method. Global perturbation. May be used for emission. Power-efficient.	Specific EMC board required.
IEC 62132-9	Near field scan immunity (NFSI)	Up to 5 GHz. Local perturbation. May be used for emission. Power-efficient. Very informative. Potential for innovations (impulse, passive matrix, etc..)	Unmatched method. Needs for very precise positioning system. Very long acquisition time for high-resolution scans.

Table 2. Immunity measurement methods applicable to integrated circuits, according to IEC 62132 [15].

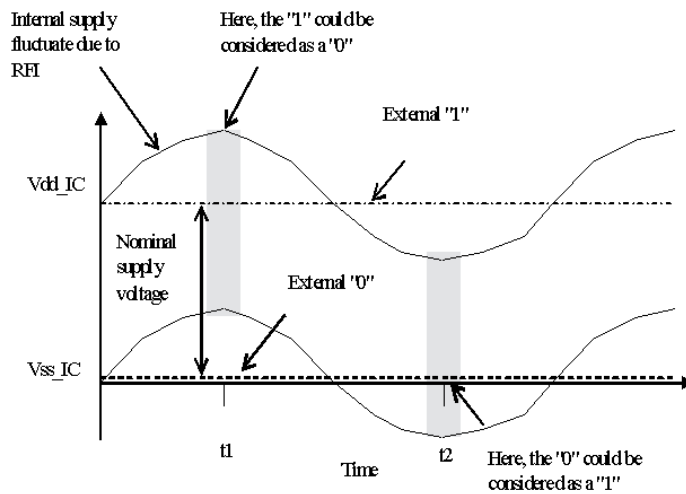


Figure 11. Susceptibility criteria based on supply-voltage fluctuation or over-current, and examples of logical errors due to voltage fluctuations

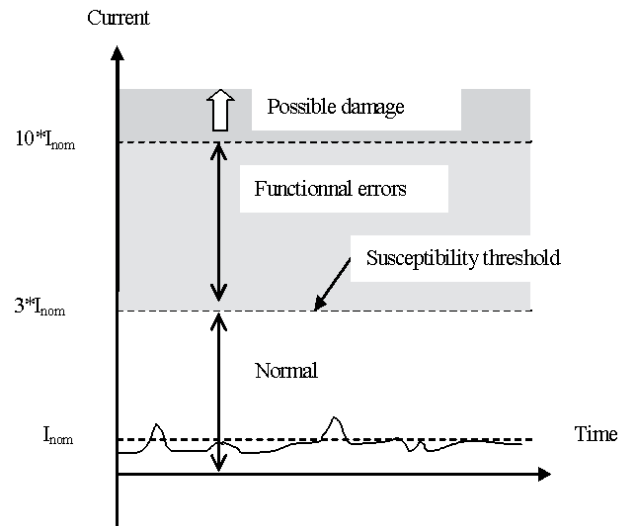


Figure 12. The susceptibility threshold based on over-current consumption.

1-1000 MHz measurement range, thus requiring a coupler and power measurement units (the left part of Figure 10). Second, the single-pin approach is not suited to very complex ICs, such as microcontrollers or FPGAs. The device under test (DUT) is usually mounted on a specific EMC board, enabling the injection of a perturbation through a discrete capacitance, and observation of the failure criterion. The criterion may be:

- A voltage threshold, as illustrated in Figure 11. This corresponds to a situation where a logic fault occurs and an erroneous value propagates inside the circuit. For example, the internal logic supply may be low enough to consider the low state as a high state.
- A decrease of the internal power-supply voltage. This notion corresponds to the difference that exists between the reference voltages V_{DD} and V_{SS} inside the IC. Below a certain margin – which is usually defined as 15% of the nominal supply voltage, V_{DD} – the switching of the logic circuits is significantly slowed. This phenomenon is at the origin of delays at the signal-distribution level, and can lead to the loss of features of logic or analog circuits.

- A current threshold. The current criterion is universal, as it applies well to most ICs. As an example, considering a nominal supply current I_{nom} . We may tolerate up to $3I_{nom}$ flowing inside the IC, which represents the susceptibility threshold (Figure 12). Possible destruction may be observed starting at $10I_{nom}$.

2.5 Recent Advances in Immunity Characterization Methods

In this section, we briefly describe measurement methods applicable to the characterization of integrated-circuit immunity, proposed by EMC researchers and engineers to overcome the limitations of existing standards.

2.5.1 Resistive RF Injection Probe (RFIP)

A new test method, called the resistive RF injection probe (RFIP), was recently proposed by Levant [16] as an improved version of the popular IEC 62 132 method, direct power injection (DPI). Using a fast digital oscilloscope and

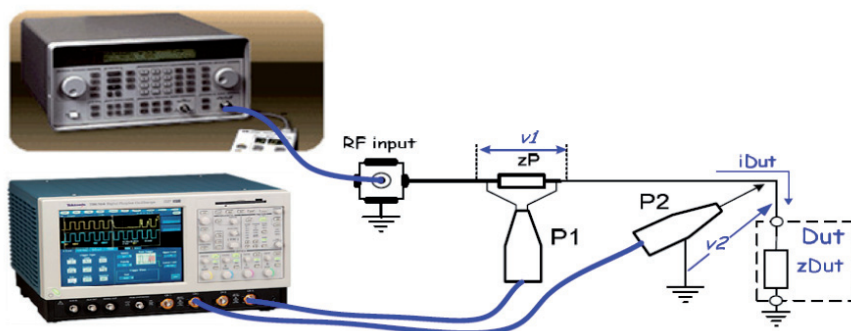


Figure 13. The measurement of voltage and current injected into the DUT [16].

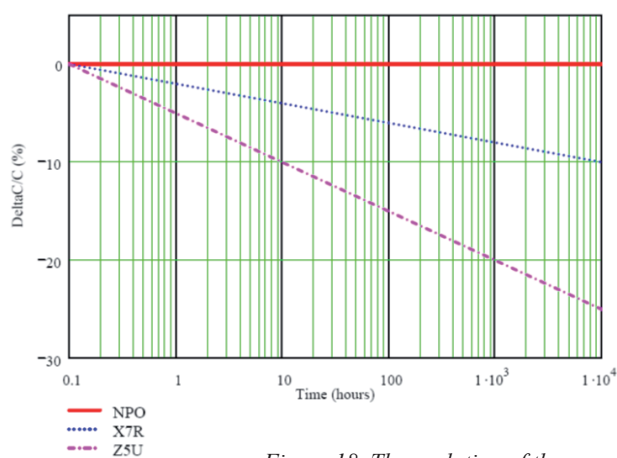


Figure 18. The evolution of the capacitance value with aging [19].

EMC margin at the system-in-package printed-circuit-board level. In [18], the susceptibility of a mixed-signal IC was characterized before and after accelerated aging, based on high-temperature cycling and electrical over-voltage stress. The immunity level was reduced up to 10 dB at some particular frequencies. Although the susceptibility of the digital part remained unaltered after aging, a voltage-controlled oscillator (VCO) suffered from a significant reduction of the immunity to radio-frequency interference (Figure 17).

In [19], Lafon studied the drift of discrete component characteristics and their consequences on immunity measurement. The author highlighted the relationship between the discrete capacitor's permittivity and its sensitivity to aging. The higher the permittivity of the dielectric used for the capacitor's construction, the higher the sensitivity to aging, as shown in Figure 18 for three types of ceramic capacitors. Nearly a 20 dB immunity variation was observed on a voltage regulator (Figure 19) due to the aging of passive components. Effects tended to decrease with the frequency, where parasitic elements (less subject to aging) were dominant.

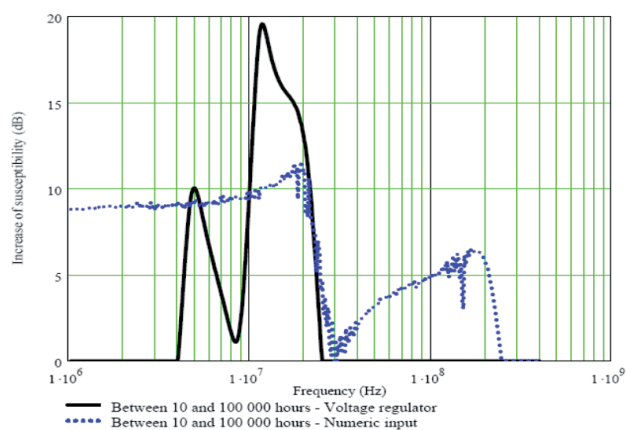


Figure 19. The susceptibility variation of two functional blocks [19]

2.5.4 On-Chip Immunity Sampling

An on-chip voltage sensor may be used to characterize the radio-frequency interference propagation inside the chip, and thus validate the immunity-modeling process. The circuit proposed by Ben Dhia [20] is based on an on-chip sample-and-hold circuit that directly probes the voltage within IC interconnects. The sensor uses a random mode acquisition to extract the probability density function (PDF) of the internal interference noise, and to consequently characterize the amplitude and statistical distribution of voltage fluctuations induced by conducted EMI. Comparisons between measured and simulated susceptibility levels on power supply lines are shown in Figure 20.

3. IC Immunity Modeling

This section details various approaches and recent research work focused on immunity modeling of integrated circuits. First, we present the general objectives of immunity modeling, and a global methodology for IC-level prediction.

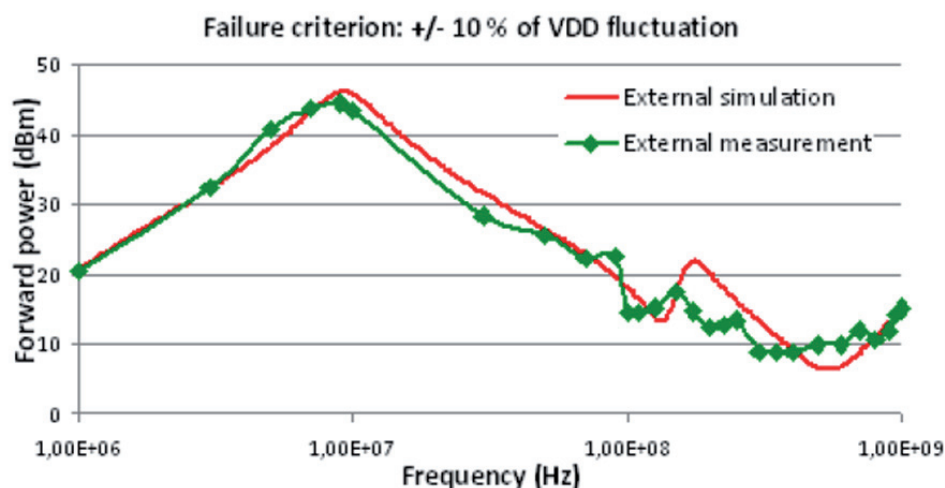


Figure 20. A comparison between measurement and simulation of the external EMI coupling [20].

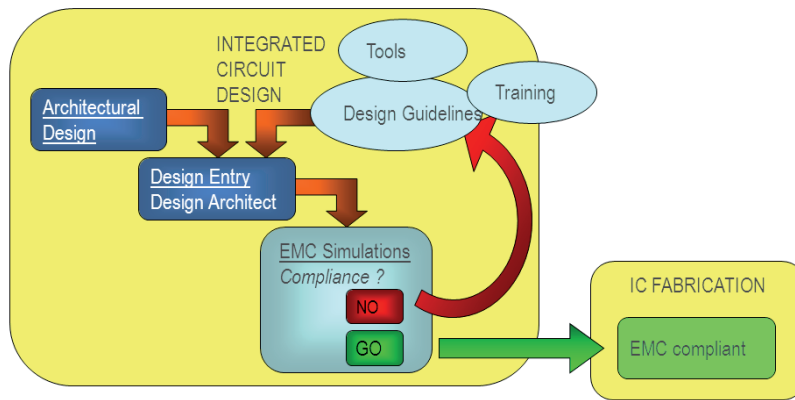


Figure 21. A generic flowchart for EMC-aware IC design.

Secondly, we go into details of passive distribution networks (PDNs). We also discuss the modeling of input/output structures, analog blocks such as an analog-to-digital converter (ADC), and describe the black-box modeling approach proposed by several researchers. Finally, we illustrate the vision of the IEC through the immunity model proposal ICIM.

3.1 Objectives

The generic goal of IC immunity prediction is to ensure EMC compliance prior to fabrication, due to the extremely high cost of IC redesign. Figure 21 highlights the important role of design guidelines and EMC tools, which are used by EMC experts to ensure that iterations converge to an EMC-aware design of the IC.

The immunity modeling of an IC can be seen as a combination of five main blocks. First (left in Figure 22), we must model the signal generator, amplifier, and power meter, in order to extract the forward and reflected power. We then model the injection path to assess the filtering effect caused on the disturbance, and to accurately forecast the current and voltage injected into the device under test. We also model the package and on-chip passive distribution

network, including the protection diodes, to derive the characteristics of the perturbation applied to the internal structures of the die. The internal behavior (IB) translates the perturbation into a failure, which can be easily simulated in the case of voltage and current thresholds.

3.2 Power Extraction from I, V Simulation

In the case of a power susceptibility criterion, the forward and reflected voltages can be expressed as complex numbers, as described in Equations (1) and (2):

$$V_{forward} = \frac{V_{in} + Z_c I_{in}}{2}, \quad (1)$$

$$V_{reflected} = \frac{V_{in} - Z_c I_{in}}{2}, \quad (2)$$

where $V_{forward}$ is the forward voltage [V], $V_{reflected}$ is the reflected voltage [V], V_{in} is the complex voltage at the input of the coupler [V], I_{in} is the complex current at the input of the coupler [A], and Z_c is the characteristic impedance of the coupler [ohms], usually 50 Ω.

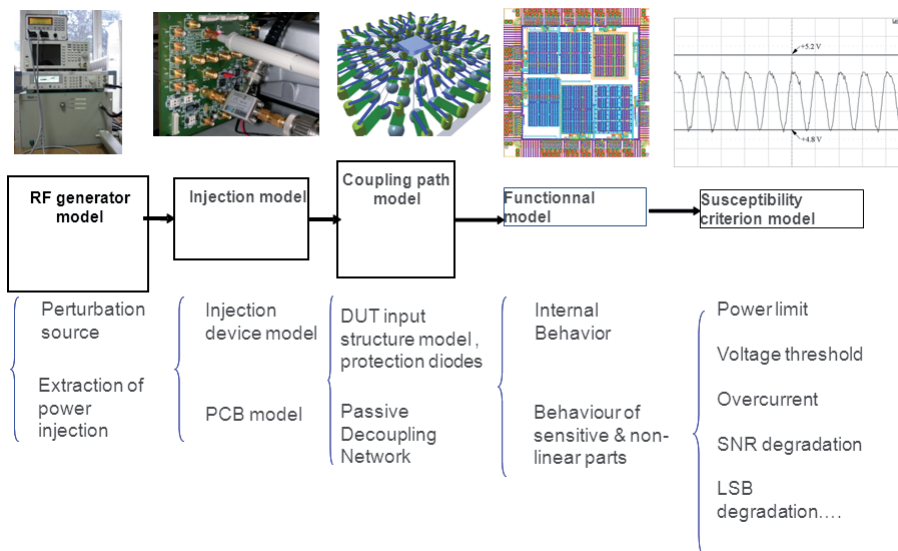
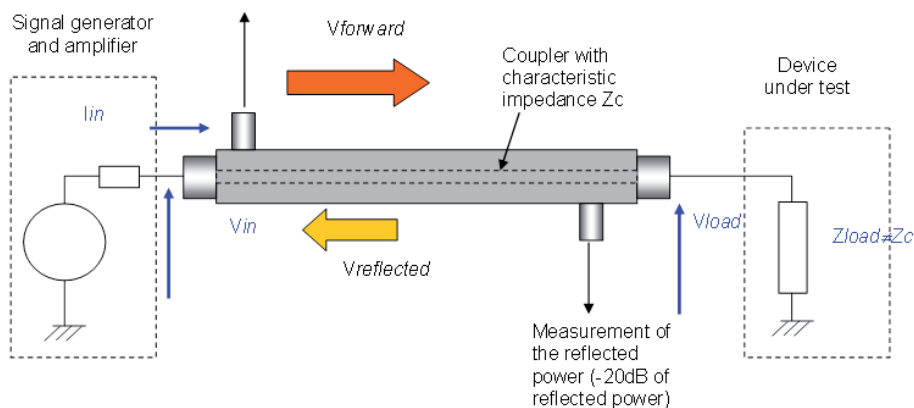


Figure 22. Performing the immunity simulation combines five types of models.

Measurement of the incident power (-20dB of forward power)

Figure 23. A coupler connected to a signal generator and a load [21].



The conversion from I, V simulations into forward and reflected power [21] is given by Equations (3) and (4):

$$P_{reflected} = 10 \log \left[\frac{1}{Z_c} \left\{ \left[\frac{\text{Re}(V_{in}) - Z_c \text{Re}(I_{in})}{2} \right]^2 + \left[\frac{\text{Im}(V_{in}) - Z_c \text{Im}(I_{in})}{2} \right]^2 \right\} \right] + 30, \quad (4)$$

$$P_{forward} = 10 \log \left[\frac{1}{Z_c} \left\{ \left[\frac{\text{Re}(V_{in}) + Z_c \text{Re}(I_{in})}{2} \right]^2 + \left[\frac{\text{Im}(V_{in}) + Z_c \text{Im}(I_{in})}{2} \right]^2 \right\} \right] + 30, \quad (3)$$

where $P_{forward}$ is the forward power in dB-milliwatts [dBm] and $P_{reflected}$ is the reflected power in dB-milliwatt [dBm].

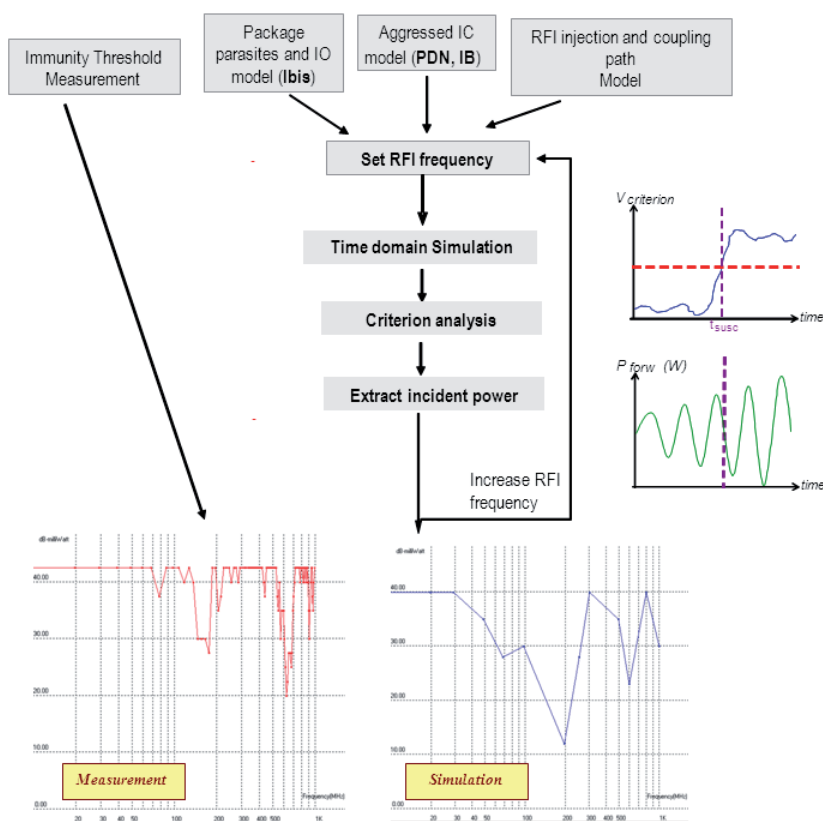


Figure 24. An example of susceptibility simulation process flow based on transient simulation [21].

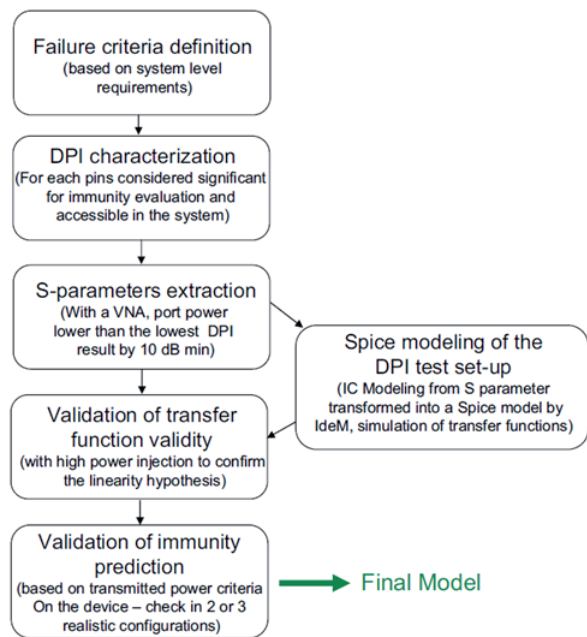


Figure 25. Direct power injection and S-parameter characterization are used to build a transfer function of the IC, later used for immunity prediction at the PCB level [22].

The power transmitted to the load can be derived from these formulations as follows:

$$P_{transmitted} = P_{forward} - P_{reflected} \quad (5)$$

3.3 Generic Flow for Immunity Prediction Using I, V Simulation

The general process flow used to achieve a comparison between susceptibility measurement and simulation using conventional analog simulators is described in Figure 24. On one side, the immunity measurement is performed using the standardized test bench [15] (direct power injection, bulk-current injection, near field, etc.). The result is usually in dB-milliwatt [dBm] as a function of frequency. To build the immunity simulation, we combine all sub-block models as discussed in Section 3.1. Transient simulation is performed, from which the forward and reflected powers are extracted for direct comparison with measurements.

The simulation process flow described in Figure 24 applies the same principle as harmonic immunity tests. The disturbance level is increased linearly for a given frequency during all the simulation duration, thanks to a sinusoidal programmable source. Forward and reflected powers are extracted from I, V transient simulations when the susceptibility criterion is reached [20].

An alternative approach was proposed by F. Lafon [22]. This consists of building a transfer function of the IC

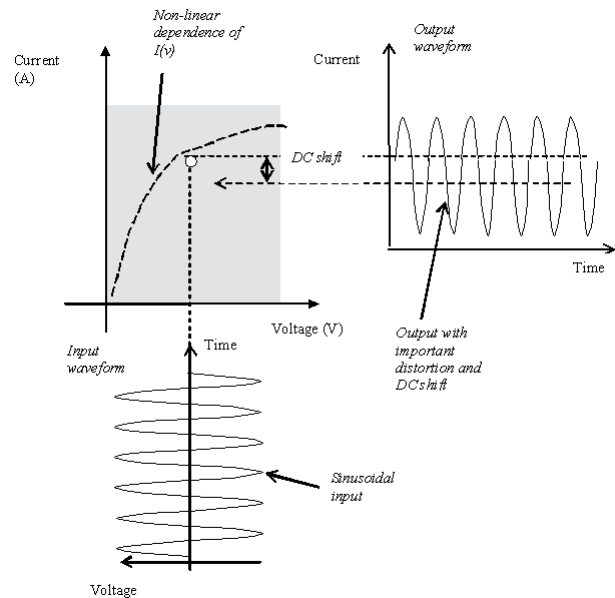


Figure 26. A nonlinear device may provoke a dc offset when a sinusoidal wave is superimposed onto a nominal voltage.

based on measurements, and then performing immunity simulation for investigation of the role of external components on the electronic board-level susceptibility (Figure 25). The immunity characterization is performed for significant IO pins (based on the direct-power-injection method in the example shown in Figure 10), and the S parameters are measured mainly on the supply rails, from which the transfer function is extracted. This approach enables predicting the immunity performance of the DUT when adding external components, such as RC filters, on critical pins. In this approach, knowledge of the internal structure and IC layout is not required. The intrinsic limitations of this approach are its inability to describe strongly nonlinear effects, and the need for S -parameter measurements prior to any immunity simulation.

Other approaches consist of simulating the IC's response to radio-frequency interference using transistor models, such as BSIM for nano-scale technologies [23]. These complex models rely on hundreds of parameters close to the technology and process, and are usually confidential. An alternative consists of describing the active-device models as voltage-controlled current sources, using a general equation such as Equation (6). The H_0 and H_1 coefficients characterize the linear dependence between the voltage, V , and the current, I . The nonlinear effects are introduced by coefficients H_2, H_3 , etc. Usually, the nonlinear modeling is limited to coefficient H_2 .

$$I(t) = H_0 + H_1V + H_2V^2 + H_3V^3 + \dots \quad (6)$$

When a sinusoidal radio-frequency interference is superimposed onto the nominal dc voltage, the current can be expressed by Equation (7):

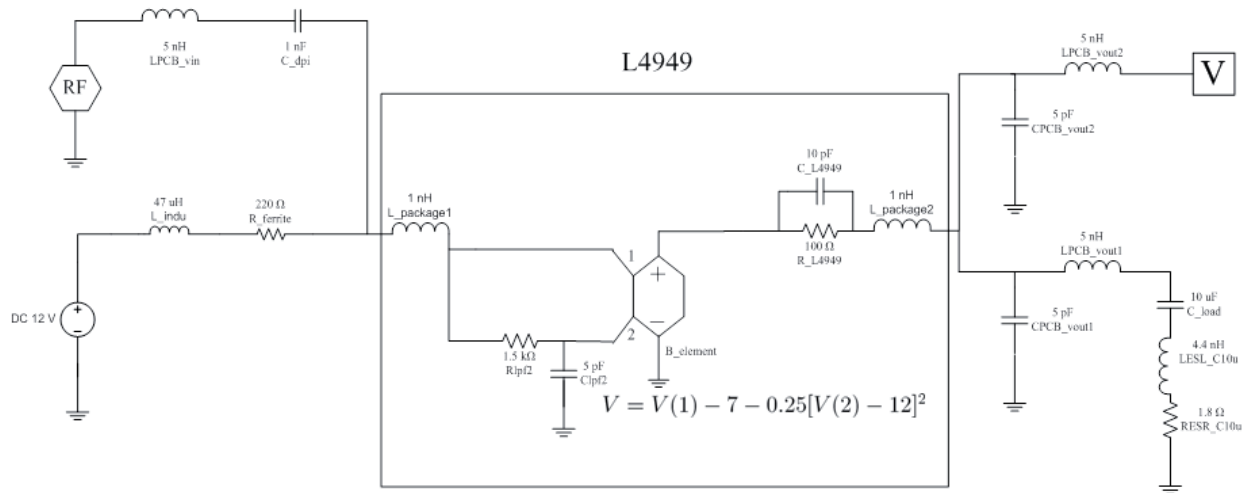


Figure 27. The nonlinear model of the voltage regulator based on a macro-model [24].

$$I(t) = H_0 + H_1 E \sin(2\pi ft) + \frac{H_2 E^2 [1 + \cos(4\pi ft)]}{2} \quad (7)$$

We can see a high-frequency component at $2f$ and a dc shift. Figure 26 clearly shows that the nonlinear device may provoke a dc offset as a consequence of the RF interference.

In [24], Wu showed a method for estimating the immunity of a low-dropout regulator by using macro-models operating in conventional transient simulation. There was good correlation with measurements up to 1 GHz (Figure 27). The RC filter at the input of the B element (a nonlinear current or voltage source in *SPICE*) was used to limit the rectification effect to the low-frequency range. As found in direct-power-injection measurements, the dc shift was significant below 100 MHz, while direct coupling through the IC's substrate and package dominated at high frequencies.

In most ICs, one critical aspect of immunity is linked to the input/output structures. These contain electrostatic-discharge (ESD) protection, including highly nonlinear

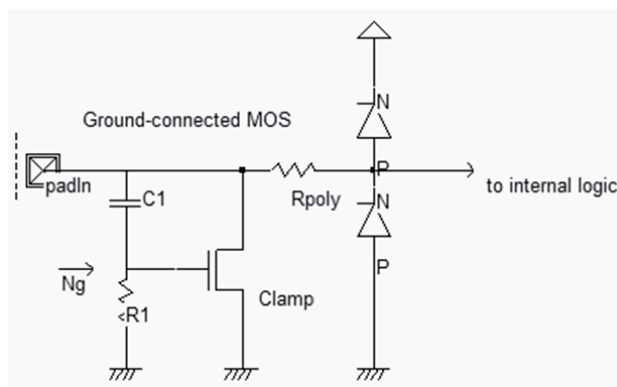


Figure 28. A ground-connected MOS used to protect against ESD.

diodes, as well as specific bipolar MOS devices, triggered by high-amplitude electrical overstress [25]. A power-clamp device for electrostatic discharge prevention is the gate-coupled NMOS, as described in Figure 28. It consists of two stages of protection: the first one handles the majority of the current, and the second one assists the first stage with relaxed stress constraints. The C1-R1 circuit is a high-pass filter. Although originally designed for ESD protection, an over-voltage such as that created by transient radio-frequency interference or high EMI harmonic interference induces a positive voltage on node Ng, which turns on the clamp MOS by capacitive coupling (Figure 29). A current path is established between the pad and the ground, until the voltage of Ng goes below the threshold voltage.

Figure 30 describes the general variation of the impedance as a function of frequency for each of the three families of I/Os: the inputs, the outputs, and the supplies.

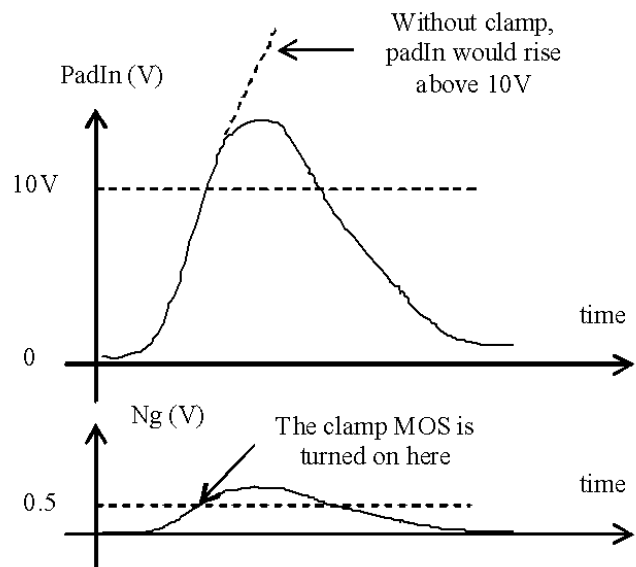


Figure 29. The ground-connected MOS may be triggered by a high-amplitude transient EMI, and shortcuts the over-voltage from the ESD pulse.

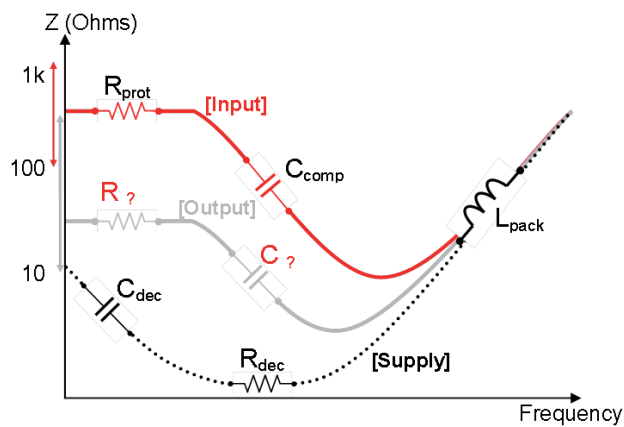


Figure 30. The impedance as a function of frequency for various types of I/Os.

At low frequencies (below 10 MHz), input pads have the highest impedance, due to ESD protection resistance. The power-supply impedance is the lowest, thanks to large on-chip decoupling. Below several MHz, inputs behave as capacitances. As such, their impedances decrease with frequency.

At high frequencies, the impedances of all types of I/O structures increase with frequency, due to the predominant effect of series parasitic inductances of the lead frames and bond wires. The IO models can be improved by impedance characterization and passive electrical-network identification, as well as from $I(V)$ characterization for an evaluation of nonlinear active elements.

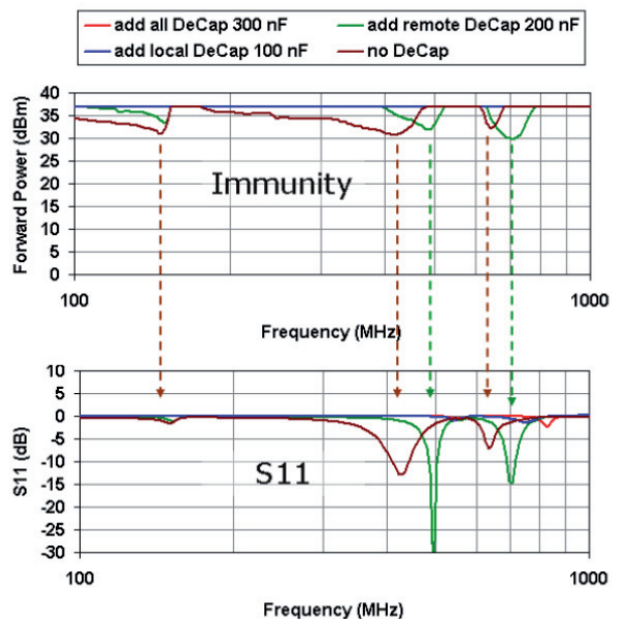


Figure 31. The correlation between the immunity and the S_{11} values measured at a core supply pin of the device [26].

3.4 Focus on Power-Distribution Network

In [26], Ichikawa highlighted the correlation between the susceptibility of the power-distribution network of a microcontroller and its impedance profile. A similar link between the IC's passive-distribution-network impedance and its immunity was established by Su in [27]. An

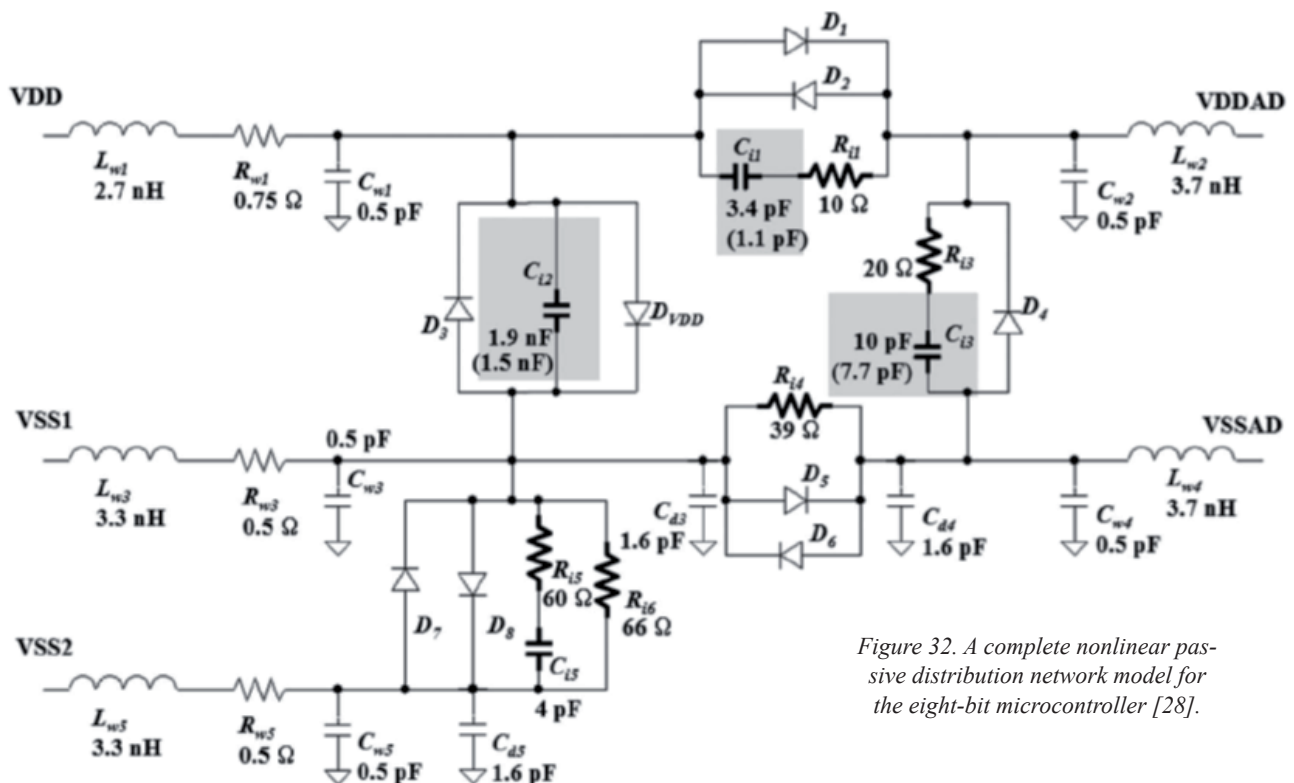


Figure 32. A complete nonlinear passive distribution network model for the eight-bit microcontroller [28].

	Conducted mode	Radiated mode
Emission	ICEM-CE <i>IEC 62433-2</i>	ICEM-RE <i>IEC 62433-3</i>
Immunity	ICIM-CE <i>IEC 62433-4</i>	ICIM-RE <i>IEC 62433-5</i>
	Impulse immunity <i>IEC 62433-6</i>	
Intra-bloc	Intra-bloc EMC <i>IEC 62433-7</i>	



Figure 33. EMC models (emission, immunity, intra-IC) according to the IEC 62433 definitions [11, 12].

application was done for a microcontroller. Four different strategies (Figure 31) of on-chip/off-chip decoupling on a given microcontroller die were characterized in terms of conducted immunity, showing a clear correlation between added high values of on-chip capacitance and high conducted immunity.

The construction of the passive-distribution-network model of an eight-bit microcontroller was described by Koo in [28]. One power network was dedicated to the core, and the second power network was dedicated to the analog-to-digital converter. As mentioned earlier, the immunity passive-distribution network differed from the emission passive-distribution network by the addition of several “back-to-back” diodes, which were used to limit voltage overstress between internal networks. These diodes featured a strongly nonlinear behavior, triggered by RF interference with voltage amplitudes above the threshold voltage, usually around 0.5 V. As mentioned by the authors, the capacitances

in the network changed with the supply voltage due to the nonlinear capacitance of P-N junctions, and due to the activation of MOS devices (Figure 32). This indicated that passive-distribution network impedance measurements at 0 V dc supply voltage may be significantly lower than those obtained at nominal dc voltages.

3.5 The Vision of the IEC

Within IEC Project 62 433, both emission and immunity modeling of ICs are being addressed (Figure 33). The Integrated Circuit Immunity Model (ICIM) under discussion in IEC technical committee TC47A is an extension for immunity of the ICEM emission model [11]. The ICIM model structure consists of two blocks [12]: a passive distribution network (PDN) and the internal behavior block (IB), as shown in Figure 34. The passive distribution network mainly consists of the power-distribution network,

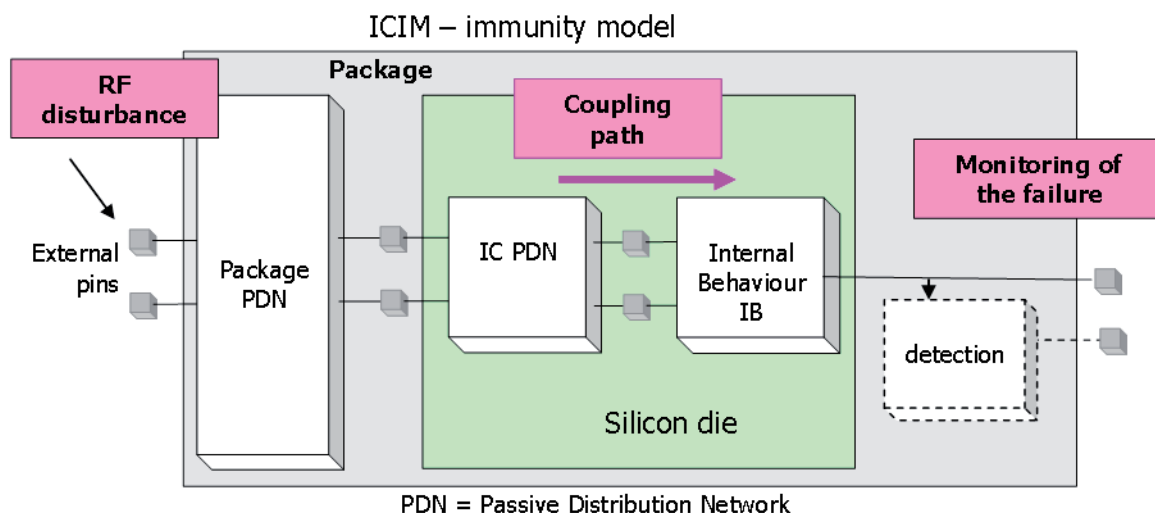


Figure 34. The generic structure of an immunity model in a conducted model [12].

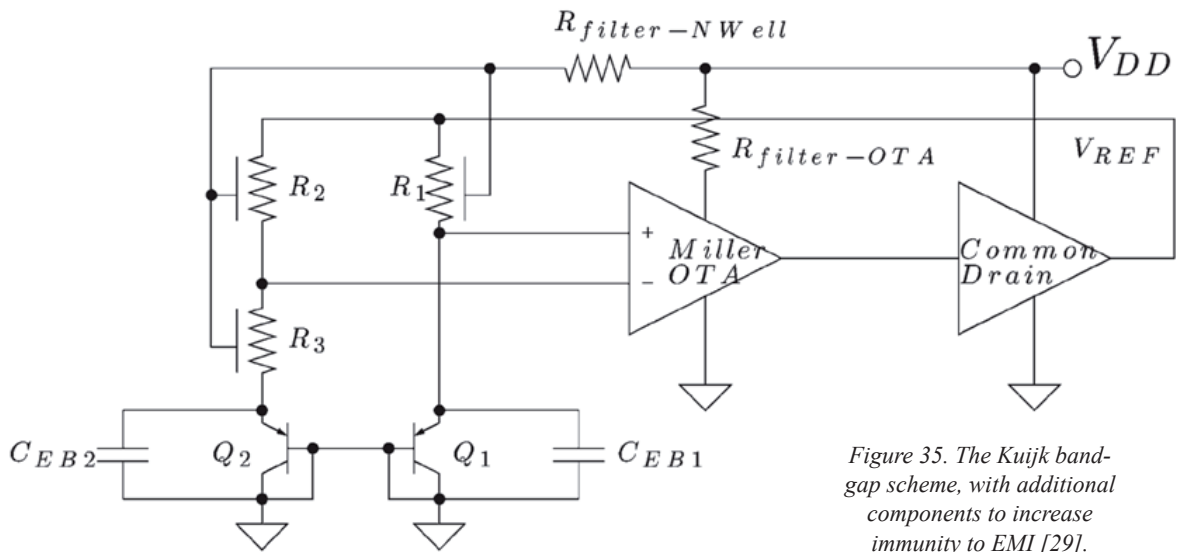


Figure 35. The Kuijk band-gap scheme, with additional components to increase immunity to EMI [29].

described either as a black box or by decomposition of passive elements R , L , and C . The novelty as compared to the ICEM model is the insertion of diodes in the passive distribution network, which may include electrostatic discharge (ESD) or electrical overstress (EOS) protection. The internal behavior block represents the behavioral response of the circuit to a radio-frequency disturbance.

The package and die impedances act as coupling paths for RF interference (V_{in} , I_{in}) to the active blocks, which can undergo a filtering effect and/or distortion through the passive distribution network and produce (V_r , I_r). The internal behavior block describes how the circuit reacts to

internal perturbations. This can be represented as (V_{out} , I_{out}) for monitoring the failure, either internally if some on-chip detection circuits are available, or off-chip using dedicated oscilloscopes or network analyzers.

4. Design Guidelines for Improved Immunity

This section aims at reviewing efficient design guidelines applicable to analog circuits, basic MOS switch functions, and logic circuits. A wide variety of approaches is proposed, including classical decoupling, filtering, isolation,

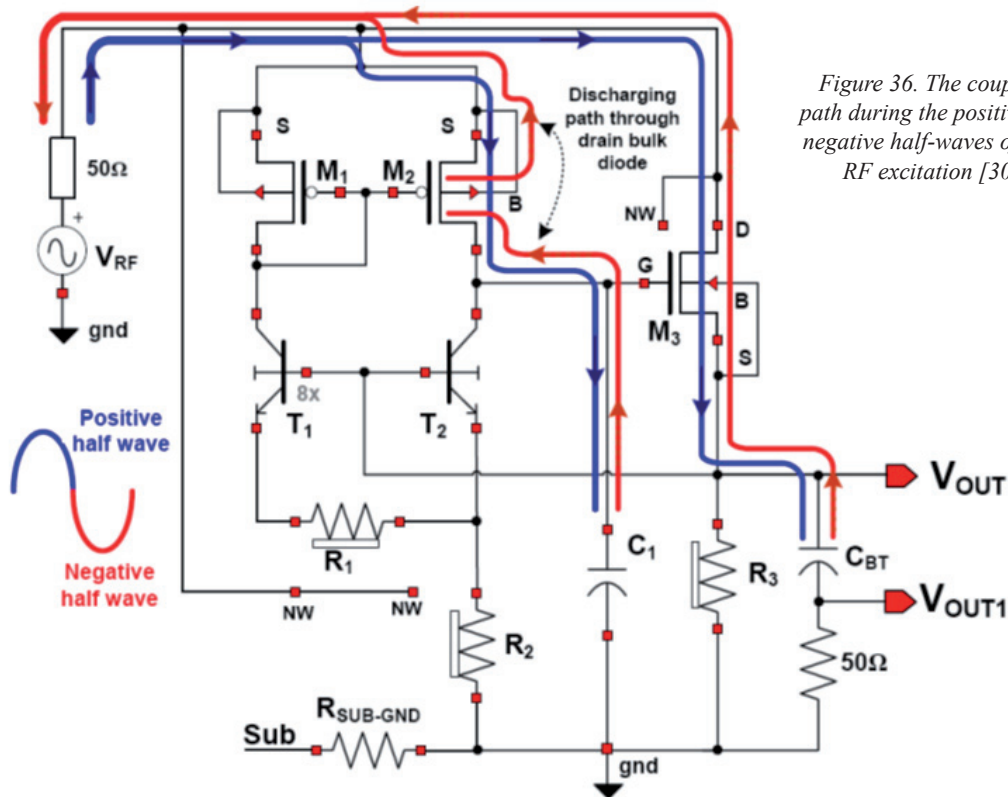


Figure 36. The coupling path during the positive and negative half-waves of high RF excitation [30].

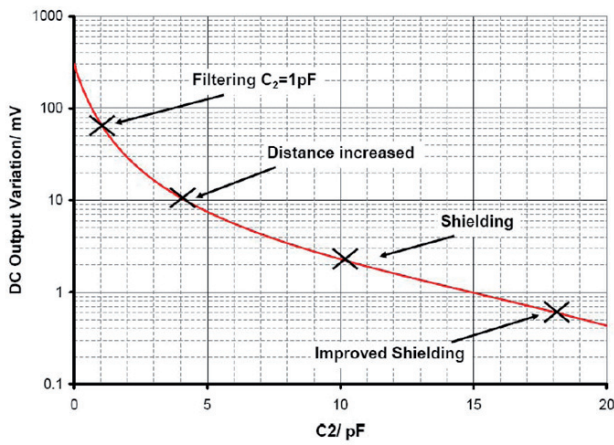


Figure 37. The impact of on-chip filtering capacitance and several other layout techniques on bandgap dc variation, for a direct power injection of 20 dBm at a frequency of 500 MHz [31].

and less-conventional techniques using improved designs, illustrated through working examples and experimental characterization. A recent book was published in 2009 by Redouté [5], where design methods that achieve a higher degree of immunity against EMI are described. We review here some of these design guidelines, and illustrate the main principles through recent publications.

4.1 Improved Immunity of Analog Integrated Circuits

4.1.1 Bandgap Circuits

Decreasing the susceptibility of a reference-voltage generator was demonstrated by Orietti [29], by adding a common-drain amplifier and decoupling capacitance (Figure 35). Direct power injection was used to perform immunity tests, and an electrical model of the circuit was also built to predict the immunity by simulation.

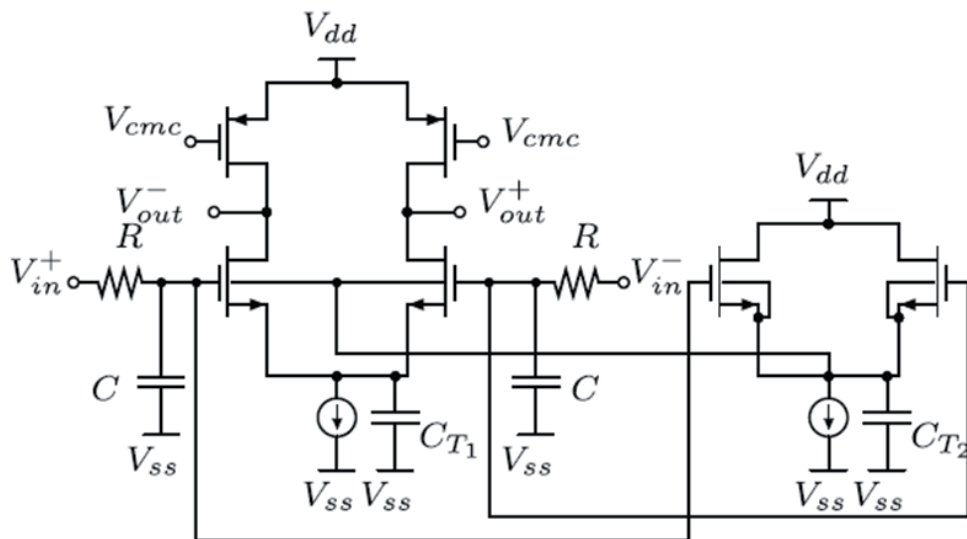


Figure 38. Improved operational-amplifier design, including RC input filtering and source buffering [32].

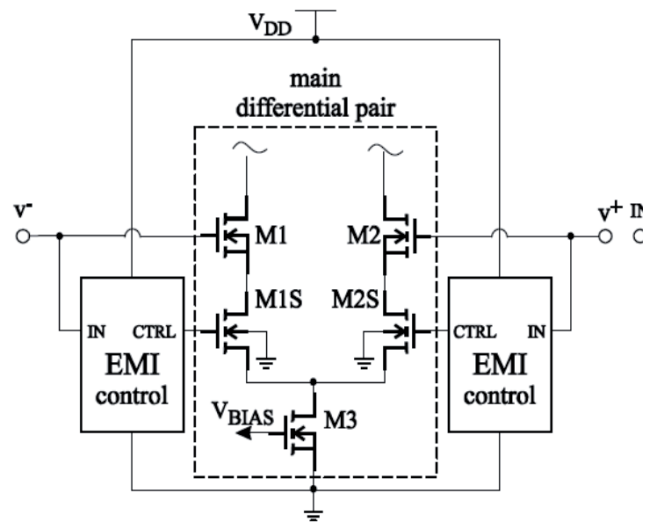


Figure 39. A schematic of the EMI-resisting differential pair [33].

Another type of voltage reference circuit was analyzed by Jovic [30] to again characterize the impact of radio-frequency interference superimposed on the power-supply voltage. The original topology was characterized. An improved version of the circuit was proposed that increased the resistivity of the coupling path and demonstrated a higher immunity, specifically from 100 MHz to 1 GHz (Figure 36).

In [31], different layout techniques that were supposed to improve the bandgap reference with respect to conducted radio-frequency interference were analyzed. The authors proposed to guard sensitive circuits from coupled RF disturbance by protecting sensitive wires from inductive and capacitive coupling with potential aggressor lines. In the situation depicted in Figure 37 (direct power injection of 20 dBm, 500 MHz), the benefits of on-chip filtering on a dc shift of the bandgap are evaluated. Isolation techniques, including increased distances between aggressor and victim wires, and conventional and improved shielding techniques are also shown.

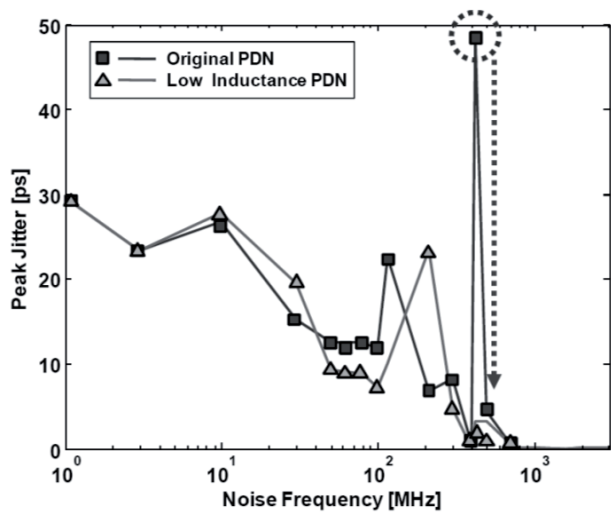


Figure 40. The power-supply noise-to-jitter transfer function of DLL for a low-inductance passive distribution network [34].

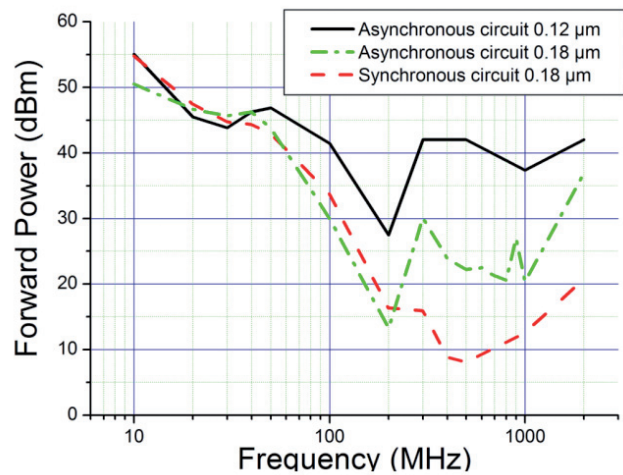


Figure 41. Measurements of the conducted susceptibility of synchronous and asynchronous versions of a crypto processor [35].

4.1.2 Operational Amplifiers

Different input topologies with resistance to electromagnetic interference (EMI) were analyzed and compared in terms of EMI reduction by Fridolin [32]. The emphasis in this study was put on solutions that strongly attenuated the EMI signal to the circuit, providing filtering, cancellation of perturbation effects, or providing buffering of reference voltages (Figure 38).

Similarly, an operational-amplifier input stage robust against high-power electromagnetic interference without any significant penalty in baseband performance was proposed by Crovetto [33]. A compensation of the disturbance signal at the AOP input was proposed (EMI control in Figure 39). At each input, a transconductance control network thus allows control of the input disturbance. Both measurements and simulations proved very significant immunity improvements from 10 MHz to 1 GHz up to 3 V radio-frequency interference amplitude.

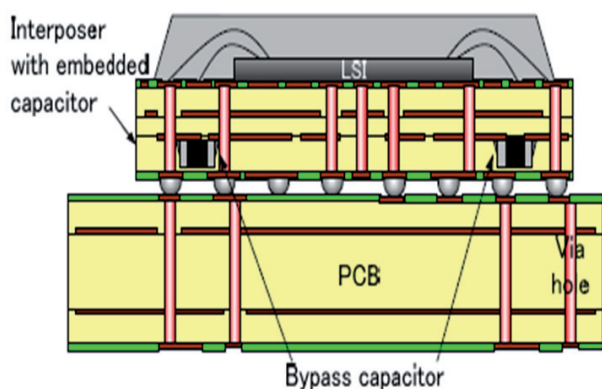


Figure 42. A two-dimensional cross section of the system-in-package (SiP) with embedded capacitor [36].

4.1.3 Oscillators

In order to reduce the sensitivity of an oscillator to conducted-mode interference on the supply network, Shin [34] added filtering capacitance and modified the inductance of the power-distribution network (PDN) of a delay-locked loop (DLL). As illustrated in Figure 40, the lowest peak jitter was obtained with the largest bias filter capacitor (34 pF), and for a low value of inductance. Note that in contrast to bandgap circuits where resistances are added in the supply, a low-inductance passive distribution network should be used for this type of circuit, according to the author.

4.2 Improved Immunity of Digital Integrated Circuits

As digital circuits are very sensitive to delay variations and supply-voltage variations, asynchronous circuit design may offer an interesting alternative for improving susceptibility. In [35], Bouesse compared the susceptibility of two versions of a crypto processor: one designed in a conventional synchronous way, and the other version designed in an asynchronous version. Figure 41 presents the susceptibility comparison of the two versions, featuring an immunity improvement of 30 dB from 200 MHz to 1 GHz, for the case of the 0.12 μm implementation. Notice that the asynchronous version was much more complex in terms of logic gates (by close to a factor of four).

In [36], Sasaki evaluated the immunity improvements thanks to embedded capacitors in the package of an image-processing LSI for digital television. Figure 42 depicts the two-dimensional cross section of the system-in-package, the embedded capacitor placement, and the benefits in terms of immunity. The immunity of the SiP was significantly improved around 100 MHz, but remained almost unchanged above 500 MHz. According to the authors, the immunity

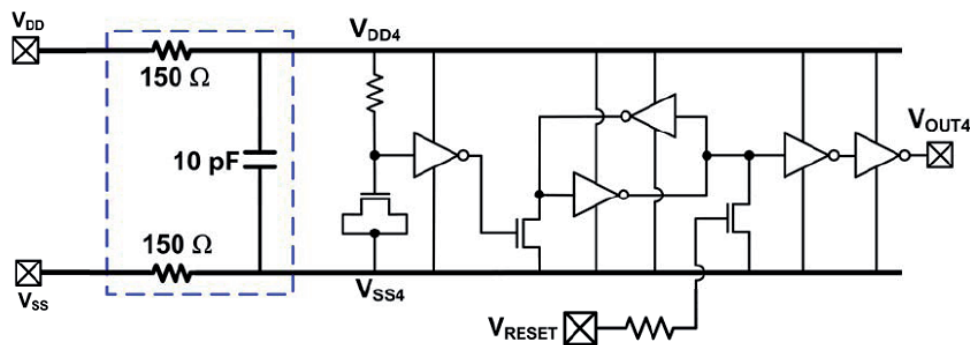


Figure 43. The proposed cell of an on-chip transient-to-digital converter for each bit [37].

characteristics could be improved over the entire frequency range, especially below 500 MHz.

The effectiveness of an on-chip RC noise filter to protect against high-amplitude electrical fast transients (EFTs) was analyzed by Yen in [37], based on an added decoupling capacitor and serial resistors on the internal supply network (Figure 43). The RC noise filter was used to reduce voltage fluctuations on V_{DD} and V_{SS} . Under a negative electrical fast transient voltage, V_{DD} decreased rapidly. V_{out} was simultaneously disturbed with a negative exponential voltage pulse coupled onto the V_{DD} power line. After the negative electrical-fast-transient-induced transient disturbance, V_{out} transitioned from 0 V to 3.3 V.

5. Conclusion

This paper has reviewed the recent publications related to the susceptibility of integrated circuits to radio-frequency interference. The general concepts of electromagnetic compatibility have been applied to the integrated-circuit level, with an evaluation of the impact of technology improvements on EMC performance of ICs. The most recent standards from the IEC in terms of measurement methods and modeling approaches applicable to the characterization and prediction of the immunity performance of ICs have also been described. Innovative measurement methods that could be potential candidates for future standardization have been reviewed. In terms of modeling, recent approaches defended by scientific experts have been reported. Some case studies covering logic, analog, and mixed blocks have been illustrated, showing an increased degree of understanding and knowledge of coupling paths and consequences of the functional behavior. Promising modeling approaches have been listed. The review also considered recent publications dealing with design guidelines for improved immunity, including novel design approaches for analog integrated circuits, and more-traditional filtering, decoupling, and protection approaches at the die and package levels for logic circuits. It should be noted that most publications have concerned measurements or modeling within the 1 MHz to 1 GHz band. Future work will require the extension of measurement standards and modeling approaches at least up to 10 GHz, which constitutes the next scientific challenge for the coming years.

6. References

1. E. Sicard, C. Marot, J. Y. Fourniols, and M. Ramdani, "Electromagnetic Compatibility for Integrated Circuits," in W. R. Stone (ed.), *Review of Radio Science: 1999-2002*, New York, Wiley/IEEE Press, 2002, pp. 453-472.
2. S. Ben Dhia, M. Ramdani, and E. Sicard, *Electromagnetic Compatibility of Integrated Circuits - Techniques for Low Emission and Susceptibility*, New York, Springer-Verlag, 2006.
3. J. J. Whalen, "Predicting RFI Effects in Semiconductor Devices at Frequencies Above 100 MHz," *IEEE Transactions on Electromagnetic Compatibility*, 21, 4, 1979, pp. 281-282.
4. M. Ramdani, E. Sicard, A. Boyer, S. Ben Dhia, J. J. Whalen, T. H. Hubing, M. Coenen, and O. Wada, "The Electromagnetic Compatibility of Integrated Circuits - Past, Present, and Future," *IEEE Transactions on Electromagnetic Compatibility*, 51, 1, 2009, pp. 78-100.
5. J. M. Redouté and M. Steyaert *EMC of Analog Integrated Circuits*, Berlin, Springer, 2009.
6. S. A. Boulingui, C. Dupoux, S. Baffreau, E. Sicard, N. Bouvier, and B. Vrignon, "An Innovative Methodology for Evaluating Multi-Chip EMC in Advanced 3G Mobile Platforms," *Proceedings of the IEEE Symposium on EMC*, Austin, 2009, pp. 145-150.
7. "International Technology Roadmap for semiconductors, Packaging and Assembly," available at <http://www.itrs.net>.
8. S. Borkar, "Design Perspectives on 22nm CMOS and Beyond," *46th ACM/IEEE Design Automation Conference*, 2009, pp. 93-94.
9. K. Choi, "Extremely Scaled Gate-First High-k/Metal Gate Stack with EOT of 0.55 nm Using Novel Interfacial Layer Scavenging Techniques for 22 nm Technology Node and Beyond," *2009 Symposium on VLSI Technology*, 2009, pp. 138-139.
10. "IBIS I/O Buffer Information Specification - Version 5.0," 2008, available at <http://www.eda.org/ibis/>.
11. "IEC 62433-2: Models of Integrated Circuits for EMI Behavioral Simulation - Conducted Emission Modelling," International Electrotechnical Commission, 2008, available at <http://www.iec.ch>.
12. "IEC 62433-4: Models of Integrated Circuits for EMI Behavioral Simulation - Conducted Immunity," International Electrotechnical Commission, 2009, available at <http://www.iec.ch>.

- 13.K. Saban, "Xilinx Stacked Silicon Interconnect Technology Delivers Breakthrough FPGA Capacity, Bandwidth, and Power Efficiency," 2011, available at <http://www.xilinx.com>.
- 14.R. Perdriau, O. Maurice, S. Dubois, M. Ramdani and E. Sicard, "Exploration of the Radiated Electromagnetic Immunity of Integrated Circuits Up to 40 GHz," *Electronics Letters*, **47**, 10, 2011, pp. 589-590.
- 15."IEC 62132-1: Integrated Circuits, Measurement of Electromagnetic Immunity, 150 KHz – 1 GHz: General Conditions and Definitions," International Electrotechnical Commission, 2007, available at <http://www.iec.ch>.
- 16.J.-L. Levant, J.-B. Gros, G. Duchamp, and M. Ramdani, "Resistive RF injection Probe Test Method," Proceedings of EMC Compo 09, Toulouse, France, 2009.
- 17.F. Grassi, F. Marliani, and S. A. Pignari, "Circuit Modeling of Injection Probes for Bulk Current Injection," *IEEE Transactions on Electromagnetic Compatibility*, **49**, 3, 2007, pp. 563-576.
- 18.A. Boyer, B. Li, S. Ben Dhia, and C. Lemoine "Impact of Aging on the Immunity of a Mixed Signal Circuit," Proceedings of EMC Europe 2010, Wroclaw, Poland, 2010.
- 19.F. Lafon, F. de Daran, L. Caves, M. Ramdani, and M. Drissi, "Influence of Aging and Environment Conditions on EMC Performances of Electronic Equipment," Proceedings of EMC Europe 2010, Wroclaw, Poland, 2010.
- 20.S. Ben Dhia, "IC Immunity Modeling Process Validation Using On-Chip Measurements," Proceedings of the IEEE Latin-American Test Workshop, Porto de Galinhas, Brazil, 2011.
- 21.E. Sicard and A. Boyer, *IC-EMC v2.5 User's Manual*, INSA Publishers, 2011, ISBN 978-2-87649-061-1.
- 22.F. Lafon, F. de Daran, M. Ramdani, R. Perdriau, and M. Drissi, "Immunity Modeling of Integrated Circuits – An Industrial Case," *IEICE Transactions on Communications*, **E93B**, 7, 2010, pp. 1723-1730.
- 23.W. Liu "Mosfet Models for SPICE Simulation Including Bsim3v3 and BSIM4," New York, John Wiley & Sons, 2001.
- 24.J. F. Wu, E. Sicard, A. Cissé Ndoye, F. Lafon, J. C. Li, and R. J. Shen, "Investigation on DPI Effects in a Low Dropout Voltage Regulator," Proceedings of EMC Compo 2011, Dubrovnik, Croatia, 2011.
- 25.S. H. Voldman, "ESD: Design and Synthesis," Chichester, UK, John Wiley & Sons, 2011.
- 26.K. Ichikawa, M. Inagaki, and Y. Sakurai, "Simulation of Integrated Circuit Immunity with LEECS Model," Proceedings of the 17th International Zurich Symposium on Electromagnetic Compatibility, 2006, pp. 308-311.
- 27.T. Su, M. Unger, T. Steinecke, and R. Weigel, "The DPI Immunity Behavior of Microcontrollers," Proceedings of EMC Compo09, Toulouse, France, 2009.
- 28.J. Koo, L. Han, S. Herrin, R. Moseley, R. Carlton, D. G. Beetner, and D. Pommerenke, "A Nonlinear Microcontroller Power Distribution Network Model for the Characterization of Immunity to Electrical Fast Transients," *IEEE Transactions on Electromagnetic Compatibility*, **51**, 3, 2009, pp. 611-619.
- 29.E. Orietti, N. Montemezzo, S. Buso, G. Meneghesso, A. Neviani, and G. Spiazzi, "Reducing the EMI Susceptibility of a Kuijk Bandgap," *IEEE Transactions on Electromagnetic Compatibility*, **50**, 4, 2008, pp. 876-886.
- 30.O. Jovic, W. Wilkening, U. Stuermer, and A. Baric, "Susceptibility of a Brokaw Bandgap to High Electromagnetic Interference," EMC Compo09, Toulouse, France, 2009.
- 31.P. Schröter and F. Klotz, "On Chip Filtering Versus Layout Techniques to Reduce RF Coupled Disturbances," IEEE International Symposium on EMC, Fort Lauderdale, USA, 2010, pp. 222-227.
- 32.M. Fridolin and S. Michiel, "Comparison of High Impedance Input Topologies with Low EMI Susceptibility," *Analog Integrated Circuit Signal Process*, **65**, 2010, pp. 299-309.
- 33.P. S. Crovetto and F. Fiori, "A CMOS Opamp Immune to EMI with no Penalty in Baseband Operation," Proceedings of the International Symposium on EMC, Kyoto, Japan, 2009.
- 34.M. Shin, C. Yoon, J. Cho, J. Shim, Y. Shim, and J. Kim, "Analysis of DLL Jitter Affected by Power Supply Noise on Power Distribution Network," Proceedings of International Symposium on EMC, Kyoto, Japan, 2009.
- 35.G. F. Bouesse, N. Ninon, G. Sicard, M. Renaudin, A. Boyer, and E. Sicard, "Asynchronous logic vs. Synchronous logic: Concrete Results on Electromagnetic Emissions and Conducted Susceptibility," Proceedings of EMC Compo 07, Torino, Italy, 2007.
- 36.C. Sasaki, Y. Saito, E. Takahashi, Y. Sugaya, and H. Kobayashi, "An Evaluation of the Immunity Characteristics of an LSI with Capacitors Embedded in an Interposer," IEEE International Symposium on EMC, Fort Lauderdale, USA, 2010, pp. 473-478.
- 37.C-C. Yen, M-D. Ker, C-S. Liao, T-Y. Chen, and C-C. Tsai, "Transient-to-Digital Converter for Protection Design in CMOS Integrated Circuits against Electrical Fast Transient," IEEE International Symposium on EMC, Austin, USA, 2009, pp. 41-44.

Radio-Frequency Radiation Safety and Health



James C. Lin

Are Radio-Frequency or Mobile-Phone Electromagnetic Fields Possibly Carcinogenic to Humans

The response to the recent International Agency for Research on Cancer (IARC) announcement that while incomplete and limited, the evidence is sufficiently strong to support a classification of possibly carcinogenic to humans for radio-frequency electromagnetic fields, was mixed, to say the least. Although the IARC's conclusion was not entirely unanimous, it acknowledged published scientific papers reporting increased risks for gliomas (a type of malignant brain cancer) and acoustic neuromas (a nonmalignant tumor of the auditory nerve on the side of the brain) among heavy or long-term users of cellular mobile telephones [1, 2].

A published summary of the IARC working group appears to suggest that while hundreds of scientific articles were reviewed, four papers played the most influential role in its conclusion [3]. These were the Interphone Study [4, 5], the Swedish pooled analysis [6], and an acoustic neuroma study from Japan [7]. The Interphone study reported increased risks of 40% for gliomas. They tended to be greater in subjects who reported usual phone use on the same side of the head as their tumor than on the opposite side of heavy users. A 270% increase in risk was found in the Swedish pooled analysis for the most common type of glioma, astrocytoma, for mobile-phone use longer than 10 years. A similar conclusion was reached from these two studies for acoustic neuroma, although the case numbers were substantially smaller than for glioma. The study from Japan found some evidence of an increased risk (from 10% to 300%) for acoustic neuroma associated with use of mobile phones on the same side of the head. However, it was acknowledged that these human epidemiological studies were susceptible to bias, or other methodological limitations such as detection or recall error and selection prejudice for participation. The working group concluded that the findings could not be dismissed as reflecting bias alone, and that a causal interpretation between exposure to mobile-phone radio-frequency electromagnetic fields and glioma or acoustic neuroma is possible.

However, what epidemiology gives, it also may take away.

Some other epidemiologists or groups of epidemiologists, reviewing the same data or papers, have concluded that the increased risk was entirely explicable by various biases or errors, believing that there is little possibility that mobile-phone use could increase the risk of glioma or acoustic neuroma in users.

For example, within the span of a month after IARC's announcement, the International Commission for Non-Ionizing Radiation Protection (ICNIRP's) Standing Committee on Epidemiology – which included two members from the Interphone group – published a lengthy commentary on the risk of gliomas [8]. With a particular focus on the recent publication of the Interphone study, the commentary concluded that within about 10 to 15 years after first use of mobile phones, there is unlikely to be a material increase in the risk of gliomas in adults. It is well to recall from brain-tumor incidence trends that the latency of brain-tumor development is considerably longer than 10 to 15 years. Furthermore, the commentary's focus on the most recent publications of the Interphone study was spotted on one of them [9]; unfortunately, this missed the other related Interphone study with the same objective [10].

It is interesting to note that these recent studies, two separate analyses [9, 10] from different members of the Interphone study group, appeared in print shortly after publication of the ICNIRP commentary. The objective of both analyses was to evaluate whether gliomas occur preferentially in the areas of the brain having the highest radio-frequency energy absorption from mobile-phone exposure. Indeed, these were the first papers to report estimates of absorbed radio-frequency energy at the center of tumors in the brain of mobile-phone users.

James C. Lin is with the University of Illinois-Chicago, 851 South Morgan Street, M/C 154, Chicago, IL 60607-7053 USA; Tel: +1 (312) 413-1052 (direct); +1 (312) 996-3423 (main office); Fax: +1 (312) 996-6465; E-mail: lin@ece.uic.edu.

One analysis included 888 gliomas between 2000 and 2004 from seven European Interphone study countries: Denmark, Finland, Germany, Italy, Norway, Sweden, and southeast England [9]. The tumor midpoints were defined by neuroradiologists on a three-dimensional grid, based on radiological images obtained from computerized X-ray tomography or magnetic-resonance imaging. The results did not indicate gliomas in mobile-phone users were preferentially located in the part of the brain with the highest deposition of radio-frequency fields from mobile phones.

In the other analysis, patients with brain tumors from the Australian, Canadian, French, Israeli, and New Zealand components of the Interphone study were considered [10]. Brain tumors localized by neuroradiologists were analyzed. The analysis included 553 glioma cases and 1762 controls. The mean age of the glioma cases was 47.2 years, and 62% were men. The total cumulative specific radio-frequency energy absorbed (in J/kg) at the tumor's estimated center was estimated by taking into account multiple radio-frequency exposures. An increased risk of glioma was seen at higher specific radio-frequency absorptions, above 3500 J/kg, corresponding to individuals with long-term and heavy use of mobile phones. The relative risk for glioma was 1.35 in subjects with localized tumor, and 1.66 in subjects with tumor centers estimated by a neuroradiologist. These results are suggestive of an increased risk of glioma in long-term mobile-phone users with high RF exposure. However, there are methodological and protocol uncertainties associated with tumor-center localization, RF energy-absorption estimation, and the sample size, which argue for caution regarding a causal interpretation of these results at the present time.

This is of course very perplexing, if not mystifying, even though there are methodological differences in these analyses. How is it that the same Interphone study produced two separate or different reports, in tandem, on the same subject matter, which conflicted with each other? Why two reports instead of one that combines and analyzes all the collected data? Are the mobile phones in use in Denmark, Finland, Germany, Italy, Norway, Sweden, and southeast England different from those popular in Australia, Canada, France, Israel, and New Zealand? Or are the brains or heads of Danes, Finlanders, Germans, Italians, Norwegians, Swedes, and southeast Englanders collectively different from those of Australians, Canadians, French, Israelis, and New Zealanders?

The skeptic may argue that science has become partisan. The corollary, if science becomes partisan: is it science or politics, or would it be political science?

That argument aside, the interval of observation (10 to 15 years) between the subjects' use of mobile phones and the occurrence of tumors might have been too short to allow detection of an effect, if there is one. Could it be unfair to ask or even expect these epidemiological studies to yield any authoritative conclusion, given the well-known long developmental latency for brain tumors?

References

1. "IARC Classifies Radiofrequency Electromagnetic Fields as Possibly Carcinogenic to Humans," IARC press release No. 208, Lyon, France, May 31, 2011.
2. J. C. Lin, "The Peculiar Circumstances of the IARC Working Group on Radio Frequency Electromagnetic Fields and Cellular Telephones," *IEEE Antennas and Propagation Magazine*, **53**, 3, June 2011, pp. 202-203; see also J. C. Lin, "Reply to Letter to the Editor," *IEEE Antennas and Propagation Magazine*, **53**, 5, October 2011, pp. 162-163.
3. R. Baan et al. (on behalf of the WHO International Agency for Research on Cancer Monograph Working Group), "Carcinogenicity of Radiofrequency Electromagnetic Fields," *The Lancet Oncology*, **12**, 7, 2011, pp. 624-626.
4. E. Cardis and the Interphone Study Group, "Brain Tumour Risk in Relation to Mobile Telephone Use: Results of the INTERPHONE International Case-Control Study," *International Journal of Epidemiology*, **39**, 3, 2010, pp. 675-694.
5. E. Cardis and the Interphone Study Group, "Acoustic Neuroma Risk in Relation to Mobile Telephone Use: Results of the INTERPHONE International Case-Control Study," *Cancer Epidemiology*, **35**, 5, 2011, pp. 453-464.
6. L. Hardell, M. Carlberg, and K. Mild Hansson, "Pooled Analysis of Case-Control Studies on Malignant Brain Tumours and the Use of Mobile and Cordless Phones Including Living and Deceased Subjects," *International Journal of Oncology*, **38**, 5, 2011, pp. 1465-1474.
7. Y. Sato, S. Akiba, O. Kubo, and N. Yamaguchi, "A Case-Case Study of Mobile Phone Use and Acoustic Neuroma Risk in Japan," *Bioelectromagnetics*, **32**, 2, 2011, pp. 85-93.
8. A. J. Swerdlow, M. Feychting, A. C. Green, L. Kheifets, and D. A. Savitz (International Commission for Non-Ionizing Radiation Protection Standing Committee on Epidemiology), "2011 Mobile Phones, Brain Tumors, and the Interphone Study: Where Are We Now?," *Environ. Health Perspect.*, **119**, 11, 2011, pp. 1534-1538.
9. S. Larjavaara, J. Schuz, A. Swerdlow, M. Feychting, C. Johansen, S. Lagorio, T. Tynes, L. Klæboe, S. Reidar Tonjer, M. Blettner, G. Berg-Beckhoff, B. Schlehofer, M. Schoemaker, J. Britton, R. Mäntylä, S. Lönn, A. Ahlbom, O. Flodmark, A. Lilja, S. Martini, E. Rastelli, A. Vidiri, V. Kähärä, J. Raitanen, S. Heinävaara, and A. [Auvinen](#), "Location of Gliomas in Relation to Mobile Telephone Use: A Case-Case and Case-Specular Analysis," *Amer. Journal of Epidemiol.*, **174**, 1, 2011, pp. 2-11.
10. E. Cardis, B. K. Armstrong, J. D. Bowman, G. C. Giles, M. Hours, D. Krewski, M. McBride, M. E. Parent, S. Sadetzki, A. Woodward, J. Brown, A. Chetrit, J. Figuerola, C. Hoffmann, A. Jarus-Hakak, L. Montestruq, L. Nadon, L. Richardson, R. Villegas, and M. Vrijheid, "Risk of Brain Tumours in Relation to Estimated RF Dose from Mobile Phones: Results from Five Interphone Countries," *Occup. Environ. Med.*, **68**, 2011, pp. 631-640.

[Essentially the same contribution appeared in the *IEEE Antennas and Propagation Magazine*, **54**, 1, February 2012, pp. 210-212; ©2012 IEEE.]

Radiowave Propagation

by Curt A. Levis, Joel T. Johnson, and Fernando L. Teixeira, New York, John Wiley & Sons, 2010,
ISBN 978-0-470-54295-8; 81,50€

It is our pleasure to have the opportunity to review this timely book on radiowave propagation, which will serve as an excellent text for senior-level engineering students as well as a useful reference for practicing engineers in the radar, communications, and remote-sensing fields. In contrast to other books on this subject – which are either mathematically terse, or tend to emphasize specific applications – the current text surveys the dominant propagation mechanisms pertinent to different applications in a pedagogical narrative, and provides first-principle derivations of the relevant mathematical equations. Such an approach is highly appealing to students and practitioners.

Chapter 1 opens with an illuminating discussion of the importance of propagation studies to system design. The chapter then provides a brief historical perspective, discusses the interrelated effects of the propagation medium and frequency on propagating signals, and identifies the dominant propagation mechanisms for different applications. A brief discussion of these mechanisms follows. The chapter closes with a summary that outlines the different applications of various propagation mechanisms, as well as the most applicable propagation mechanisms for each frequency band. On the topic of ducting, the authors state that this mechanism is most important at VHF and UHF on the basis that antenna beamwidths at higher frequencies do not couple into atmospheric ducts as efficiently. However, for terrestrial links and surface-based radar systems, ducting has an enormous impact, because these systems often operate at very low elevations and they couple into the ducts very well at frequencies up to 10 GHz and beyond. A recommendation is to broaden the applicable systems for which ducting is a very important phenomenon to include terrestrial communications and radar systems, particularly in coastal and marine environments.

Chapter 2 provides a concise overview of the important material characteristics of propagation media encountered in practical propagation scenarios. Special emphasis is given to the frequency-dependent behavior of dispersive media. Both conduction and polarization losses in materials are introduced, and their macroscopic equivalence is established.

Chapter 3 outlines the fundamental concepts pertaining to plane-wave propagation in simple media, as well as in lossy and dispersive media. The subjects of phase and group velocities are then introduced, followed by a concise discussion of wave polarization.

Chapter 4's development of the receiving-antenna concepts based on generalizing the equations of a short dipole is more appealing to undergraduate students and practicing engineers. The usual, more-rigorous development using the reciprocity theorem/equivalence principle is more suitable for graduate students. The development of the receiving-antenna concepts is followed by a succinct discussion of internal system noise, external noise, and source brightness temperature.

Chapter 5 delineates the classical derivation of the Friis transmission formula for direct transmission. An illuminating discussion of the frequency-dependent atmospheric-loss mechanisms follows. The section on rain attenuation provides a comprehensive discussion on this topic, and includes sample calculations, based on ITU-R Recommendations, for Earth-satellite and terrestrial paths through rain. The concept of site diversity is also introduced and demonstrated, which is very useful. Compared with the rain-attenuation section, the gaseous-attenuation section is much more concise, and relies on the reader referring to the noted ITU-R Recommendations. A brief discussion of the Lorentzian function approach to loss due to water vapor and oxygen would have been useful. Such a summary is presented in Chapter 5 of Ulaby, et al., *Microwave Remote Sensing: Active and Passive, Volume 1* (Reading, MA, Addison-Wesley, 1981).

Chapter 6 introduces the subjects of reflection and refraction, and provides a first-principles derivation of the polarization-dependent Fresnel reflection coefficients for normal and oblique incidence. A simple derivation of Snell's law of refraction in a spherically stratified atmosphere is then given, followed by a discussion of the effective-Earth-radius approximation. The discussion of the different atmospheric refractive conditions and various duct types that follows is highly instructive. Some of the qualitative comments on ducting could be a bit more precise, particularly regarding frequency dependence of the various duct types, but the discussion is generally accurate. More discussion of the differences in refractive conditions experienced in marine versus over-land situations would be useful. Figure 6-14c presents a notional evaporation duct, and this type of profile is generally represented by a log-linear shape, rather than the two-segment profile shown. Section 6.9 provides a basic description of a ray-tracing recipe. It seems that the term under the square root in Equation (6.109) needs to be replaced by its absolute value.

Chapter 7 delineates the basic physical mechanisms of multipath interference due to terrain reflection. It introduces the concept of Fresnel zones, describes the construction of path profiles and the effect of Earth curvature of these profiles, and outlines the principles underlying the design of a microwave link. Effects of diffraction of received power by terrain obstructions are then quantified through the canonical examples of diffraction by a spherical surface and knife-edge diffraction. The chapter concludes by introducing numerical methods used for path-loss analysis, the most popular among those being the parabolic-equation (PE) method. Further discussion of the parabolic-equation method, along with additional end-of-the-chapter references, is highly recommended for the second edition of the book. The use of the Method of Moments (MoM) for path-loss prediction is also briefly discussed. It should be pointed out that the use of the MoM is generally limited to a homogeneous atmosphere. Attempts to couple the MoM with the parabolic equation to accommodate a variable atmospheric refractivity are reported in the literature.

Chapter 8 introduces empirical methods for calculating median path loss, as well as slow and fast channel fading. The probability theory concepts necessary for the statistical description of fading are succinctly covered. The distinction between the techniques used to characterize narrowband compared to wideband fading is made, and the use of channel diversity for narrowband-fading mitigation is clearly described. The concepts of channel equalization, coherence bandwidth, delay spread, coherence time, and Doppler spread are briefly outlined. The details of these topics are beyond the scope of the book, and a list of end-of-the-chapter references is provided for further study. This chapter serves as a good introduction for undergraduates to empirical models, as well as a quick refresher of these models for the practitioner. The calculations pertaining to median path loss and fading presented in the chapter are directly applicable to realistic propagation scenarios.

Chapter 9 deals with the fascinating subject of groundwave propagation. The authors rightfully point out that the mathematical details pertaining to this subject are not for the faint-hearted. Consequently, the chapter focuses on presenting practical mathematical formulas that represent the end results of the tedious mathematical analysis undertaken by several researchers. Also in the introduction, the authors state that groundwave propagation dominates during the daytime, and skywave propagation dominates at night. While it is true that nighttime may bring long-range interference into an HF receiver (e.g., an AM radio at night), system designs typically select groundwave or skywave based on the terrain and desired ranges, rather than daytime/nighttime operation. In the case of radar applications, groundwave is used over the sea out to 150 km or so, and much-longer-range propagation is supported (in different modes) by skywave. The pivotal role of the numerical distance parameter in groundwave calculations is clearly delineated in the chapter. Groundwave

attenuations as a function of distance, polarization, and frequency for a planar Earth and for antennas sufficiently close to the ground are completely characterized by the numerical distance parameter. Modified formulas for the calculation of groundwave propagation involving elevated antennas are also presented. The subject of groundwave propagation over a spherical Earth is then introduced. The expression for the complex field associated with non-line-of-sight propagation between antennas over a spherical Earth is provided and discussed. Methods for approximate groundwave calculation are delineated, and worked examples at both 1 MHz and 10 MHz are presented. It is well known that the subject of groundwave propagation triggered a long-standing controversy in electromagnetic theory. It is the experience of the reviewers that students are usually fascinated by this topic, and we feel that a high-level account of this controversy in a future edition of the book would be a well-received addition. An excellent reference in this regard is the seminal 2004 paper by the late Prof. Robert E. Collin. The reviewers would also like to point out that some parabolic-equation models correctly represent groundwave (surface-wave) propagation for most situations, including rough surfaces. This is demonstrated in published literature and summarized in M. Levy's book *Parabolic Equation Methods for Electromagnetic Wave Propagation* (IEE Electromagnetic Waves Series 45, 2000).

Chapter 10 provides a systematic derivation of the electron number density in the ionosphere based on the Chapman theory. This is followed by a discussion of the different ionospheric regions, their daytime and nighttime characteristics, and their impact on HF communications. Ionospheric variability in the electron number density due to seasonal variations of the sun's zenith angle, atmospheric motion, and variations in the solar flux is then discussed in an informative fashion.

Chapter 11 delves into the subject of ionospheric propagation. Without resorting to tensor analysis, the authors manage to provide a first-principle derivation of the Appleton-Hartree equations describing the dispersion relation governing allowable ionospheric modes. A discussion of the so-called ordinary and extraordinary waves follows. The use of ionosondes for mapping the ionospheric conditions is then discussed, and data from deployed ionograms is presented and discussed. Theorems needed to facilitate the overlay of ionogram measurements (virtual heights versus vertical frequencies) and transmission curves are derived from first principles. The resulting graphs are then used to define important channel parameters, such as maximum usable frequency and skip distance. A brief discussion of ionospheric signal dispersion, absorption, and scintillation due to small-scale ionospheric irregularities follows. The chapter also provides a short description of the available ionospheric prediction tools and their capabilities.

The book closes with a discussion of other propagation mechanisms that were mentioned in passing in earlier chapters, namely tropospheric scatter and meteor scatter.

Our overall impression of the book is very good. It is highly recommended for any RF engineer who is concerned with the effects of the propagation channel on his or her system's performance. An excellent feature of the book is the frequent references to the recommendations of the Radiocommunication Sector of the International Telecommunication Union (ITU-R). We think that a well-designed set of end-of-chapter exercises and additional

worked examples are needed in future editions, to maximize the effectiveness of the book as an undergraduate textbook.

Reviewed by:
Ra'id S. Awadallah and G. Daniel Dockery
Johns Hopkins University Applied Physics Laboratory
Laurel, MD 20723 USA
E-mail: Dan.Dockery@jhuapl.edu

Book Review by an URSI Young Scientist

Antennas for All Applications, Third Edition

by John D. Kraus and Ronald J. Marhefka, New York, McGraw-Hill, 2002, 960 pp.; ISBN: 978-0072321036

Antennas, an integral part of wireless systems, can effectively transmit and receive electromagnetic signals in specified spectra, directions, and polarizations. State of the art antenna technologies have incredibly changed everyone's daily life, such as through communications, entertainment, defense, and many other applications. The field of antennas is a continually active field, considering the annual large volume of journal publications and conference proceedings, as well as courses for both undergraduates and graduates. Among the textbooks in widespread use, this book by John D. Kraus and Ronald J. Marhefka is preferred for its application orientation and illustrative explanations, avoiding troublesome mathematics. The authors also share some valuable experiences in their pioneering research, design, and engineering work.

Prof. Kraus is widely known as the inventor of the helical beam antenna and the corner-reflector antenna for early satellites. For his outstanding contributions, he was elected to the US National Academy of Engineering, and received many awards. Dr. Marhefka played a key role in the development of the *Numerical Electromagnetics Code—Basic Scattering Code (NEC-BSC)*, which has been widely used for the design of various antenna systems.

This book could be ideally divided into two parts. The first twelve chapters present preliminary knowledge. With suitable trimming they could perfectly fit a one-semester course. The last twelve chapters introduce the theoretical and numerical treatments, several advanced antennas, and system integration. Selected references for further readings could facilitate young scientists in starting new research.

The first three chapters deal with the fundamentals. More specifically, Chapter 1 introduces the units, symbols, and notations in this book. The antenna basics, including bandwidth, pattern, field, and polarization, are detailed in Chapter 2, which could be frequently used as performance criteria. Chapter 3 briefly introduces the families of antennas. With the help of the illustrations, one can get familiar with many antennas, and soon remember their characteristics.

Chapters 4 and 5 describe the point source and some interesting findings when point sources are arrayed.

Undoubtedly, the point source makes an important assumption in theory, and directly leads to the development of arrays, which substantially boost the capabilities of current antennas.

Chapter 6 begins with the short electric dipole, and then mathematically deduces its fields for the general and far-field cases. With these equations, other parameters such as the radiation pattern and radiation resistance can be easily obtained. The remaining part of Chapter 6 introduces more practical linear antennas, such as the half-wavelength dipole and traveling-wave antennas. Loop antennas are discussed in Chapter 7. The reader soon finds that the small loop has very similar characteristics to the short dipole, and the Duality Principle may be understood, although it is not included in this part.

Chapter 8 introduces the helical antenna, including the original design, operating modes, design considerations, and applications. Chapter 9 introduces a categorized group known as aperture antennas, including the slot, patch, and horn antennas. The governing theory, Babinet's Principle, is discussed in an illustrative way, and thus the physical fundamentals and characteristics of various slot antennas can be easily understood. Chapter 10 explains how to achieve directional patterns with higher directivity by flat, corner, and parabolic reflectors. Broadband antennas are discussed in Chapter 11, and then the frequency-independent antennas are introduced along with Rumsey's Principle. The first part is concluded in Chapter 12, dealing with antenna temperature, remote sensing, and radar cross section.

Chapter 13 starts with the Reciprocity Theorem, which shows the identity of the transmitting and receiving patterns for any antenna under certain conditions. The self and mutual impedances of thin linear antennas are discussed through an approximated surface-current distribution. More-general cases, such as the thick cylindrical, spherical, and conical antennas, are examined in Chapter 14 through the Method of Moments.

Chapters 15 and 16 present several advanced topics involving the radiation capabilities of continuous apertures and their discrete samplings (arrays). This solves the issues

of what kind of aperture distributions can provide a desired radiation performance, and how to achieve this through array technologies. The effects of the ground on radiation patterns are explored, and then heavy materials are arranged to briefly introduce the most popular arrays.

Chapter 17 begins with Fermat's Principle, describing the path rule for electromagnetic waves in a dielectric. This is followed by the dielectric, metal-plate, helical, and Luneburg lenses. Chapter 18 discusses the wave-propagation characteristics of frequency-selective surfaces for radome applications, which includes the dipole, slot, and hybrid types, and the cases with oblique angles of incidence.

Chapters 19 to 22 present a series of seminars on design issues and considerations, such as the most famous

large aperture antennas around the world, THz antennas, and about thirty other antennas. The book is concluded after the introduction of baluns and antenna measurements, followed by a rich set of tools in the Appendix.

This book would be a decent textbook for college students, and a helpful resource for researchers and professionals working with antennas. It also has a large popularity in China since the publication of the Chinese version, translated by Prof. Wenxun Zhang from Southeast University.

Reviewed by:
Dr. Qi Wu
Beihang University
E-mail: qwu@buaa.edu.cn

Letter to the Editor

Comments on the Review of Fundamentals of Wave Phenomena

In the review of our book, *Fundamentals of Wave Phenomena*, [*Radio Science Bulletin*, No. 337, June 2011, p. 72] there appear to be some misunderstandings on the part of the reviewer, Dr. Klaus Wilhelm.

- This particular book was not "edited" by the authors, it was "written" by the authors.
- The book is meant to be a textbook for undergraduates and beginning graduate students. As such, one should not expect that it would provide profound results for the professional, only a coherent interpretation of the physical phenomena for students.
- Concerning the use of the MKS rather than SI notation in the preface: this was a choice of the authors, who view the two as being synonymous. In fact, the system is often referred to as the MKSA system of units. In addition, symbols such as Å are of common use in optics, even though they are not a standard SI unit. The symbol ϵ is reserved for the dielectric constant rather than for the exponential term. The letter e is reserved for the charge of the electron. The symbols are defined in the appendix.
- The notation for the square root of -1 is different in the disciplines of engineering (j) and mathematics and physics (i).
- The tsunami is just an example of a nonlinear wave and it was not presented in detail in this text, therefore it was not included in the index.

- The reviewer suggests that Equation (8.9) is incorrect. We disagree. Equation (8.9) is correct for a small relative velocity between the source and observer when all velocities (wave velocity, source velocity, and observer's velocity) are aligned in the same direction. The equation below Equation (8.9),

$$v' = \frac{\sqrt{1-(u/c)^2}}{1-(u/c)\cos\theta} v_0$$

is for the case when a source is approaching an observer with velocity u at an angle θ relative to the direction from the observer to the source. In terms of the wave-emission angle, θ_s , in the reference frame of the source, the Doppler-shifted frequency can alternatively be given by

$$v' = \frac{1+(u/c)\cos\theta_s}{\sqrt{1-(u/c)^2}} v_0.$$

The two angles θ and θ_s are related through

$$\cos\theta = \frac{\cos\theta_s + \beta}{1 + \beta\cos\theta_s},$$

where $\beta = u/c$.

- The reviewer suggests that Equation (15.59) is incorrect. This particular nonlinear resonance phenomenon for solitary waves and solitons in higher dimensions was originally predicted by Miles (*J. Fluid Mech.*, **79**, 1977, p. 171) with relation to shallow-water waves, and is described with the higher-dimensional KdV or KP equation. Although the theoretical description in the book is of the “back of the envelope” type, it has been verified using inverse-scattering theory for the resonance of two, three, and four equal-amplitude solitons, where the new soliton will have an amplitude of four, nine, and 16 times the initial soliton, respectively. The results of this prediction have been verified in laboratory experiments performed in plasma physics

and in water-wave experiments (see, e.g., *Chin. Phys. B*, **20**, 2011, 015205, and references therein).

- The suggestions that the Poynting theorem can be used to illustrate how a resistor would start to heat is a “back of the envelope” derivation to hopefully increase the physical intuition of the reader.

Akira Hirose
E-mail: akira.hirose@usask.ca

Karl E. Lonngren
E-mail: lonngren@engineering.uiowa.edu



INTERNATIONAL REFERENCE IONOSPHERE (IRI) WORKSHOP 2011

Hermanus, South Africa, 10 - 14 October 2011

The 2011 IRI Workshop was hosted by the Space Science Directorate of the South African National Space Agency (SANSA), SANSA Space Science, formerly the Hermanus Magnetic Observatory (HMO), in Hermanus, South Africa. The meeting took place from October 10 to 14, 2011 and was attended by 60 participants representing 20 countries including a sizable group of attendees from African countries (16 representing 7 countries). The special emphasis of the 2011 workshop was on improving IRI over the African Region. The 65 presentations were grouped into sessions on IRI in the African Sector: Topside Ionosphere: Storm-Time and Real-Time IRI; F Peak Height and Density; TEC and related Parameters; The Ionosphere and IRI During the Recent Solar Minimum; Lower Ionosphere; Inputs for IRI; IRI Applications; and Final Discussions. The workshop has received financial support from COSPAR, URSI, NSF, SANSA, Cape Town Routes Unlimited, and the Overstrand Municipality.

The meeting provided an excellent opportunity to review the many IRI-related science and educational activities in Africa and to focus on shortcomings of the IRI model over this large and important longitude sector. Most of the research activities reported at this meeting were based on ionospheric parameters deduced from ionosonde and GPS measurements. But there were also important contributions that relied on satellite sounder and in situ measurements including data from the older Alouette and ISIS topside sounders and from the more recent TIMED and C/NOFS satellites. It became quite clear that additional work is needed to more accurately represent the African zone and particular the Equatorial Ionization Anomaly (EIA) region in IRI.

An important event during this workshop was the presentation of the latest version of the IRI model, IRI-2012 (Bilitza, USA). This new version includes several improvements and new additions: (1) A better representation of the bottomside electron density profile based on the work of Altadill, Blanch, and Torta (Spain) with a large volume of worldwide ionosonde data; (2) A better representation of the profile of molecular ion composition in the bottomside ionosphere based on normalizing the photochemistry from the FLIP model with the IRI electron density (Richards and Bilitza, USA); A new model for the electron temperature that now accounts also for solar activity variations based on a large volume of in situ measurements (Truhlik, Bilitza, and

Triskova, Czech Republic and USA); Inclusion of auroral boundaries and their movement with magnetic activity based on the TIMED/GUVI model of Zhang and Paxton (USA); Adding a model describing storm effects in the E region based on TIMED/SABER data (Mertens, USA); Using the latest model version for the Earth's magnetic field (International Geomagnetic Reference Field, IGRF-11) and the Earth's atmosphere (NRL-MSIS-00 model of Picone and Drob, USA); Inclusion of Corrected Geomagnetic Coordinates (CGM) (Papitashvili, USA) and of several additional solar indices: F10.7 daily, 81-day, 12-month running mean, and PF10.7. Workshop participants received a beta version of the IRI-2012 Fortran code and will help to test the new code before it is officially released later in the year.

Storm-time conditions and the quality of IRI predictions were studied in a number presentations based on ionosonde measurements (Buresova, Czech Republic; Oyeyemi, Nigeria; Pietrella, Italy; Pezzopane, Italy; Ngwira, South Africa; Cherniak, Ukraine). The need for a Real-Time IRI (IRI-RT) becomes very clear from these presentations. A possible approach was presented by Galkin (USA) assimilating data from the digisonde network into IRI (GIRO). But most storm-modeling is so far limited to the F2 peak density, although it is clear that the peak height (hmF2) is also severely affected by the storm (Buresova; Ngwira). A first step towards a better representation of hmF2 in IRI was presented by Altadill (Spain) who introduced a global model for the quiet-time hmF2 based on a large volume of values scaled from ionograms. This is an important improvement because in the current IRI hmF2 is obtained indirectly through its relationship with the propagation factor M(3000)F2 also scaled from ionograms.

The talks presented at this meeting made use of a number of data sources including ionosondes, GPS, COSMIC, ISIS, ISS-b, Hinotori, CHAMP, C/NOFS, TIMED, Demeter, and DMSP. Like in earlier workshops ionosondes were the prime data sources including data from African stations (McKinnell, Mbambo, Sessanga, South Africa; Oyeyemi, Nigeria; Ahoua, Ivory Coast), European stations (Buresova; Altadill; Pietrella; Mosert; Bilitza), Argentine and Antarctic stations (Mosert; Gularte), Chinese stations (Wang; Shi), Indian stations (Srinivas), Brazilian stations (de Souza and Bilitza) and Thai stations (Wichaipanich; Kenpankho). Studies of spread-F occurrence

over Thailand (Wichaipanich) and over China (Shi) are bearing promise for a future extension of the IRI spread-F model from currently the Brazilian longitude sector to a global model. Another widely used data source were GPS-TEC measurements including data from ground receivers located in China (Wang; Shi), Argentina (Mosert), Russia (Zakharenkova) and in several African countries (Olwendo, Kenya; Ochieng, Kenya; Okoh, Nigeria; Mbambo, South Africa; Cilliers, South Africa). The data were used to evaluate IRI over the respective region and to point out times and regions where improvements are needed. Tomographic techniques have evolved to the point where they can help to get information for the IRI peak and profile models (Chartier, UK). The IGS IONO group continues its role as main liaison between the GPS and IRI community and as producer of the definitive GPS TEC maps and new products like the ROTI index (Krankowski, Poland). New initiatives in Argentina bear great potential for future inputs to IRI modeling (Gularte, Argentina) including the Argentine Network for the Study of the Upper Atmosphere (RAPEAS) and the Argentina Ionospheric Radar Experiment Station (AIRES).

An important topic was the investigation of IRI performance during the recent very low and extended solar maximum using ionosonde data (Fuller-Rowell; Bilitza; Buresova), C/NOFS data (Klenzing, USA), and GPS TEC (Cherniak; Cilliers). Since there is good agreement at the F-peak, the discrepancy found above the peak with C/NOFS and CHAMP satellite measurements must be due to an overestimation in IRI of hmF2 and/or the topside shape. CHAMP and C/NOFS data will help to introduce the required improvements into IRI.

The IRI team continues its involvement and support of international science unions. The International Telecommunication Union (ITU) and the International Union of Radio Science (URSI) have asked the IRI team to help facilitate the science transfer from URSI studies to ITU recommendations. IRI was invited to present the IRI F-peak mapping status and plans at the ITU-R meeting

in Genève in October 17-21, 2011 (Reinisch, USA). IRI is also actively involved in efforts by the International Standardization Organization (ISO) to establish ISO standards for the Near-Earth space environment. The IRI-ISO standard document has now been sent out to the international ionosphere community for review (Bilitza, USA and Gulyaeva, Russia).

Papers from the 2009 IRI Workshop in Kagoshima, Japan have now been published in a first issue of *Earth, Planets, and Space* (EPS, Volume 63, Number 4, 2011) and a second special EPS issue will be published soon. A special issue of *Advances in Space Research* is in preparation with the presentation from the IRI session during the 2010 Scientific Assembly of the Committee on Space Research (COSPAR). The IRI group has submitted a session proposal for the 2012 COSPAR meeting in Mysore, India (July 16-21), which now has been approved. The session will be on 'Global and Regional Representation of Ionospheric Peak Parameters for Space Weather Applications'. For its 2013 Workshop the IRI community has been invited to the University of Warmia and Mazury in Olsztyn, Poland with A. Krankowski as the local organizer. Two new members were elected to join the IRI Working Group: Patrick Sibanda (University of Zambia, Lusaka, Zambia), and Jiankui Shi (Center for Space Science and Applied Research, CAS, Beijing, China).

The workshop was expertly organized by the SANSa team led by Lee-Anne McKinnell; John Bosco Habarulema deserves a special mention for his untiring support of participants' needs before and throughout the workshop week from pick-up at the airport to drop-off. The little seaside town of Hermanus fully lived up to its title as one of the world's prime location for whale sightings. An excursion to the Hemel en Aarde Valley near Hermanus with food pairing and dinner at local wineries convinced the attendees that the valley carries its name rightfully, "Heaven on Earth". The Executive Mayor of the Overstrand Municipality Nicolle Botha-Guthrie and SANSa CEO Dr. Sandile Malinga welcomed the delegates at the dinner reception.

THE 13TH INTERNATIONAL SYMPOSIUM ON EQUATORIAL AERONOMY

Paracus, Peru, 12 - 16 March 2012

The 13th International Symposium on Equatorial Aeronomy (ISEA13) was held on March 12-16, 2012 in Paracus Peru. ISEA's meet every three to four years. They are a major gathering of scientists around the world interested in the low-latitude atmosphere and ionosphere, and their coupling to other latitudes and altitudes. Each ISEA meeting represents an opportunity for researchers to share their most recent results and discuss possibilities for future campaigns and experiments.

The objective of the symposium is to bring together the leaders in the field of equatorial, low-, and mid-latitude

aeronomy to advance our knowledge of these regions of the Earth's atmosphere. Topics for the workshops cover a wide range of research areas, reflecting the need to study the Earth's ionosphere/atmosphere system in a coupled sense. ISEA13 participants joined the celebration of two important events: the 50th Anniversary of the Jicamarca Radio Observatory (JRO) and also the first ISEA meeting-ISEA1 - which took place in Huaychulo, Peru, in 1962. The celebration day for JRO's 50th anniversary was held on Saturday March 17th 2012 at the observatory grounds. The celebration program included a detailed tour of the facilities with the Jicamarca scientists and technicians and frequent users participating as "tour guides".

The celebration program was attended by approximately 150 guests, partially overlapping the 150 participants of ISEA-13. The participants of ISEA-13 included 25 students and representatives from 23 countries. Also, 120 oral talks were presented and 95 posters were displayed during two poster sessions. The oral and poster presentations were aligned with the following eight topical sessions: (1) Irregularity Physics, (2) E and F region coupling (low and mid latitude coupling), (3) Wave propagation between low/middle atmosphere and ionosphere, (4) Plasma neutral coupling, (5) Low and mid latitude Aeronomy and Electrodynamics, (6) Ionospheric storms and Space weather effects at low and mid latitudes, (7) New techniques, experiments, campaigns, and results, and (8) Future trends and challenges. More information about ISEA13, including an access to the program and abstracts, can be found at <http://jro.igp.gob.pe/isea13>. ISEA13 was supported by the US National Science Foundation (NSF), the US Air Force Office of Scientific Research (AFOSR) and the Southern Office of Aerospace Research and Development (SOARD), Scientific Committee On Solar-Terrestrial Physics (SCOSTEP) and Climate And Weather of the Sun-Earth System (CAWSES), the

International Association of Geomagnetism and Aeronomy (IAGA), the International Union of Radio Science (URSI) - Commission G, the Consejo Nacional De Ciencia Y Tecnología del Perú (CONCYTEC). In addition, ISEA received support from private companies in Peru. Most of this was devoted to support the participation of young scientists and researchers from developing countries. The results of the workshop will be published in a special issue in the Journal for Atmospheric and Solar Terrestrial Physics. The deadline for submission of papers is July 31st, 2012. Ethiopia was chosen as the site of the next ISEA meeting to be held in 2015/2016 time window.

ISEA13 Support for Participants

As indicated in the symposium report we received support from different funding agencies and Peruvian companies. We have supported 66 participants, the majority of them students, young scientists, and scientists from developing countries. The complete list can be found in the following link <http://jro-app.igp.gob.pe/isea/index.php?pag=financial>



Figure 1. ISEA13 group picture.

URSI CONFERENCE CALENDAR

An up-to-date version of this conference calendar, with links to various conference web sites can be found at <http://www.ursi.org/en/events.asp>

and Informatics at Bulgarian Academy of Sciences, 1113 Sofia, Bulgaria, Fax :+359 2971 3649, E-mail: bshishkov@math.bas.bg

June 2012

FEM2012 - 11th International Workshop on Finite Elements for Microwave Engineering

Estes Park, Colorado, USA, 4-6 June 2012

Contact: Dr. Branislav M. Notaros, Department of Electrical and Computer Engineering, Colorado State University, 1373 Campus Delivery, Fort Collins, CO 80523-1373, USA, Fax: +1 (970) 491-2249, E-mail: notaros@colostate.edu

July 2012

EUROEM 2012 - European Electromagnetics

Toulouse, France, 2 - 6 July 2012

Contact: Dr. Jean-Philippe Parmantier, ONERA, DEMR/CDE, BP4025, Avenue Edouard Belin, 31055 TOULOUSE Cedex 4, FRANCE, Fax : +33 5 62 25 25 77, E-mail: euroem2012@onera.fr

IEEE 2012 AP-S/URSI Intl. Symposium

Chicago, IL, USA, 8-13 July 2012

Contact: Dr. D. Erricolo, IEEE 2012 AP-S/URSI, University of Illinois at Chicago, Dept of Electrical and Computer Eng, 1020 SEO (MC 154), 851 S. Morgan Street, Chicago, IL 60607-7053, USA, Fax: (+1) 312 996 6465, erricolo@ece.uic.edu

COSPAR 2012 - 39th Scientific Assembly of the Committee on Space Research (COSPAR) and Associated Events

Mysore, India, 14 - 22 July 2012

Contact: COSPAR Secretariat, c/o CNES, 2 place Maurice Quentin, 75039 Paris Cedex 01, France, Fax: +33 1 44 76 74 37, cospar@cosparhq.cnes.fr, <http://www.cospar-assembly.org/>

International School of Physics «Enrico Fermi», Metrology and Physical Constants

Varenna, Italy, 17-27 July 2012

Contact: Prof. Elio Bava, strada delle cacce 91, I-10135 Torino, Italy, Fax +39 011 346384, E-mail: [Elio Bava <e.bava@inrim.it>](mailto:Elio.Bava@inrim.it)

August 2012

ICTRS 2012 - First International Conference on Telecommunications and Remote Sensing

Sofia, Bulgaria, 29-31 August 2012

Contact: Prof. Blagovest Shishkov, Institute of Mathematics

September 2012

ICEAA 2012 - International Conference on Electromagnetics in Advanced Applications

Cape Town, South Africa, 2-8 September 2012

Contact: ICEAA-IEEE 2012 Conference, Consult US (Pty) Ltd, PO Box 19063, Tygerberg, 750, Fax +27 21 933 2649, E-mail: iceaa12@iceaa.polito.it

VERSIM Workshop

Sao Paulo, Brazil, 2-8 September 2012

Contact: Prof. F.C.P. Bertoni, CRAAM/EE/UPM, Rue da Consolacao 896 Prédio T, 7 andar, CEP 01302-907 Sao Paulo, SP, Brazil

Metamaterials 2012

St. Petersburg, Russia, 17-22 September 2012

E-mail : contact@congress2012.metamorphose-vi.org
EMC Europe 2012, Rome, Italy, 17-21 September 2012 Contact: Marcello D Amore, Department of Electrical Engineering, Sapienza University of Rome, Rome, Italy, Via Eudossiana 18, I-00184 Rome, Italy, marcello.damore@uniroma1.it

RADIO 2012 - Radio and Antenna Days of the Indian Ocean

Mauritius, 24-27 September 2012

Contact: Vikass Monebhurrn, Dept of Electromagnetics, DRE-L2S, SUPELEC, 3, Rue Joliot-Curie, 91192 Gif-sur-Yvette Cedex, France, Fax +33 1 69851569, E-mail vikass.monebhurrn@supelec.fr

October 2012

ISSSE 2012 - International Symposium on Signals Systems and Electronics

Potsdam, Germany, 3-5 October 2012

Prof. Rolf Kraemer, IHP GmbH, Dept. System Design, Im Technologiepark 25, 15236 Frankfurt (O), Germany, E-mail: Kraemer@ihp-microelectronics.com

November 2012

ISAP2012-2012 International Symposium on Antennas and Propagation

Nagoya, Japan, 29 October - 2 November 2012

Professor Koichi Ito, General Chair of ISAP2012, Chiba University, 1-33 Yayoi-cho, Inage-ku, Chiba-shi, Chiba 263-8522, Japan, Fax: +81-43-290-3327, E-mail: ito.koichi@faculty.chiba-u.jp

RFID-Technology and Applications 2012

Nice, France, 5-7 November 2012

Contact: Smail TEDJINI, General Chair of IEEE RFID-TA
2012, NPG-ESISAR, LCIS, 50, rue B. de Laffemas, BP
54, F-26902 VALENCE CEDEX 9, FRANCE, Fax +33
4 75 43 5642

September 2013

ICEAA-APWC-EMS conferences

Torino, Italy, 9-13 September 2013

Contacts: Prof. W.A. Davis, EMS Chair wadavis@vt.edu
and Prof. Y. Koyama, EMS Vice-Chair koyama@nict.go.jp

URSI cannot be held responsible for any errors contained in this list of meetings

Information for authors



Content

The *Radio Science Bulletin* is published four times per year by the Radio Science Press on behalf of URSI, the International Union of Radio Science. The content of the *Bulletin* falls into three categories: peer-reviewed scientific papers, correspondence items (short technical notes, letters to the editor, reports on meetings, and reviews), and general and administrative information issued by the URSI Secretariat. Scientific papers may be invited (such as papers in the *Reviews of Radio Science* series, from the Commissions of URSI) or contributed. Papers may include original contributions, but should preferably also be of a sufficiently tutorial or review nature to be of interest to a wide range of radio scientists. The *Radio Science Bulletin* is indexed and abstracted by INSPEC.

Scientific papers are subjected to peer review. The content should be original and should not duplicate information or material that has been previously published (if use is made of previously published material, this must be identified to the Editor at the time of submission). Submission of a manuscript constitutes an implicit statement by the author(s) that it has not been submitted, accepted for publication, published, or copyrighted elsewhere, unless stated differently by the author(s) at time of submission. Accepted material will not be returned unless requested by the author(s) at time of submission.

Submissions

Material submitted for publication in the scientific section of the *Bulletin* should be addressed to the Editor, whereas administrative material is handled directly with the Secretariat. Submission in electronic format according to the instructions below is preferred. There are typically no page charges for contributions following the guidelines. No free reprints are provided.

Style and Format

There are no set limits on the length of papers, but they typically range from three to 15 published pages including figures. The official languages of URSI are French and English: contributions in either language are acceptable. No specific style for the manuscript is required as the final layout of the material is done by the URSI Secretariat. Manuscripts should generally be prepared in one column for printing on one side of the paper, with as little use of automatic formatting features of word processors as possible. A complete style guide for the *Reviews of Radio Science* can be downloaded from <http://www.ips.gov.au/IPSHosted/NCRS/reviews/>. The style instructions in this can be followed for all other *Bulletin* contributions, as well. The name, affiliation, address, telephone and fax numbers, and e-mail address for all authors must be included with

All papers accepted for publication are subject to editing to provide uniformity of style and clarity of language. The publication schedule does not usually permit providing galleys to the author.

Figure captions should be on a separate page in proper style; see the above guide or any issue for examples. All lettering on figures must be of sufficient size to be at least 9 pt in size after reduction to column width. Each illustration should be identified on the back or at the bottom of the sheet with the figure number and name of author(s). If possible, the figures should also be provided in electronic format. TIF is preferred, although other formats are possible as well: please contact the Editor. Electronic versions of figures *must* be of sufficient resolution to permit good quality in print. As a rough guideline, when sized to column width, line art should have a minimum resolution of 300 dpi; color photographs should have a minimum resolution of 150 dpi with a color depth of 24 bits. 72 dpi images intended for the Web are generally *not* acceptable. Contact the Editor for further information.

Electronic Submission

A version of Microsoft *Word* is the preferred format for submissions. Submissions in versions of T_EX can be accepted in some circumstances: please contact the Editor before submitting. *A paper copy of all electronic submissions must be mailed to the Editor, including originals of all figures.* Please do *not* include figures in the same file as the text of a contribution. Electronic files can be sent to the Editor in three ways: (1) By sending a floppy diskette or CD-R; (2) By attachment to an e-mail message to the Editor (the maximum size for attachments *after* MIME encoding is about 7 MB); (3) By e-mailing the Editor instructions for downloading the material from an ftp site.

Review Process

The review process usually requires about three months. Authors may be asked to modify the manuscript if it is not accepted in its original form. The elapsed time between receipt of a manuscript and publication is usually less than twelve months.

Copyright

Submission of a contribution to the *Radio Science Bulletin* will be interpreted as assignment and release of copyright and any and all other rights to the Radio Science Press, acting as agent and trustee for URSI. Submission for publication implicitly indicates the author(s) agreement with such assignment, and certification that publication will not violate any other copyrights or other rights associated with the submitted material.

APPLICATION FOR AN URSI RADIOSCIENTIST

I have not attended the last URSI General Assembly, and I wish to remain/become an URSI Radioscientist in the 2012-2014 triennium. Subscription to *The Radio Science Bulletin* is included in the fee.

(please type or print in BLOCK LETTERS)

Name : Prof./Dr./Mr./Mrs./Ms. _____
Family Name First Name Middle Initials

Present job title: _____

Years of professional experience: _____

Professional affiliation: _____

I request that all information be sent to my home business address, i.e.:

Company name: _____

Department: _____

Street address: _____

City and postal/zip code: _____

Province/State: _____ Country: _____

Phone: _____ ext. _____ Fax: _____

E-mail: _____

Areas of interest (Please tick)

- | | |
|--|---|
| <input type="checkbox"/> A Electromagnetic Metrology | <input type="checkbox"/> F Wave Propagation & Remote Sensing |
| <input type="checkbox"/> B Fields and Waves | <input type="checkbox"/> G Ionospheric Radio and Propagation |
| <input type="checkbox"/> C Radio-Communication Systems & Signal Processing | <input type="checkbox"/> H Waves in Plasmas |
| <input type="checkbox"/> D Electronics and Photonics | <input type="checkbox"/> J Radio Astronomy |
| <input type="checkbox"/> E Electromagnetic Environment & Interference | <input type="checkbox"/> K Electromagnetics in Biology & Medicine |

I would like to order :

- An electronic version of the RSB downloadable from the URSI web site

(The URSI Board of Officers will consider waiving the fee if a case is made to them in writing.)

40 Euro

Method of payment : VISA / MASTERCARD (we do not accept cheques)

Credit card No Exp. date _____

CVC Code: _____ Date : _____ Signed _____

Please return this signed form to :

The URSI Secretariat
c/o Ghent University / INTEC
Sint-Pietersnieuwstraat 41
B-9000 GHENT, BELGIUM
fax (32) 9-264.42.88